Capstone Team Project

MENG411/ MECT411

Name of Project: *ROBOTIC SOLAR PANEL CLEANER*

Group Name: *ROBOTIC SOLAR CLEANER*

Group Members:

Student ID: 20910981 Student Name: Mehdi Ahmad

Student ID: 18701377 Student Name: Mmesoma Mario Alaneme

Student ID: 19700189 Student Name: Thabo Allen Baalora

Student ID: 19700713 Student Name: Mohammad Alhaj Mousa

Student ID: 19700715 Student Name: Mohammad Diwan

Supervisor: *Assist. Prof. Dr. Omid Shekoofa*

Semester: *Spring 2022/2023*

Submission Date: 6th *of June 2023*

Eastern Mediterranean University
Department of Mechanical Engineering

ABSTRACT

This project aimed to design and develop a low-cost, remotely controlled robotic system for cleaning solar panels to improve their performance and efficiency. The robot utilizes a chassis made from 3mm aluminum sheet, manufactured using CNC laser cutting. Mechanical locomotion of the robot is achieved using timing belts, providing an efficient and reliable movement mechanism. The robot is controlled wirelessly through a mobile phone, making it user-friendly and easy to operate. The gear wheels were 3D printed, allowing for customization and cost-effectiveness. The electrical compartment box was made from plexiglass, providing durability and transparency, the brush cover was also made from plexiglass to ensure efficient cleaning and component protection. The robot utilizes a motor driven circular brush and water nozzles for cleaning, ensuring effective dirt and dust removal from solar panels. The robot also utilizes IR and Ultrasonic Sensors for edge and dust detection. Through a thorough review and study of existing robotic solar panel cleaners, the project incorporated the most effective and efficient features to maximize the efficiency of the panels in generating renewable energy. The aim was on using inexpensive materials, employing economical manufacturing processes, and reducing complexity for end users. Detailed cost analysis, mechanical design, operating subsystems, and standards used were presented in the project, contributing to the overall goal of maintaining solar panels and optimizing their energy generation efficiency.

TABLE OF CONTENTS

LIST OF FIGURES

LIST OF TABLES

CHAPTER 1 - INTRODUCTION

1.1. Detailed Definition of the Project

The design, development, and manufacturing of a low-cost remotely controlled robotic system for solar panel cleaning is the main purpose of this project. Different robotic solar panel cleaners would be examined with respect to mechanical locomotion across inclined surfaces as well as the process of operation. The solar robot cleaner would be built on an aluminum chassis with a compartment to house the controller circuitry. A remote control is used to wirelessly transmit control movement instructions to the solar robot cleaner. The robot is equipped with a microprocessor unit which controls the movement of the motors based on the input received from the operator. We opted for gear wheels attached to rubber belts for the mechanical locomotion of the solar panel cleaner which ensures the robot adheres properly to the surface of the solar panels. The cleaning components of the robot are roller brushes fixed at the front of the system and water sprayers which facilitate the removal of accumulated particles such as dust, dirt on the surface of the solar panel. The robotic solar panel is developed for efficient cleaning via wireless remote control thus improving the performance and efficiency of solar panels.

1.2. Significance of the Project

The concept of generating power from renewable sources is an approach that has grown exceedingly in recent years because of increasing demand for energy and environmental concerns of harmful emissions. Renewable energy, particularly solar energy, is an important means for decarbonizing the energy system. Solar panels are effective means of harnessing solar energy from the sun as they possess features that include simple installation, low maintenance cost, eliminated fuel cost and no harmful emission to the environment. Achieving maximum efficiency from solar panels can be challenging and the efficiency of the solar panels varies as a result of various environmental factors that reduce the performance of the solar panels during their life cycle. Some of the factors affecting the performance and efficiency of solar panels include the accumulation of particles like dust, dirt, bird feces, etc. To maintain maximum efficiency in power generation, solar panels need to be cleaned regularly. However, manual cleaning of solar panels can be time consuming, labor-intensive, costly, and hazardous especially in large scale solar panel systems.

The accumulation of dust or dirt on the surface of solar panels can increase its temperature and also block the solar radiation resulting in reduced efficiency and decrease of power output. The development of solar panel cleaning robots' aids in maintaining the performance and efficiency of solar power generation by ensuring the solar panels are kept clean. Various robotic solar panel cleaners are being designed, developed, and manufactured for automatic cleaning of solar panels. Similar to solar power plants used in large scale industrial applications, the developed solar robot cleaners can also be used to improve the efficiency in small scale applications like rooftop solar panels in houses and offices.

1.3. Detailed Project Objectives

The focus of this project is to incorporate existing designs, components, and technologies to the development of the robotic solar panel cleaner such that it improves the performance and efficiency of solar panels on both small- and large-scale applications. We aim to develop a low-cost solar panel cleaning system by using inexpensive materials and components as well as economical manufacturing processes. The robotic solar panel cleaner would also be developed to be sustainable so it would be able to perform regular cleaning operations over a long-life span. Additionally, the robot would integrate user friendly operations by reducing the complexity of control making it easy to use and operate for end users. To provide a much wider perspective of how the robotic solar panel cleaner would be developed, we outlined the main goals and objectives for developing the system below.

- **Design for Cost** - To develop a cost-effective robot cleaning system we would utilize inexpensive and readily available materials and components as well as economical manufacturing processes. This approach is aimed at minimizing the cost of developing the cleaning system without limiting the robot's performance or deviating from the main objectives.
- **Design for Manufacturability** - We aim to design a robotic system that is easy to manufacture using available materials while also outsourcing related components and implementing economical manufacturing processes.
- **Design for Safety** - A key aspect of this project is to design and develop a robot solar cleaning system that is safe to use and operate without causing any damage to the user and solar panels. Some methods of achieving this are to ensure all wires are insulated and covered properly and smoothing sharp edges on the body of the robot.
- **Design for Sustainability** - We aim to develop the robot to be sustainable so it would be able to perform regular cleaning operations over a long-life span. We would achieve this by utilizing durable materials and selecting components that don't wear out easily and can be easily replaced if need be.
- **Design for Environment** - The robot would be developed with little to no harmful emission of waste products. We would also implement proper disposal of worn-out batteries and the water tank would be made of plastic which can be easily recycled.

1.4. Detailed Project Constraints

- **Cost** - For the project, cost is an important parameter to factor. The project should be economically affordable therefore efficient use of budget for the materials, components, and manufacturing is of importance.
- **Time** - The start and completion of the design and development of the project should be done within a specified time frame.
- **Manufacturability** - The manufacturability of the robotic solar panel cleaner would be determined with respect to the materials selected during the design stages as well as the availability of the materials. Additionally, economic manufacturing techniques would be used without reducing the overall performance of the robotic system.
- **Sustainability** - It is necessary to have a well-defined life span, from its origin to its disposal, as well as considering environmental factors in the design. Hence, the robotic solar panel cleaner should be sustainable and robust.
- **Safety** - Implementing a user-friendly design which poses no risk of harm or damage to the user or solar panels should be considered. This would mean that the structure of the cleaning robot should be devoid of sharp edges and include proper insulation of the electrical unit.
- **Environmental Factors** - Components like batteries should be properly disposed of and also the plastic features of the robot can be recycled. Good control of waste disposal and proper monitoring should be incorporated.

1.5. Report Organization

- In chapter 1, an introduction to the report is given. The chapter also discusses the significance of the project, as well as the objective and constraints related to the project.

- Chapter 2 gives a broader discussion and review about existing robotic solar panel cleaners with different operations, use, functionality, and design developed over time. Additionally, it gives background information about solar cleaning robot systems and a good overview of various control systems incorporated into robotic solar panel cleaners. Furthermore, concurrent solutions related to robotic solar panel cleaning systems were illustrated their engineering standards as well.

- Chapter 3 lays emphasis on the proposed design of the robotic solar panel cleaner and also gives a detailed analysis on the electrical, and mechanical components of the robot cleaning system. The components of the robotic cleaner are highlighted and analyzed with a summary of their technical specification and operation. Also, some simplified calculations were made for the robotic solar panel cleaner and cost analysis was also provided.

- Chapter 4 focuses on the manufacturing of robotic solar panel cleaners. Various manufacturing processes were described, and the manufacturing materials were also discussed. The selection criteria for both the manufacturing process and material were highlighted in this section.

- Chapter 5 discusses the implementation of the testing methods for an efficient functioning of the robotic solar panel cleaner which entails the verification of the objectives of the project and the applied engineering standards.

- Chapter 6 provides a discussion on the results, engineering standards and constraints of the project.
- Chapter 7 gives a conclusion on the design and development of the project and provides insights into future works relating to the project.
- Finally, the appendixes include the detailed engineering drawing of the designed robotic solar panel cleaner, logbook, and timeline of the project.

CHAPTER 2 - LITERATURE REVIEW

2.1 BACKGROUND INFORMATION

Since the development of silicon photovoltaic cells back in 1954, this invention has played a crucial role in the development of innovative technology. Utilizing the renewable energy source from the sun enabled the first satellites to be autonomous for a long time. Nevertheless, it was around the mid 70's that scientists began to recognize photovoltaic energy as an efficient source for future non-fossil energy supply. Despite this development, modern research shows that there is more to be done to improve the technology in terms of size, manufacturing, and efficiency.

A photovoltaic cell of a solar panel absorbs photons hitting the semiconducting material of the panel when exposed to sunlight. Electrons are excited and move up to an atomic orbital or higher molecule. In order to dissipate the excess energy, the electrons can either revert back to their original orbital, by converting the extra energy into heat, or by traveling through the material to an electrode thereby negating the potential. A normal cell would generate around 0.45volts DC regardless of its size. This suggests that the available power generated by the cell will be very dependent on the area of the cell the sun irradiates and the material used to absorb the photons. To achieve higher voltages, cells are installed in series. The types of cells which are available commercially can be divided into 3 main groups:

- Thin film cells: smaller ecological footprint but heavy
- Crystalline silicon cells: the most used bulk material for PV cells
- Multijunction cells: currently experimental, used originally in space however terrestrial solar concentrators make them also effective on earth.

These three types of cells can be subdivided into different groups, depending on the materials and methods dependent on the available spectrum and the cost-effectiveness of the cells. The two commonly used materials are polycrystalline and monocrystalline silicon cells. Monocrystalline silicon cells have a higher efficiency but are also more expensive compared to polycrystalline cells. Though, because of technological advances, the cost of monocrystalline cells has decreased with increasing usage.

For the protection of PV cells of solar panels against the wear and tear of the operational environment, they are developed with a material, preferably glass or polycarbonate, that has both good optical qualities in terms of transmittance and provides protection against humidity, impact etc. (KU Leuven, 2014)

The output power generated by photovoltaic cells is directly related with the time, date, and weather as shown in the below figure.

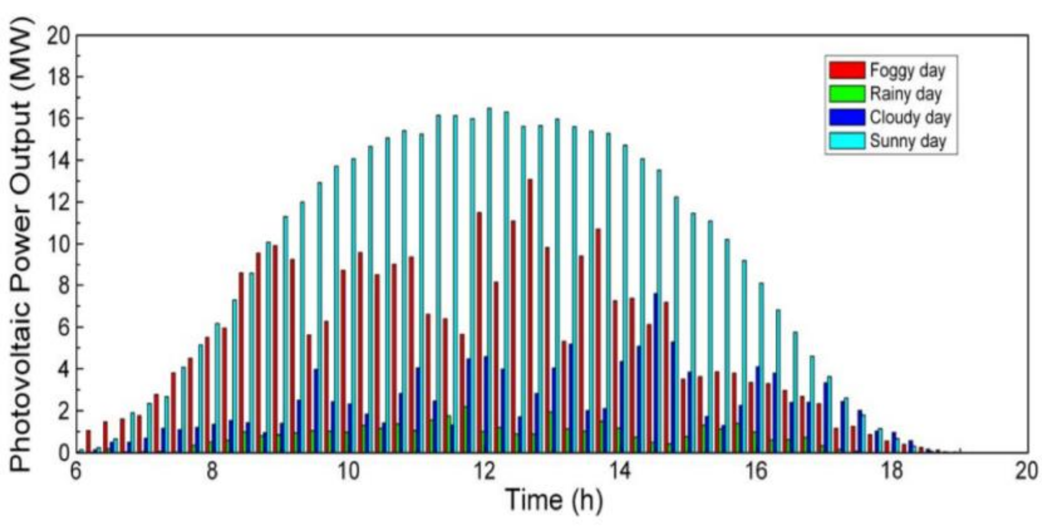

Figure 1: Power output of solar panel systems under varying weather conditions

(“KU Leuven: Power output forecast of PV systems”, 2012)

From the model developed from reports and studies, solar panels generate the most power output on sunny days with the least power output generated on rainy days. The models also highlight the estimated power output of solar panels on other days which include cloudy and foggy days.

Modern innovations have brought about the development of different robotic solar panel cleaners which include:

Ecoppia E4 which is a fully autonomous robot that uses microfiber brushes to sweep dust off solar panels. This robot is designed for large rows of solar panels installed in dry and sandy environments. Utilizing the effect of gravity, the brushes move downwards while spinning which creates an airflow that helps blow off dust. The robotic cleaner uses an on-board solar panel and battery to store energy which enables the robot to clean at night. Horizontal and vertical translation is made possible using a guide rail and wheels. (KU Leuven, 2014)

Figure 2 : Ecoppia E4

(“Ecoppia: Field proven automatic, water-free solar panel cleaning system”, 2014)

Another developed robotic solar panel cleaner is washpanel systems that cleans arrays of solar panels by moving a vertical brush horizontally across rows of solar panels. This system can be deployed automatically. A water hose is attached to the robot for wetting the solar panels while it cleans. Unlike the Ecoppia E4 this system does not require a track.

Figure 3: A Wash panel system

("Washpanel systems: Product ranges", n.d.)

Additionally, there is the hyCleaner Solar facelift cleaning robot that allows for easy, economic, and fast cleaning. This robotic cleaning system is controlled by a radio remote control and draws its power from lithium-ion batteries without an external power source enabling the operator to achieve an optimum cleaning result without physical efforts.

Figure 4 : hyCleaner Solar facelift

("hyCleaner: Solar panel cleaning robot - Product specification", n.d.)

There are several other developed solar cleaning systems that are used for both small- and large-scale applications to effectively clean solar panels for proper maintenance.

2.1.1 Losses in Solar panel systems

As sunlight is converted into usable electricity there are different losses lowering the solar panel systems power output. To evaluate the performance of solar systems a performance ratio is used. The performance ratio represents the final yield (Y_F) divided by the reference yield (Y_R). Additionally, the performance ratio compares the AC output power with the DC power exiting the panel, thereby evaluating the losses. These losses can be linked with:

Panel degradation (η_{deg}), temperature(η_{tem}), soiling(η_{soil}), internal network(η_{net}), inverter(η_{inv}), transformer(η_{tran}), systems availability and grid connection network(η_{ppc}).

The performance ratio (PR) is then expressed as:

$$PR = \frac{Y_F}{Y_R} = \eta_{deg}.\eta_{tem}.\eta_{soil}.\eta_{net}.\eta_{inv}.\eta_{tran}.\eta_{ppc}$$

The performance of transformers and inverters is improving because of technological advances. However, soiling can be improved irrespective of the installed technology simply by keeping the glass panels clean. The following section would go into details of the mechanism for soiling and degradation. (KU Leuven, 2014)

Soiling

As time passes, operational solar panel systems become covered with layers of dirt, hence reducing the amount of sunlight hitting the PV cells. The amount of power lost as a result of soiling depends on several factors.

Firstly, it depends on the type of dirt deposited on the panel. The dirt may be from pollen or air pollution matter, sea salt, construction, agricultural activity, and other natural sources.

Secondly, the influence of precipitation. The amount of rainfall and the time between rain events alter the layer of precipitation. A substantial amount of the accumulated pollution is washed away by rainfall while during periods of drought losses rapidly increase. All these factors can be linked to the geographical location and the climate the system operates in.

Lastly, the angle at which the solar panels are tilted is an important factor. The lower the angle, the faster dirt accumulates with maximal effect when solar panels are installed horizontally.

Soiling decreases the transmittance of the glass thus affecting the short circuit current resulting in power losses that differ considerably. (KU Leuven, 2014)

Snow

The summer is the best period for utilizing solar panels, regardless of the higher temperatures reduce the overall efficiency of the solar panels. Winter has a smaller share in the annual power output yield, but the snowfall effects can be seen clearly in report statistics. Snow can be viewed as a major form of soiling. Layers of snow limit the amount of radiation penetrating through to the cells, hence reducing the output yield. Even with partially covered areas of snow, the impact is still substantial because of the bypass diodes disabling cells. On tilted panels the snow may slip, and the output power increases gradually, however on flat solar panels, the snow will cover the panels until they melt. (KU Leuven, 2014)

Researchers in Munich evaluated data obtained from a local 38100m^2 large PV array to analyze the effect of snow on the annual yield of the solar plant. According to their results, the impact of snow depends on several parameters including the weight and height of snow as well as tilt angle of the solar panels.

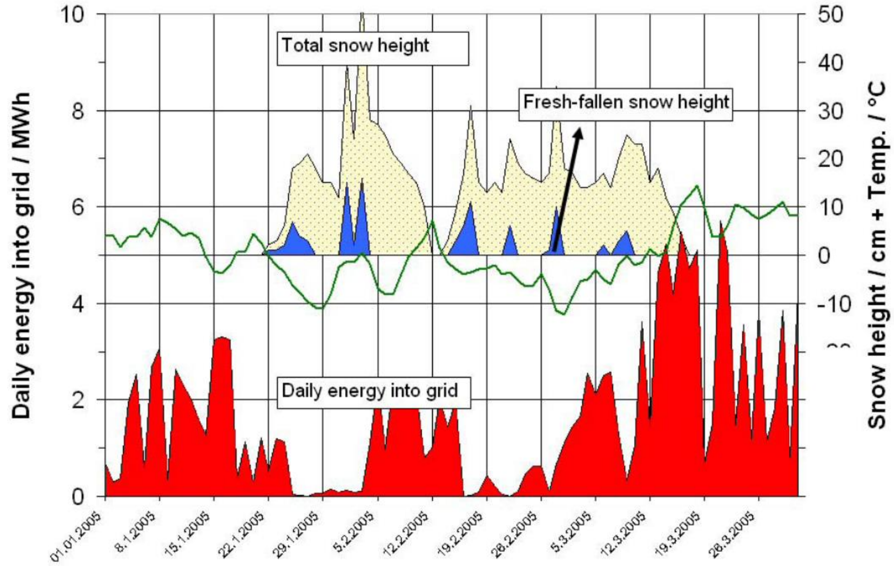

Figure 5 : Influence of snowfall and total snow height on energy yield

("KU Leuven: Snow impact on PV systems. Proc. European PVSEC", 2006)

Degradation

Solar panel degradation refers to the loss of efficiency or performance of solar panels over time. This can be caused by a variety of factors, including exposure to the elements, wear and tear, and manufacturing defects. Degradation can occur at different rates and can be classified into two main types: simple degradation and permanent degradation.

Simple degradation, also known as natural degradation, refers to the gradual loss of efficiency that occurs as a solar panel ages. This type of degradation is typically slow and predictable, and it can be compensated for by properly sizing a solar system and choosing high-quality panels. Simple degradation is usually caused by factors such as: temperature and humidity. Permanent degradation, on the other hand, refers to damage or loss of efficiency that cannot be reversed or compensated for. This can be caused by a variety of factors, including corrosion and physical damage from storms, hail, or falling debris.

Dirt, dust, debris and other environmental contaminants can cause degradation in solar panels When these contaminants accumulate on the surface of a solar panel, they can block some of the sunlight that would normally be absorbed by the panel. This can reduce the amount of electricity that the panel is able to produce, leading to a decrease in efficiency. In addition to reducing efficiency, dirt, dust, and other contaminants can also cause physical damage to solar panels over time. When contaminants are allowed to build up on the surface of a solar panel, they can cause scratches and abrasions on the panel's surface. These scratches can weaken the panel and make it more susceptible to damage from physical impacts or weather events. Therefore, it is very important to keep solar panel cleans in order to minimize degradation and ensure optimal performance. This can be achieved with robotic solar panel cleaners. (KU Leuven, 2014)

2.1.2. Cleaning methods for solar panels

1. **Robotics:** Robotics is an interesting new technology that is being utilized to clean solar panels. One of the most efficient and time-saving approaches is to use robotics to clean solar panels. This results in a more effective cleaning operation that takes less time, lowering the danger of scratches or damage to the solar panel's surface. This will also reduce the amount of damage and injuries that workers may sustain when cleaning panels in hazardous places.
2. **Waterless Vibration:** It's also simple and doesn't require any special equipment or tools. The fundamental procedure is shaking the surface of your solar panel with a strong equipment known as an industrial vibrator (sometimes referred to as "Vibra-clean"). This approach employs high-frequency vibrations to break down grime and oil on the surface of your solar panel while causing no damage to the surface or interior components. Because of the high frequency vibration, this approach may cause damage to the solar panel.

3. **Nanoparticle Coating:** Another method for cleaning your solar panels is to use nanoparticle coatings that are specifically intended for cleaning solar panels. These nanoparticle coatings are deposited using an electrostatic spray gun or roller on both metal and glass surfaces. They operate by eliminating dirt and grime from both sides of your solar panels while they are still in their protective containers during storage or shipping, allowing them to be installed quickly after cleaning.

2.2 CONCURRENT SOLUTIONS

2.2.1 Four Wheel Holonomic-Drive System

IEEE published in 2018 a type of mobile robot system that has flexibility in rotational movement which allows the robot to reduce unnecessary cleaning time. Most mobile robot systems have flexibility in cleaning since it doesn't require installation of a rail system on the top of the solar panel or extra equipment. Moreover, mobile robot systems can cover all the panel areas without any restrictions. However, when it comes to time most mobile robot systems spend unnecessary cleaning time while slowly turning from left to right or vice versa and this disadvantage can be real time consuming especially for continuous panels in solar farms. Luckily, IEEE proposed in 2018 a type of drive system that can reduce unnecessary cleaning time by adopting a 4 Wheel Holonomic-Drive System Robot. "What is a Holonomic-Drive System?" If a robot adapted a controllable degree of freedom equal to its total degree of freedom (DOF) the robot can be Holonomic. However, to adapt such drive system Omni wheels were the only solution to achieve the Holonomic-Drive System because omni wheels can allow the robot to move freely in all directions as well as allow it to move even in the moving direction that is perpendicular to the wheels. Figure 1 illustrates the dynamics behind the four wheel Holonomic-Drive System that allows the robot to move freely without rotating on itself.

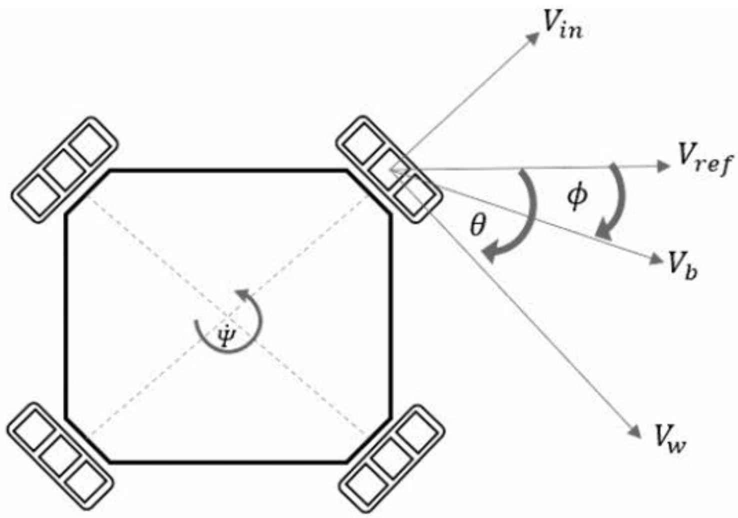

Figure 6. Four Wheel Holonomic-Drive System

("IEEE: Rooftop solar panel cleaning robot using Omni wheels", 2018)

IEEE aimed for this new driving system to improve the cleaning speed compared to other robots as well as to maintain accurate control of the robot in inclined planes. To achieve that goal IEE made multiple performance tests between Omni-wheel movement (Holonomic) and Non-omni-wheel movement (non-holonomic). The results were tabulated in table 1 and 2.

Omni-wheel movement (Holonomic)				
Number of Laps	Average Error X (mm)	Average Error Y (mm)	%Position Error /Distance	Average moving time (sec)
1	-2	72	1.8%	11.2
2	39	17	0.5%	21.7
3	30	-27	0.3%	31.8

Figure 7. Table 1 of tabulated results

("IEEE: Rooftop solar panel cleaning robot using Omni wheels", 2018)

Non-omni-wheel movement (Non-holonomic)				
Number of Laps	Average Error X (mm)	Average Error Y (mm)	%Position Error /Distance	Average moving time (sec)
1	-14	16	0.5%	28.4
2	-43	27	0.6%	64.1
3	-17	39	0.4%	87.8

Figure 8. Table 2 of tabulated results

("IEEE: Rooftop solar panel cleaning robot using Omni wheels", 2018)

By looking at both tables Omni-wheel movement has saved 64% of cleaning time for 3 laps compared to non-omni-wheel movement. Therefore, IEEE has achieved its goal of improving the cleaning speed of the robot by implanting the proposed new driving system using omni wheels.

2.2.2. Automated dual axis moving frame and a rotating brush

Swain et al. (2021) proposed a self-powered solar panel automated cleaning system that consists of a rail system. The mechanism behind it is two motor M3 drives mounted at the top side of the panel and another two motor M3 drives installed at the bottom side of the panel figure (1). The proposed system consists of two parts: electrical and mechanical. The first part consists of a DC motor, IR Sensor, Microcontroller, Motor driver. The second part consists of two frames for different moving actions. The first frame is set to move horizontally between left and right. The second frame is set to move vertically up and down while the brush is mounted on the top of the vertical frame. Moreover, the proposed design will be self-powered by two small solar panels to energize the automated cleaning system. However, the proposed design by Swain et al. will be more like a rail system which will take longer time to clean because the vertical cleaning brush has a small cleaning area. Moreover, this cleaning system is fixed type so that it is permanently attached to solar panels. Therefore, the proposed design works efficiently for continuous flat panels in solar farms.

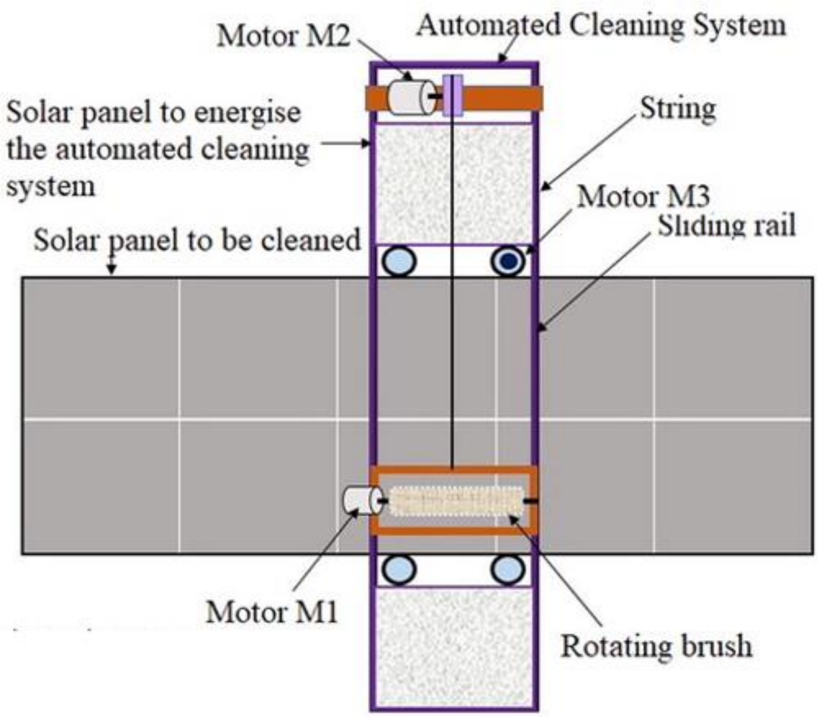

Figure 9. Automated dual axis moving frame and a rotating brush.

("Manoj K. Swain, Manohar Mishra, Ramesh C. Bansal & Shazia Hasa: A Self-Powered Solar Panel Automated Cleaning System," 2021)

2.2.3. Track Driven- Dual Brush Design

In a study published by (Antonelli et al., 2020), a solar cleaning robot shown in Fig 4, that consists of two motorized tracks for the locomotion and two helical brushes located at the two ends of the robot to perform the cleaning process of the PVP. In this design, the helical brushes located at the front and rear end of the robot allow the robot to achieve forward and backward motion, this eliminates the need for the robot to perform a 180 degree turn when changing direction. As a result, the structure of each brush helix has been structured with opposing helix angles to allow brushing away thick layers of sand toward PVP array areas that will be cleaned later during the cleaning process. The brushes must ordinarily work in such a way that only the brush facing the robot motion direction brushes the sand away forwards and downwards until it falls out of the PVP surface, far from previously cleaned PVP surfaces. The cleaning procedure is shown in Fig 3. As for the locomotion of the robot, two independent closed belts that perform the function of two tracks, allow for the motion of the robot. The tracks help to distribute the mass of the robot on the solar panels, enhance traction capability and improve the traction capability of the robot. In this design the belts/tracks were covered with a 2.4mm thick layer of Linatex, a high friction red coloured natural rubber that has a friction coefficient ranging from 1 to 1.65. The robot prototype was subjected to a series of laboratory experimental tests by using 2 x 4 PV panels for PVP slope angles from 0-30 as shown in the figure.

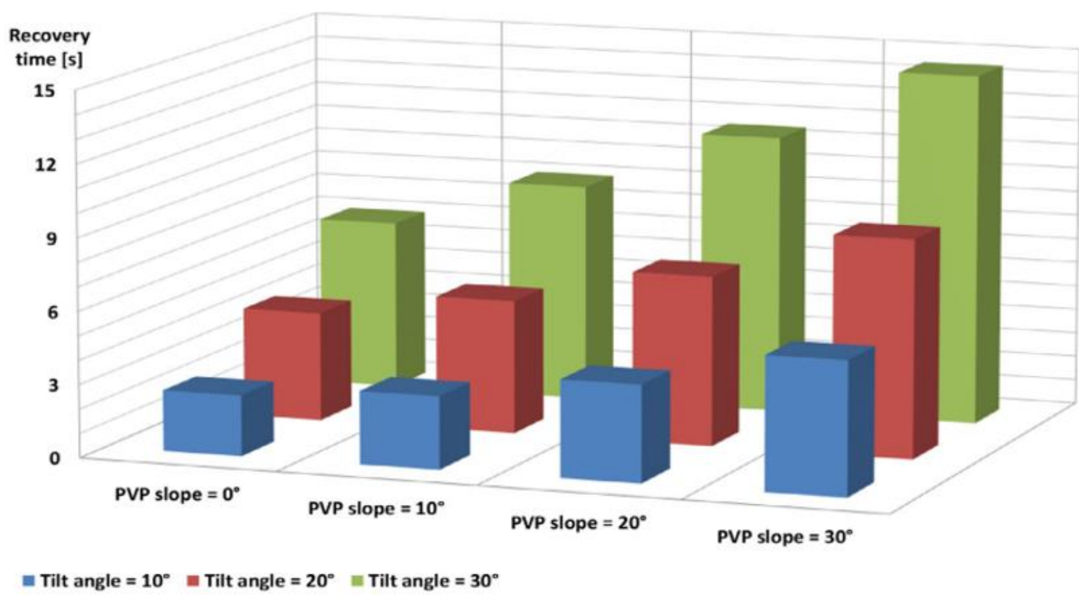

Figure 10. Recovery time vs Slope/Tilt Angle

(“Antonelli, M. G., Beomonte Zobel, P., De Marcellis, A., & Palange, E: Autonomous robot for cleaning photovoltaic panels in desert zones.”, 2020)

Experimental laboratory tests: resulting cleaning times of the robot moving along a PVP cleaning path (length of about 6.5 m) as a function of the PVP array slope.

PVP array slope [degree]	Average cleaning time [s]	Average cruise speed [m/s]
0	25.0	0.26
10	26.3	0.25
20	28.3	0.23
30	31.2	0.21

Figure 11. Experimental Laboratory tests: cleaning time as function of PVP Slope

("Antonelli, M. G., Beomonte Zobel, P., De Marcellis, A., & Palange, E: Autonomous robot for cleaning photovoltaic panels in desert zones.", 2020)

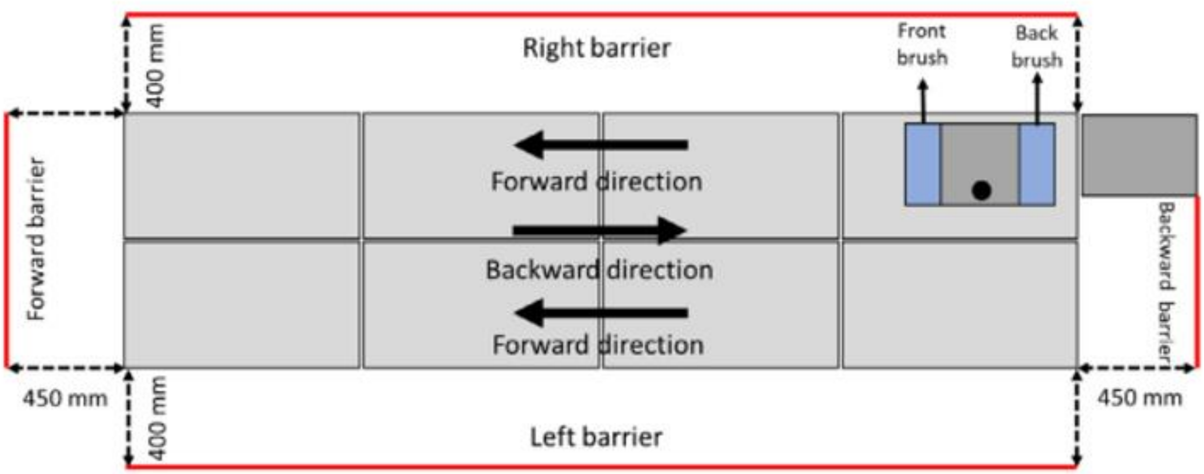

Figure 12. Laboratory experimental verifications of robot motion and cleaning schematic/procedure

("Antonelli, M. G., Beomonte Zobel, P., De Marcellis, A., & Palange, E: Autonomous robot for cleaning photovoltaic panels in desert zones.", 2020)

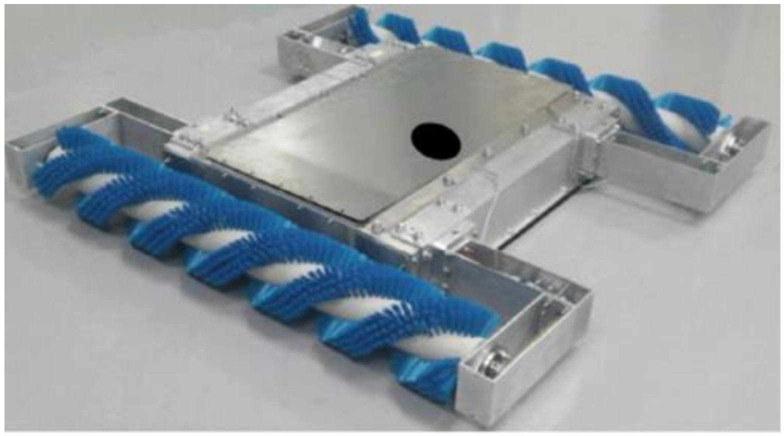

Figure 13. Track Driven- Dual Brush Design

(“Antonelli, M. G., Beomonte Zobel, P., De Marcellis, A., & Palange, E: Autonomous robot for cleaning photovoltaic panels in desert zones.”, 2020)

2.2.4. Wheel Driven - Single Brush Design

In a study published by (Hassan et al., 2018), a solar cleaning robot that consists of a roller brush to remove dust from PV modules, a ducted fan to generate adhesion to the PV module to avoid slippage, four differential drive motors and four running wheels for smooth locomotion, and a blower fan to remove dust from PV modules as shown in Fig 1. In this design, the locomotion constraints caused by slippage while traversing a smooth surface and the inclination of PV modules are addressed using ducted fan and runner wheels. The ducted fan creates adhesion, which allows the robotic cleaner to stick to the PV module, reducing the effect of slippage. The proposed system's roller brush scratches dust from PV modules and allows the blower fan to remove this dust by providing a strong thrust of blowing air. The strong thrust of blowing air removes dust and other particles from PV modules, leaving the glassy surface gleaming and clear. Because the robotic cleaner must climb PV modules inclined at 25°. The use of rubber wheels in this design in conjunction with the ducted fan reduces slippage of robot wheels caused by the protection glass of PV modules. The robot's excellent grip in this design is provided by the rubber wheels. A graph of maximum power generated by the PVP over time for a cleaned PVP and a dirty PVP was plotted in Figure 2. To show the significant increase in performance of the PVP because of the cleaning done by the proposed design.

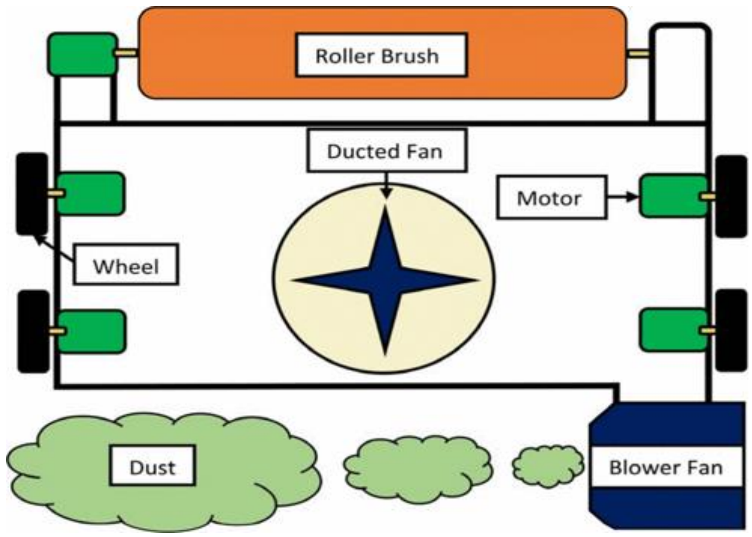

Figure 14. Schematic of Wheel Driven -Single Brush Design

("Hassan, M. U., Nawaz, M. I., & Iqbal, J: Towards autonomous cleaning of photovoltaic modules", 2018)

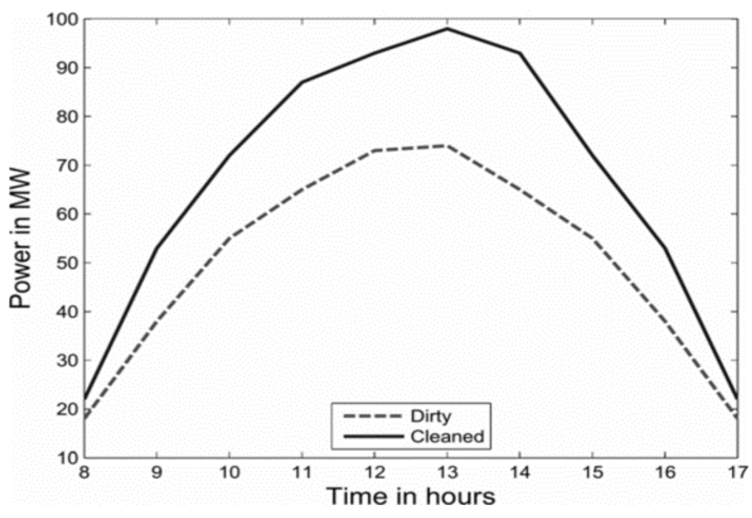

Figure 15. Impact of cleaning on PVP performance

("Hassan, M. U: Towards autonomous cleaning of photovoltaic modules", 2018)

2.3. Comparisons of the concurrent solutions

In this section the above reviewed articles with different designs in section 2.2 were compared with the help of Pugh's matrix so that the team could decide on which concept to adopt for the new design of the Robotic solar cleaner. However, before comparison we summarized robot capabilities in the above reviewed designs for the simplicity of the reader to be able to distinguish the differences between these concepts.

Four Wheel Holonomic-Drive System: is a type of robot that adopts the Holonomic-Drive System. IEEE introduced this new system in 2018.Moreover, Holonomic robot refers to a robot that has a controllable degree of freedom equal to its total degrees of freedom (DOF). Omni wheels were the only solution to achieve the Holonomic-Drive System because omni wheels can allow the robot to move freely in all directions. In addition, the robot performance has recorded fast cleaning time as well as high flexibility and stability.

Automated Dual Axis Moving Frame and a Rotating Brush: is a type of automated rail cleaning system, but this automated system is self-powered by small solar panels. This system was introduced by Swain et al. in 2021. Moreover, it consists of two parts: electrical and mechanical. Electrical part has a DC motor, IR Sensor, Microcontroller, Motor driver. Mechanical part has two frames for different moving actions. The mechanism behind it is that the first frame is set to move horizontally between left and right. The second frame is set to move vertically up and down while the brush is mounted on the top of the vertical frame.

Track Driven Dual Brush Design: is a robot that has two motorized tracks for locomotion. This design was introduced by Antonelli et al. in 2020. Moreover, they implemented two independent closed belts that perform the function of two tracks which allow for the motion of the robot. The tracks help to distribute the mass of the robot on the solar panels for high stability and improve the traction capability of the robot. In this design the belts/tracks were covered with a 2.4mm thick layer of Linatex, a high friction red colored natural rubber to avoid slipping on water. In addition, the helical brushes located at the front and rear end of the robot allow the robot to achieve forward and backward motion, this eliminates the need for the robot to perform a 180 degree turn when changing direction.

Wheel Driven Single Brush Design: is a robot that has four differential drive motors attached to four wheels for smooth locomotion. This design was introduced by Hassan et al. in 2018.Moreover, they implemented on this design a ducted fan that creates adhesion so that the robot sticks on the surface of PV modules and runner wheels to avoid robot slippage and to traverse a smooth surface. In addition, a blower fan to remove dust from PV was used in this design as well as a roller brush to have high cleaning performance on solar panels.

After the team has reviewed the previous designs Pugh's matrix was executed in the below tables. However, comparing 4 different concept designs with different ideas was not professional since all these concepts have advantages as well as disadvantages. Therefore, as a team we made sure to compare these concept designs according to the cost since the team was looking for a low cost but reliable robot. Secondly, the robot cleaner should be light in weight since PV modules are sensitive to heavy weight. Thirdly, the robot cleaner must be stable since PV modules have inclined surfaces and it might slip. Fourthly, the robot cleaner must be flexible and able to clean wide areas of the PV modules. Fifthly, the robot cleaner should be fast during the cleaning phase otherwise it will not be reliable in a solar farm. Therefore, these 4 concept designs were compared in table 1 according to Cost, Weight, Stability, Flexibility and Reliability.

Table 1. Pugh matrix for concept selection for robotic solar panel cleaner

Concept **1→Worst** **10 →Best**	**Four Wheel Holonomic-Drive System**	**Automated Dual Axis Moving Frame**	**Track Driven Dual Brush Design**	**Wheel Driven Single Brush Design**
Cost	2	10	7	3
Weight	9	10	4	8
Stability	8	6	10	8
Flexibility	9	3	10	8
Reliability	10	2	10	9
Total	38	31	42	36

From the table the concept of Track Driven Dual Brush Design had the highest score; therefore, the team decided to implement the concept of track driven robot on their design because track Drive-System satisfies the team needs of having stable, flexible, and reliable robot. However, most PV modules are sensitive to heavy weight and they might crack from high load, so the team decided to improve their design by choosing light components. Therefore, from table 2, 3 and 4 Pugh's matrices were carried out for these components to choose the ones with the highest score.

Table 2. Pugh's matrix for brush selection

Concept **1→Worst** **10 →Best**	**Roller Brush**	**Dual Spiral brush**
Cost	10	5
Weight	9	5
Stability	8	8
Flexibility	7	8
Reliability	6	9
Total	40	35

Pugh's matrix was executed in the above table to choose the first component in our design. Although Dual Spiral Brush had higher flexibility as well as reliability compared to Roller Brush, adding dual brush to our design is risky because the excessive load on the PV module might break it. Therefore, the team decided to choose Roller Brush because it has the highest score compared to Dual Brush and has good aspects such as light weight and moderate performance.

Table 3. Pugh's matrix for body selection

Concept **1→Worst** **10 →Best**	**Aluminum robot body**	**3D-Printed robot body**
Cost	7	5
Weight	8	10
Stability	8	7
Flexibility	8	7
Reliability	9	6
Total	40	35

Pugh's matrix was carried out in the above table to choose the second component in our design. The team decided to select an Aluminum Robot body 3D-printed robot body because it has a higher score compared to the 3D-printed robot body and very good aspects such as high reliability and Stability.

Table 4. Pugh's matrix for track belt selection

Concept **1→Worst** **10 →Best**	**Rubber Track belts**	**Plastic Track belt**
Cost	7	10
Weight	10	8
Stability	10	5
Flexibility	10	8
Reliability	10	8
Total	47	39

Finally for the last component Pugh's matrix was carried out in the table above. After analyzing the results, the team decided to select Rubber Tracks Belt because it has a higher score compared to plastic tracks and outstanding aspects such as high stability, high flexibility, high reliability and finally the most important characteristic which is light weight.

2.4. Engineering standards of the concurrent solutions

In engineering and closely linked technological domains, standards are important technical documents. A technical standard is a rule or condition that has been set. Typically, standardized engineering or technical standards, methodologies, procedures, and practices are established in a formal document. Organizations may assist to guarantee that their goods and services are uniform, interoperable, secure, and efficient by implementing standards. Standards are more crucial than ever since goods are now constructed from parts produced in several nations and marketed all over the world.

ISO 17212:2012 & ISO 17212:2004 — illustrates the typical methods for preparation of component surfaces before bonding, which can be used for construction or laboratory testing. It is appropriate to ordinary surfaces made of metal and plastic.

ISO/DIS 10218-2 ROBOTICS — Safety standards for robot systems used in industrial environment — PART 2: Robot systems, robot applications and robot cells integration.

ISO 8373:2012 Terms related to robots and robotic devices — that operate in both industrial and non-industrial environments are defined by the phrase "robots and robotic devices."

ISO/IEC DIS 23510 Information technology — 3D scanning and printing — Framework for service platform for additive manufacturing

ISO/TR 20218-2:2017 International organization of standardization - Safety design for industrial robot systems

ISO/CD 10218 International organization of standardization – safety requirements for industrial robots

ISO 13482:2014 Robots and robotic devices — Personal care robot safety regulations.

CHAPTER 3: DESIGN AND ANALYSIS

3.1. Quality Function Deployment (QFD)

To develop the engineering specifications for the robotic solar panel cleaner, a quality function deployment analysis is done. The Quality Function Deployment (QFD) is a systematic approach for translating customer requirements into engineering design and production specifications. It involves a series of steps that helps our project group to identify and prioritize customer needs, and then translate those needs into specific design and production requirements. In the context of a robotic solar panel cleaner, QFD would involve the following steps:

1. Identify the customer needs: This involves gathering input from customers to understand their requirements for the robotic solar panel cleaner. This might include things like the speed of cleaning, the ability to navigate around obstacles, and the level of dust and dirt it can handle.
2. Develop a House of Quality: This is a visual tool that represents the relationships between customer needs and design requirements. It consists of a matrix with customer needs on one axis and design requirements on the other. The intersections between the two axes are used to indicate the strength of the relationship between each need and requirement.
3. Prioritize customer needs: Based on the information gathered in the first step, the team will prioritize the customer needs in terms of their importance to the overall product. This will help the team focus on the most important features and requirements first.
4. Develop design requirements: Using the prioritized list of customer needs, the team will develop specific design requirements that will meet those needs. These requirements would be measurable and quantifiable, so that they can be tested and validated during the design process.

5. Allocate design requirements: The team will then allocate the design requirements to specific parts or subsystems of the product. This will help to ensure that all of the necessary requirements are addressed in the final design.
6. Develop a production plan: The final step in the QFD process is to develop a plan for how the product will be manufactured and assembled. This will involve identifying the necessary materials and processes, as well as establishing a timeline and budget for the production process.

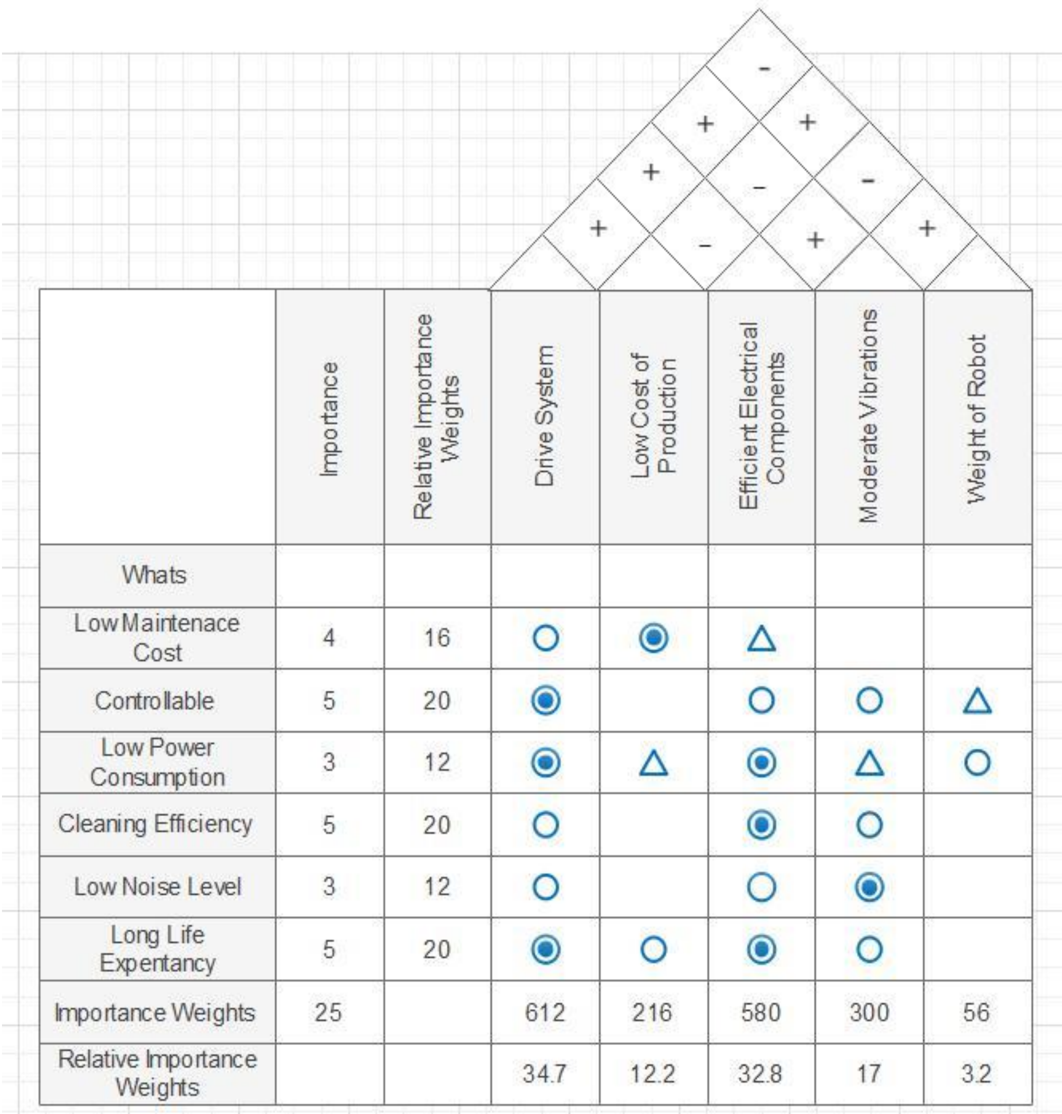

Figure 16. Quality Function Deployment for the robotic solar panel cleaner

Relationship weighing Factors for QFD

◎ - Strong (5)

○ - Moderate (3)

△ - Weak (1)

The goal of QFD is to ensure that the final product meets the needs of the customer as closely as possible, while also being feasible and cost-effective to produce. By following these steps, our project group can create a robotic system that meets the needs of the customers. Above the QFD is shown. The weight of the relationship factors is from 1-5 as shown above. From the QFD, the highest weighted specifications are the drive system and efficient electrical components. So, during our design, we would focus on an efficient drive system to ensure that the robotic solar panel cleaner does not slip or fall as a result of the inclination of solar panels. We would also make more effort to ensure that the electrical components in the robot are very efficient for smooth operation of the cleaning robot.

3.1.1. Description for design selection

With respect to the Quality Function deployment (QFD) analysis done in section 3.1. We developed three designs of which we would make a suitable selection. The first design is a robotic system with dual disc brushes for the cleaning mechanism. The robot has a pulley belt mechanism for locomotion and with a water tank and pipe built with the robot. It also has a main body compartment for housing the controller circuitry. The second design is quite similar to the first design but in this case, it uses roller brushes fitted at the front of the robot to aid the cleaning mechanism. It also has a water supply intake port mounted on top of the robot which draws water from an external water tank. The third design is a fixed frame design which moves linearly across the solar panel to perform the cleaning operation.

The team decided to select the second design with the roller brush and water supply intake port to get cleaning fluid from an external source. The images of the selected design are shown in section 3.2 while the images of the other two designs are shown in section 3.3 of this chapter. The selected design has roller brushes fitted in a brush case and attached to the front of the robot.

Regarding the cleaning mechanism of the solar panels, the first proposed design has a water tank built with the robot. Later on, we decided that by having a water reservoir attached to the robot structure, it makes the system statically imbalanced and this imbalance will affect the motion of the robot especially in inclined solar panels. Hence, in the selected design we eliminated the water tank and instead opted for an external water reservoir. The system would draw water from the reservoir via an intake port and a hose. The third proposed design was a frame semi-automated structure with dual roller brushes. This semi-automated frame can be considered as a simpler design compared to the selected design. However, when it comes to flexibility this design doesn't meet the team's criteria and standards. Therefore, the design that we selected as a team has better efficiency and flexibility compared to the other two proposed designs.

3.2 PROPOSED/SELECTED DESIGN

The proposed robotic solar cleaner is shown in the figure below. It consists of a chassis which is the main frame of the robot where other parts and components would be attached, a brush mechanism fitted in front of the robot with water supply connections for the cleaning operation. A box that houses the electrical components for operating the robotic system. The robotic system is also equipped with two rubber timing belts driven by motors attached to gear wheels for locomotion. Similar to the mechanism used in tanks.

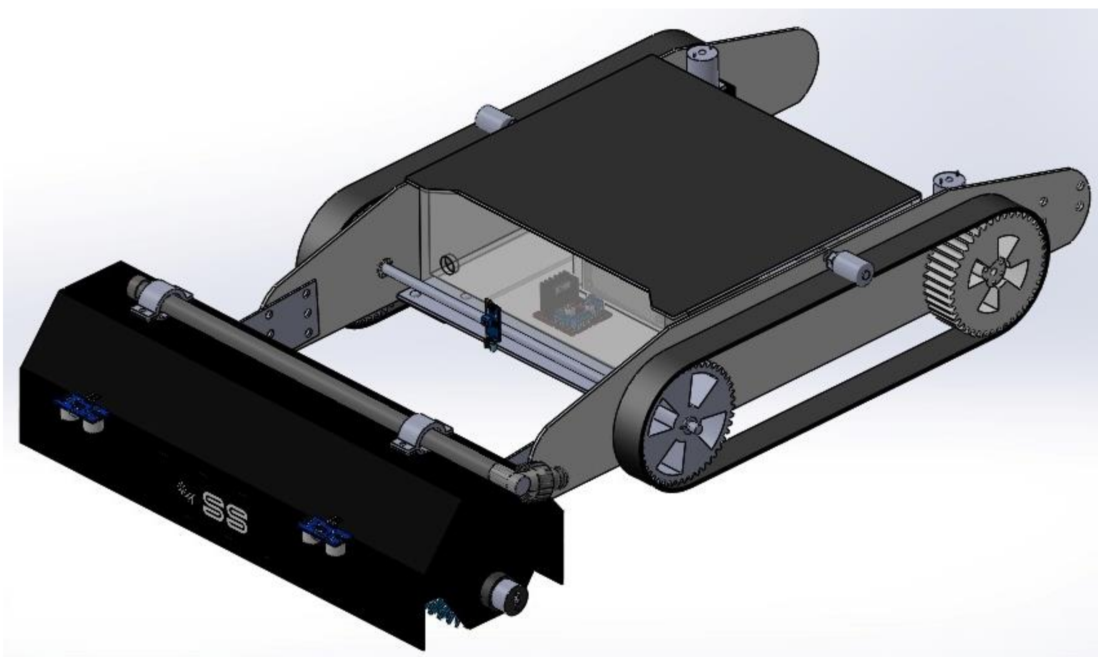

Figure 17. Selected Design

3.2.1 Mechanical Subsystems

The mechanical parts of the robotic solar panel cleaner would be shown in this section.

Chassis: The chassis is the fundamental component of the robotic solar panel cleaning system which provides structural support to house and integrate various mechanisms and components of the robotic system

Table 5. Decision matrix for chassis material selection.

			Weighing scale 1 → 10		
			Material		
			PLA +	**Aluminum (7075)**	**Steel (4340)**
Priority Scale 1 → 5	**Criteria**	**Rating** ↑~ High ↓~ Low			
3	Cost per Pound ($/lb)	↓	4 4×3=12	8 8×3=24	6 6×3=18
6	Availability	↑	1 9×6=54	5.25 6×6=36	0.9 10×6=60
2	Yield Strength (MPa)	↑	26 1×2=2	200 7×2=14	470 10×2=20
5	Durability	↑	1 1×5=5	10 10×5=50	7 7×5=35
4	Density (g/cm^3)	↓	1.24 10×4=40	2.81 8×4=32	7.85 2×4=8
1	Tensile Strength (MPa)	↑	37 1×1=1	230 6×1=6	745 10×1=10
Total			114	162	151

From the above analysis, Aluminum is the suitable material that would be selected for the chassis of the robotic solar panel cleaner based on the specified criteria. Aluminum makes a good balance between cost, availability, strength and density making it a good choice for building a robotic solar panel cleaner.

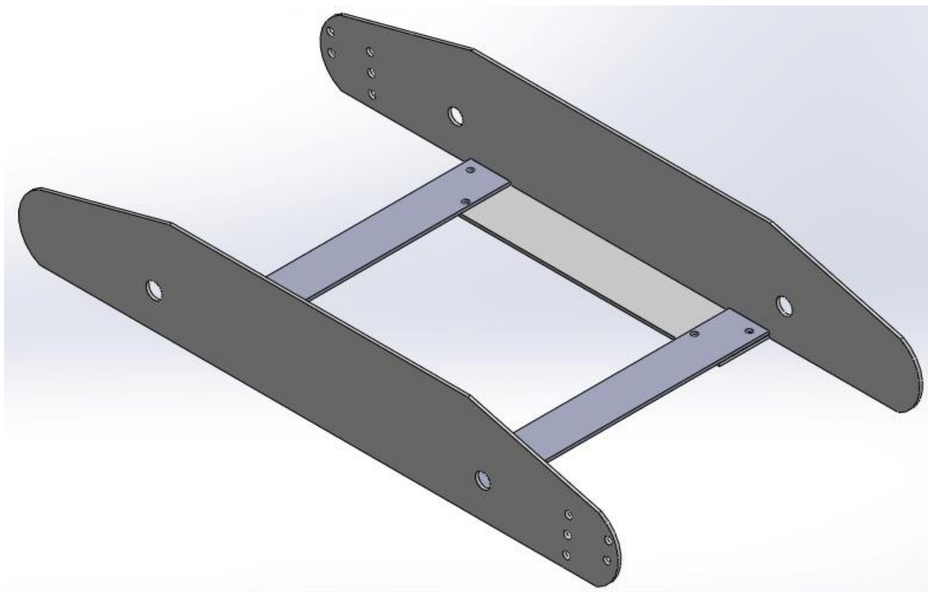

Figure 18.Chassis

Box: The box compartment of the robotic solar panel cleaner is the central part of the robot where the electrical components are placed. These components allow the robot to navigate around the solar panel, detect and avoid obstacles, and perform the cleaning tasks. The box of the robotic solar panel cleaner typically contains a power source, such as a battery, which provides the energy needed to run the robot. It would also include a microcontroller and other control components for operating the robotic system.

Table 6. Decision matrix for box material selection.

			Weighing scale 1 → 10			
			Material			
			PLA+	**Aluminum (7075)**	**Steel (4340)**	**Plexiglass**
Priority Scale 1 → 5	**Criteria**	**Rating** ↑~ High ↓~ Low				
3	Availability	↑	4 4×3=12	8 8×3=24	6 6×3=18	8 8×3=24
6	Cost per Pound ($/lb)	↓	1 7×6=42	5.25 3×6=18	0.9 8×6=48	0.7 10×6=60
5	Durability	↑	1 1×5=5	9 9×5=45	7 7×5=35	8 8×5=40
4	Density (g/cm^3)	↓	1.24 9×4=40	2.81 8×4=32	7.85 1×4=4	1.18 10×4=40
1	Tensile Strength (MPa)	↑	37 1×1=1	230 6×1=6	745 10×1=10	83.4 2×1=4
Total			96	125	115	168

From the above analysis, Plexiglass is the suitable material selected for the box of the robotic solar panel cleaner based on the specified criteria as it offers a good balance between cost, availability, strength and density making it a good choice.

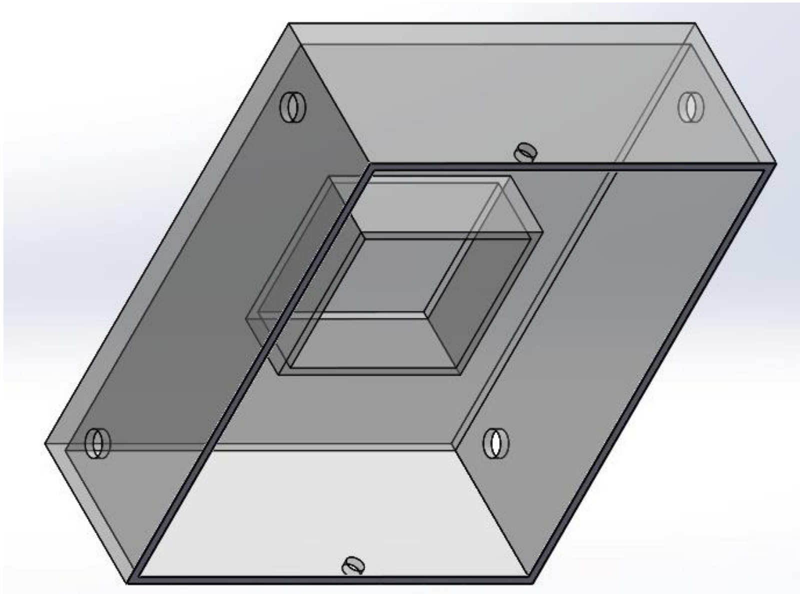

Figure 19. Box

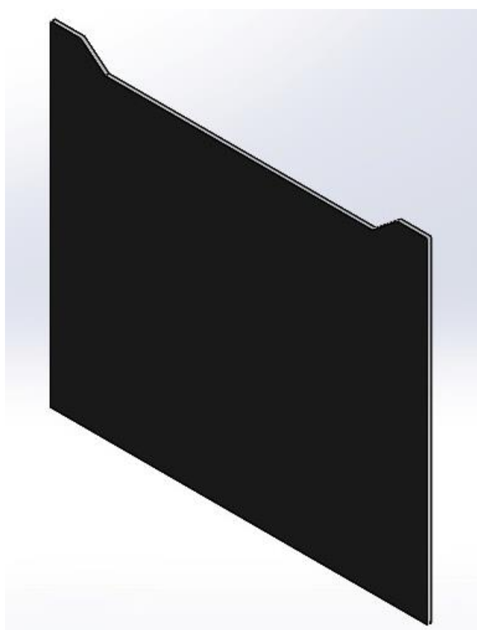

Figure 20. Box Cover

Gear Wheels: The wheels enable mobility and maneuverability of the robotic system. These wheels are specifically designed to facilitate efficient movement across various surfaces, including the solar panels themselves.

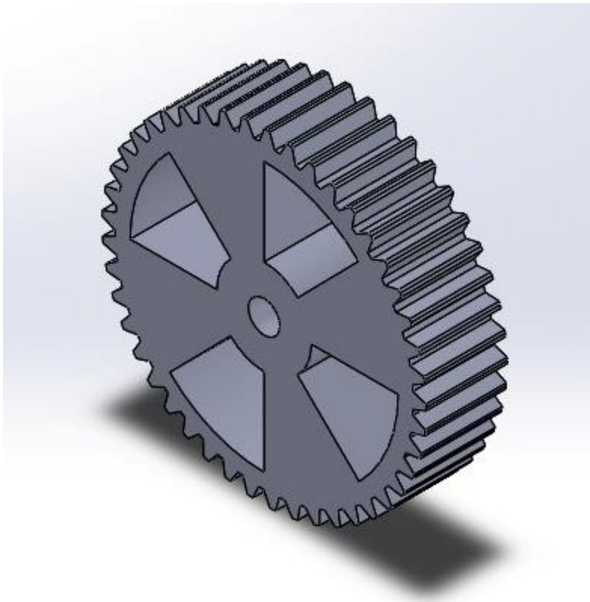

Figure 21. Front Gear Wheel

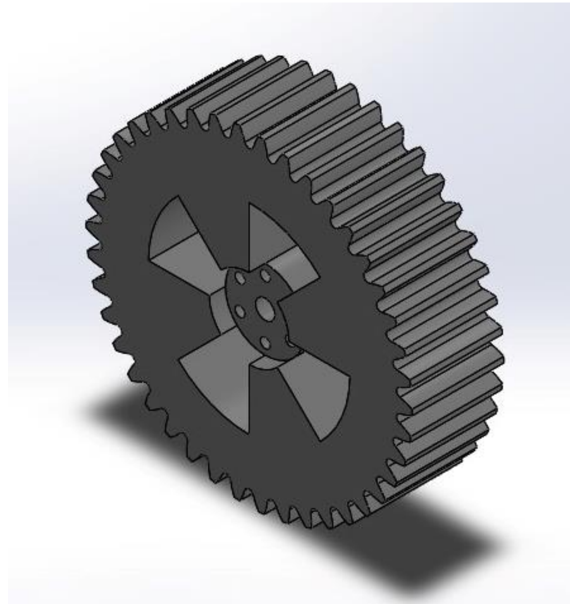

Figure 22. Rear Gear Wheel

Wheel Hub: The wheel hub is the component used to connect the gear wheels to the motor. It provides a firm connection between the wheel and the motor shaft and is held in place with M3 screws fitted by an Allen key.

Figure 23. Wheel hub

("Botland: Aluminum Mounting Hub", n.d.)

Wheel Shaft: The wheel shaft supports the wheels and serves as the axis on which the front wheels are mounted. It is mounted along with bearings to allow the wheel to rotate freely enabling the robot to move efficiently across various surfaces. Cotton pins are attached to the shaft to secure the wheels in place.

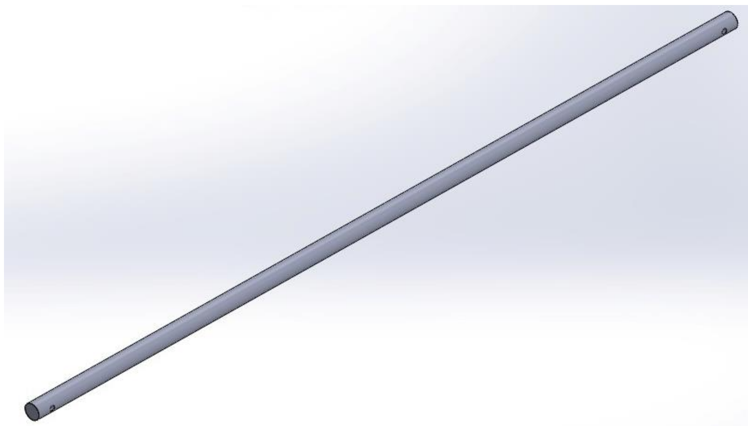

Figure 24. Wheel Shaft

Figure 25. Bearings

Figure 26. Cotton Pin

Timing Belts: Belts are used for the locomotion of the robotic system. They work in conjunction with the gear wheels and motors to transmit rotational motion and facilitate efficient movement of the solar panel cleaning system.

Table 7. Decision matrix for timing belts

			Weighing scale 1 → 10			
			Material			
			Cotton	**Polyamide (Nylon)**	**Polyester (Rubber)**	**Steel**
Priority Scale 1 → 5	**Criteria**	**Rating** ↑~ High ↓~ Low				
4	Density (g/cm^3)	↓	1.55 8×4=32	1.14 10×4=40	1.38 9×4=36	7.85 1×4=4
5	Cost per Pound ($/lb)	↓	0.86 10×5=50	1.65 6×5=30	1 8×5=40	0.9 9×5=45
1	Ease of Manufacturing	↑	4×1= 4	6×1=6	7×1=7	9×1=9
3	Availability	↑	4×3=12	8×3=24	10×3=30	7×3=21
2	Tensile strength (MPa)	↑	410 5×2=10	90 2×2=4	90 2×2=4	841 10×2=20
Total			108	104	117	99

Rubber is the selected material for the time belt based on the specified criteria. The timing belt is typically made of a durable and wear-resistant material which allows it to withstand the forces of continuous operation without breaking or wearing out. The belts have tooth profiles and the gear wheels are designed to fit well with belts for a synchronized movement between the two parts. The wheel is connected to the motor which provides the rotational force needed to move the belt. As the motor shaft turns, the wheels and timing belt moves transmitting motion from the motor to the robot.

Figure 27. Timing Belt

(“Tara Textile Spares: Rubber Timing Belt”, n.d.)

Tension Pulley: The tensioner pulley is a component of the robotic solar panel cleaning system used to ensure proper tension and alignment of the belts with the gear wheels. The pulley maintains optimal tension on the belts. The tensioner pulley helps to optimize the traction and grip of the wheels on the surface of the solar panels.

Figure 28. Tension Pulley

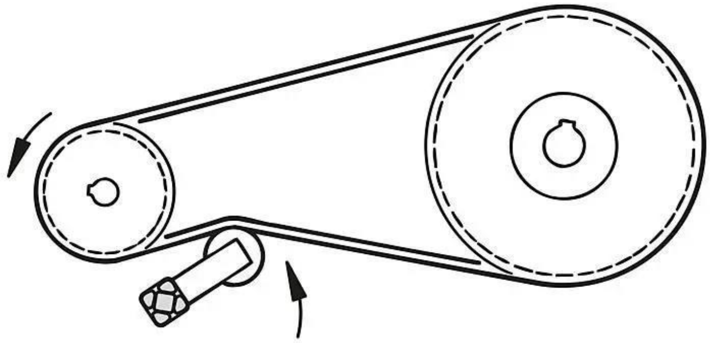

Figure 29. Illustration of belt tensioning

(“Norelem:Tension pulleys”, 2023)

Brushes: The brushes of the robotic solar panel cleaner are used to sweep away dirt, dust, and other contaminants from the surface of the solar panels. These contaminants can accumulate on the solar panels over time and reduce their efficiency and effectiveness by blocking sunlight from reaching the photovoltaic cells. By removing these contaminants, the brushes help to maintain the performance and efficiency of the solar panels. The brushes on the robotic solar panel cleaner are powered by a motor and are mounted on a rotating mechanism that allows them to move across the surface of the solar panels.

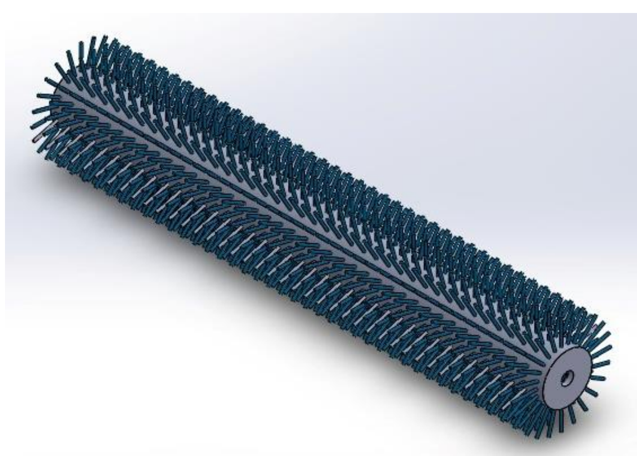

Figure 30. Brush

Table 8. Decision matrix for brushes

		Types		
		Roller rotating brush	**Rotating dual disc brush**	**Drill brush**
Weight **1→ Worst** **10→ Best**	**Rating** ↑~ High ↓~ Low			
Cost	↓	10	5	7
Flexibility	↑	9	10	5
Stability	↑	8	10	6
Weight	↓	10	4	9
Reliability	↑	7	6	3
Total		44	34	30

From the decision matrix, roller brushes would be used for the cleaning mechanism of the robot.

Brush case: The brush casing for the robotic solar panel cleaner is a protective cover that surrounds the brushes and helps to keep them in place. The brush casing serves several important functions, including protecting the brushes, containing the brushes, and providing structural support for the cleaning mechanism. The brush case is attached to the chassis using brackets.

Table 9. Decision matrix for brush case material selection.

			Weighing scale 1 → 10			
			Material			
			PLA+	**Aluminum (7075)**	**Steel (4340)**	**Plexiglass**
Priority Scale 1 → 5	**Criteria**	**Rating** ↑~ High ↓~ Low		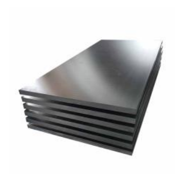		
3	Availability	↑	4 4×3=12	8 8×3=24	6 6×3=18	8 8×3=24
6	Cost per Pound ($/lb)	↓	1 7×6=42	5.25 3×6=18	0.9 8×6=48	0.7 10×6=60
5	Durability	↑	1 1×5=5	9 9×5=45	7 7×5=35	8 8×5=40
4	Density (g/cm^3)	↓	1.24 9×4=40	2.81 8×4=32	7.85 1×4=4	1.18 10×4=40
1	Tensile Strength (MPa)	↑	37 1×1=1	230 6×1=6	745 10×1=10	83.4 2×1=4
Total			96	125	115	168

From the decision matrix, the brush case would be made from plexiglass.

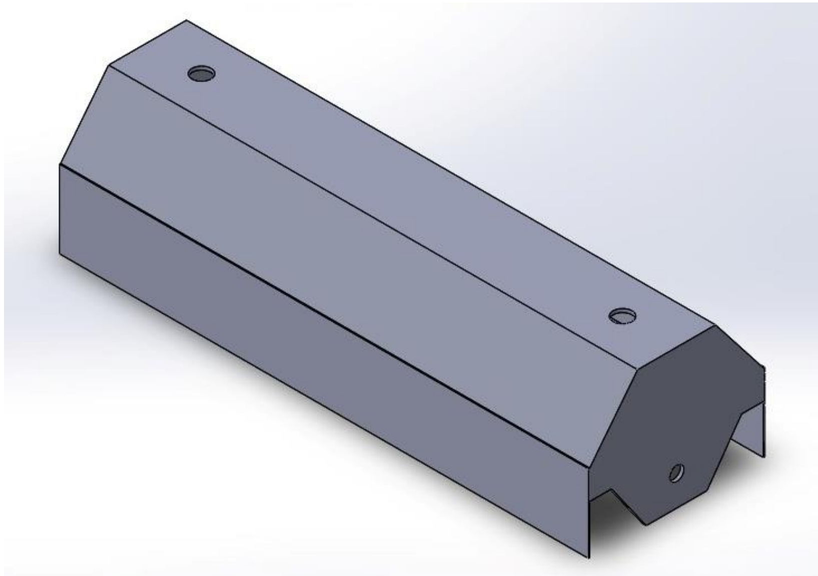

Figure 31. Brush case

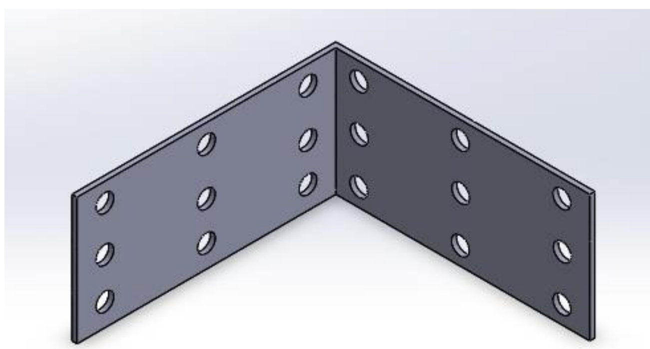

Figure 32. Bracket

Hose: The hose or pipe serves as a channel for the flow of water or cleaning fluid for the cleaning operation of the robotic system. It transports the cleaning fluid from the source to the cleaning mechanism. Rubber hoses would be used for the water cleaning mechanism.

Figure 33. Rubber Hose

("The Home Depot: Worth Garden", n.d.)

Nozzles: The nozzles are essential components that facilitate the efficient spraying of water onto the solar panel for the cleaning operation. The nozzle features orifices that control the spray pattern and flow rate. They can provide a wide-angle spray for broad coverage or a focused jet for targeted cleaning. The nozzles are typically connected to a water supply system through hoses or pipes. It utilizes threaded fittings for secure and leak-free connection ensuring efficient and consistent water delivery during the cleaning operation.

Figure 34. Nozzles

("Lechler Inc: Flat Fan Nozzles", n.d.)

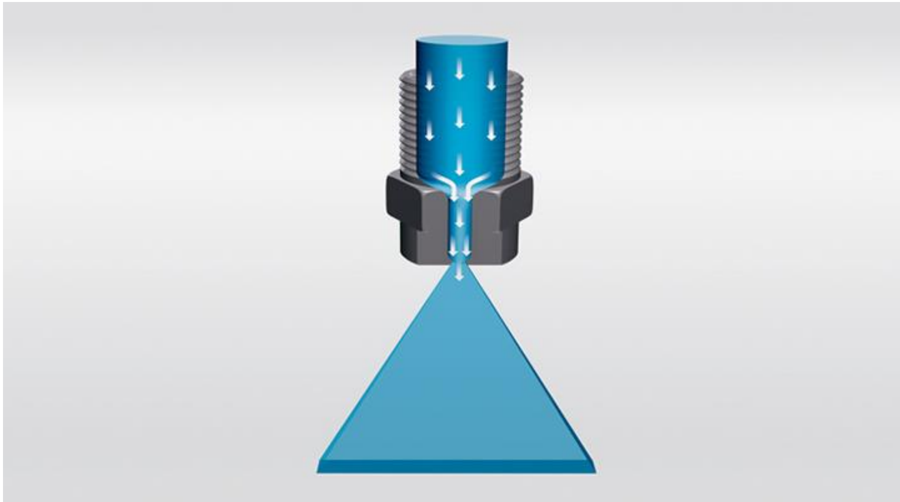

Figure 35. Water Spraying Pattern

(“Lechler Inc: Flat Fan Nozzles”, n.d.)

3.2.2 Electrical subsystems

Note: Technical specifications of the electrical components are provided in the appendix

Motors: The robotic solar panel cleaner would use motors to aid the movement and cleaning mechanism of the system. The motors are one of the key electrical components for the robotic system that provide the necessary power and motion to drive the robot’s movement and cleaning mechanisms. The motors are designed to deliver adequate torque and speed for efficient movement and cleaning operations. They are equipped with gearboxes to optimize the torque output and ensure smooth and precise movement of the robot. The motors are controlled and managed by the solar robot’s system which sends signals and commands to regulate their speed, direction, and operation. This enables the robot to navigate the solar panels with accuracy and execute cleaning maneuvers with precision.

A decision matrix would be done to aid in selecting a suitable motor for the robot.

Table 10. Decision matrix for motors

			Weighing scale 1 → 10		
			Types		
			Stepper Motor	**Servo Motor**	**DC Motor**
Priority Scale 1 → 5	**Criteria**	**Rating** ↑~ High ↓~ Low			
4	Cost	↓	7	6	10
5	Torque	↑	7	6	10
3	Speed	↑	7	9	8
5	Control	↑	9	8	7
2	Size	↓	7	8	7
Total			143	137	163

Based on the decision matrix for motors, DC motors are suitable motors to implement in the development of the robotic solar panel cleaner. DC motors incorporate a good balance between the stated criteria which makes it a good motor choice. The DC motors convert electrical energy into mechanical motion which allows the robot to move across the solar panel and perform cleaning tasks.

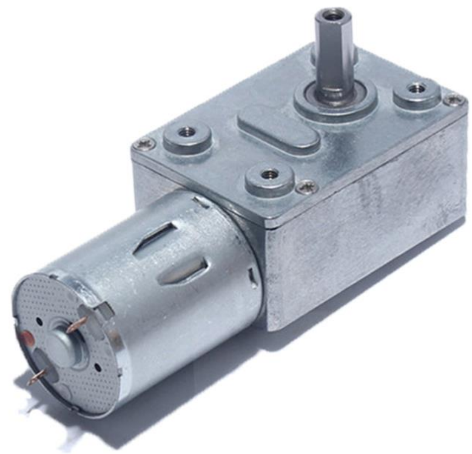

Figure 36. Motor

(“Alibaba: DC Motors”, n.d.)

Motor Driver: The motor driver manages the operation of the motors used in the movement of the robot. It acts as an interface between the robot’s control system and the motors to enable control and coordination of speed, direction and torque for the robotic system.

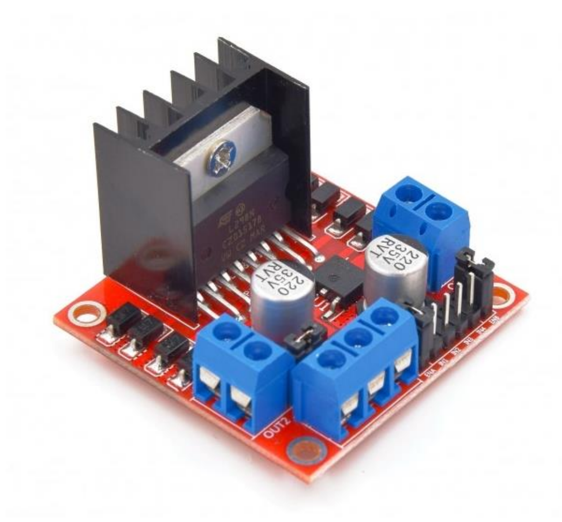

Figure 37. Motor Driver

(“Smart Prototyping: Dual H-Bridge Motor Driver”, n.d.)

Microcontroller: The microcontroller is a small, self-contained computer that is used to control the robot system. It typically has a CPU, memory, and input/output (I/O) peripherals and is programmed to perform a specific task. The microcontroller is the brain of the robotic solar panel cleaner, responsible for controlling all of the other components and making decisions based on received input.

Table 11. Decision matrix for Arduino.

			Weighing scale 1 → 10		
			Types		
			Arduino Uno	**Arduino Mega 2560**	**Arduino Micro**
Priority Scale 1 → 5	**Criteria**	**Rating** ↑~ High ↓~ Low			
5	Price ($)	↓	10	5	1
4	Dimension (Inches)	↓	10	7	4
4	Clock speed (MHz)	↑	3	7	9
3	Digital I/O pins	↑	6	8	10
Total			29	27	23

From the decision matrix based on the highlighted criteria, Arduino Uno would be the microcontroller used in the design and development of the robotic solar panel cleaner.

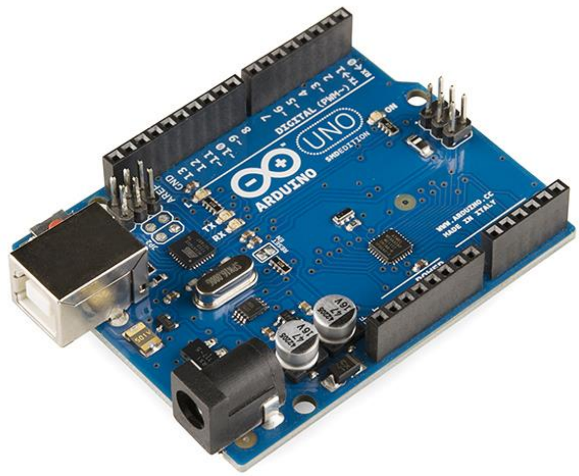

Figure 38. Arduino Uno

("Solarduino: Infrared (IR) Sensor Module with Arduino", 2020)

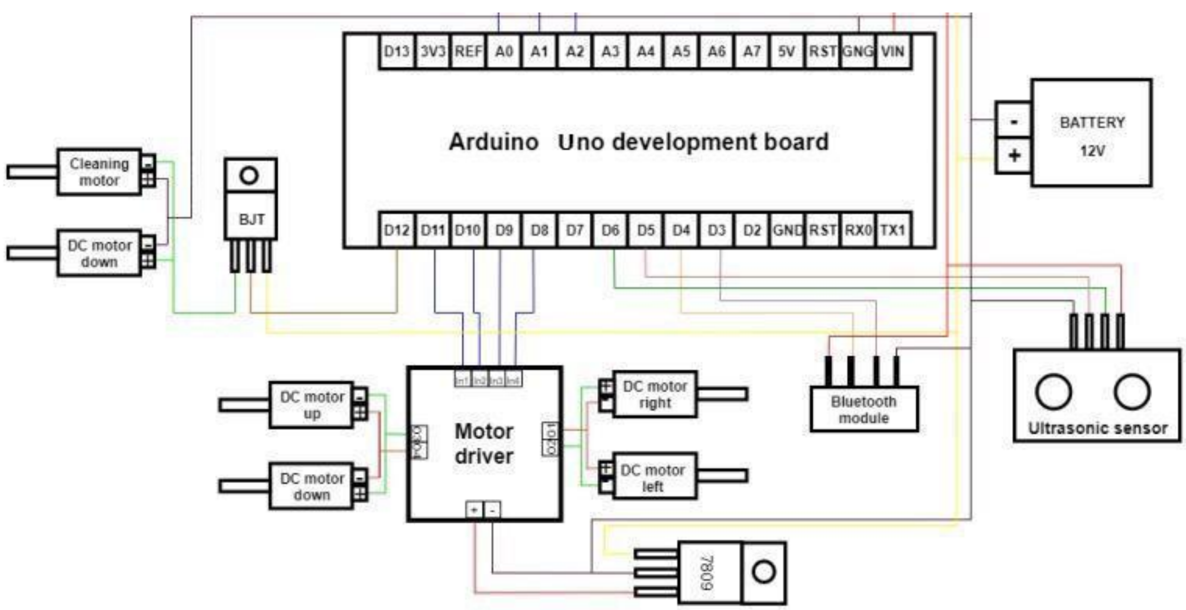

Figure 39. Arduino Uno development board.

Battery: The battery is the main power source for robotic solar panel cleaners because they allow the robot to operate independently and do not require a connection to an electrical grid. The battery stores electrical energy in the form of chemical reactions, which can be converted back into electricity as needed to power the motors and other components of the robotic cleaner. In addition to providing power for the motors, the battery in the robotic solar panel cleaner is used to power other components of the device, such as sensors, control circuits, and communication systems. It is important to choose a battery that can meet the power demands of the cleaner and has a long enough lifespan to make the device practical and cost-effective to use.

Table 12. Decision matrix for battery

		Lithium Battery	**Lead Acid Battery**
Weight **1→ 5**	**Rating** ↑~ High ↓~ Low		
Cost	↓	5	3
Material Weight	↓	3	1
Robustness	↑	3	2
Performance	↑	3	2
Charging	↑	4	3
Total		18	11

From the decision matrix, a lithium battery would be used to power the robotic solar panel cleaners.

Ultrasonic Sensor: The ultrasonic sensor enables precise and accurate detection of the solar panel's surface and surrounding environment. The sensor emits high-frequency sound waves and measures the time it takes for the waves to bounce back after hitting an object allowing for precise distance calculation for proper navigation of the robotic system. The ultrasonic sensor used for the robotic solar panel cleaner is the HC-SR04. The 4-pin HC-SR04 ultrasonic sensor module has the following pin names: V_{cc}, Trigger, Echo, and Ground. An ultrasonic wave is transmitted by an ultrasonic transmitter.

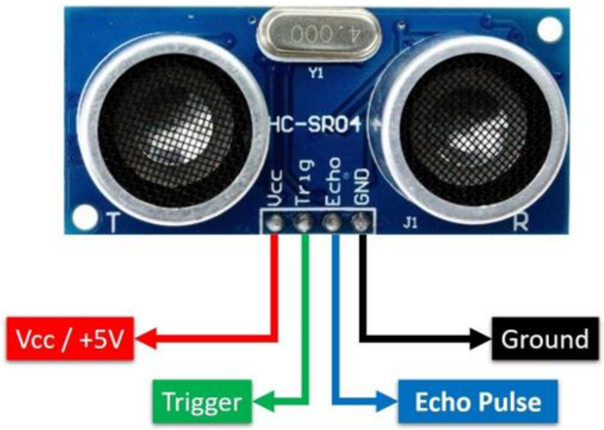

Figure 40. Pin labelling of Ultrasonic sensor

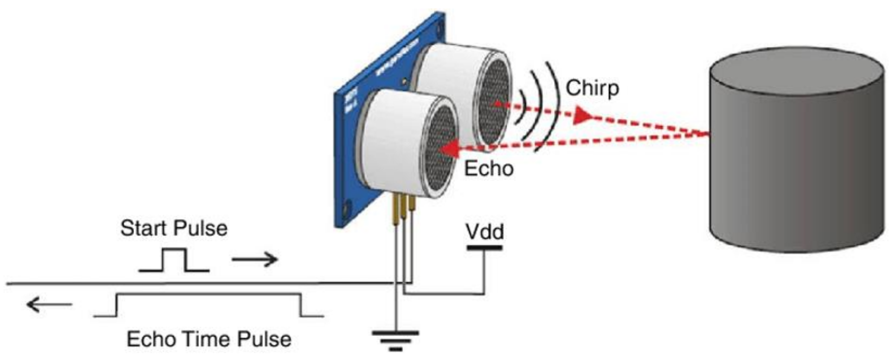

Figure 41. Working principle of ultrasonic sensor

IR Sensor: The IR(Infrared) sensor enables the detection/monitoring of objects or surfaces based on infrared radiation. The sensor used infrared light to measure distances, detect obstacles, and identify changes in the environment which provides essential feedback for navigation.

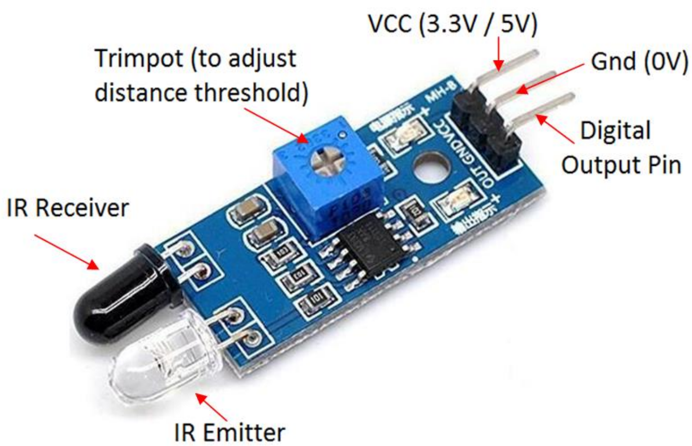

Figure 42. IR Sensor

(“Solarduino: Infrared (IR) Sensor Module with Arduino”, 2020)

Phone/Bluetooth control: The robotic solar panel cleaner would be controlled via phone/Bluetooth control. This can be accomplished using a Bluetooth module that is integrated into the microcontroller board of the robot. By ensuring the phone control is compatible with Bluetooth accessories, it can be connected to the robotic solar panel cleaner by which we can send commands. The Bluetooth module used is the HC-O5 module.

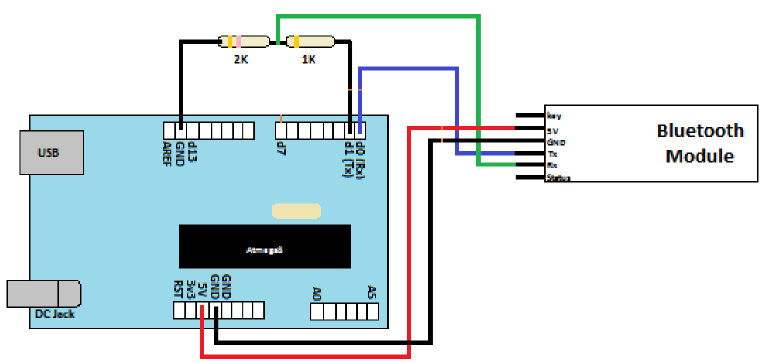

Figure 43. Circuit diagram of Arduino and Bluetooth module interfacing

(“Engineers garage: Android phone control-controlled robot using Arduino”, n.d.)

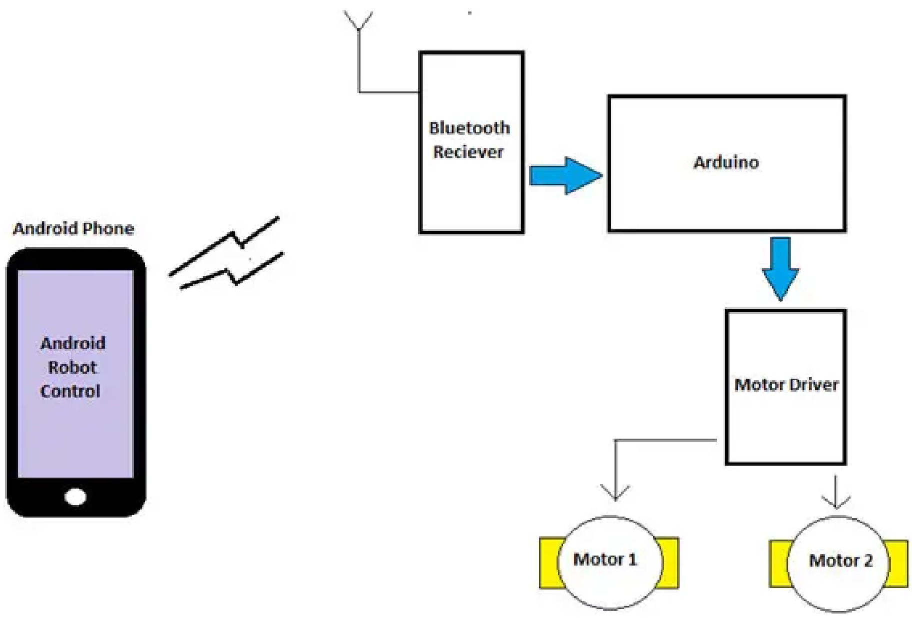

Figure 44. Phone control layout

(“Engineers garage: Android phone control-controlled robot using Arduino”, n.d.)

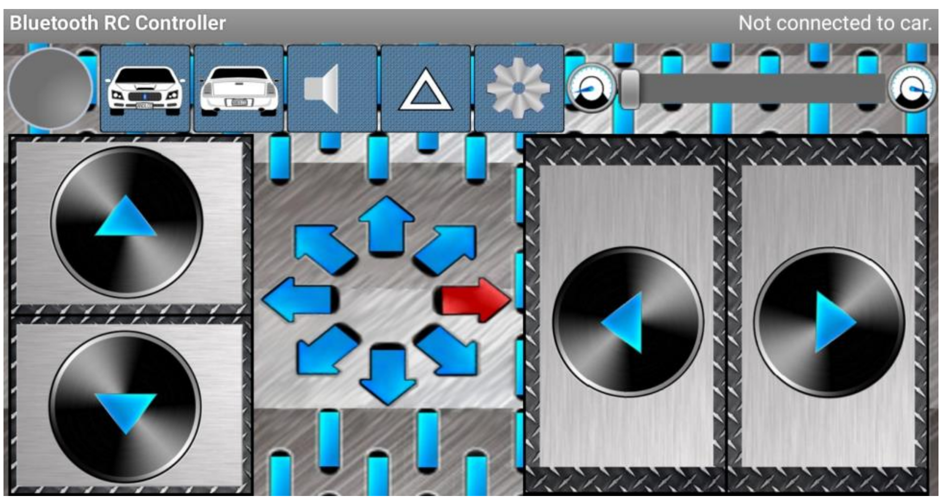

Figure 45. Phone Control Menu

3.2.3 System breakdown structure

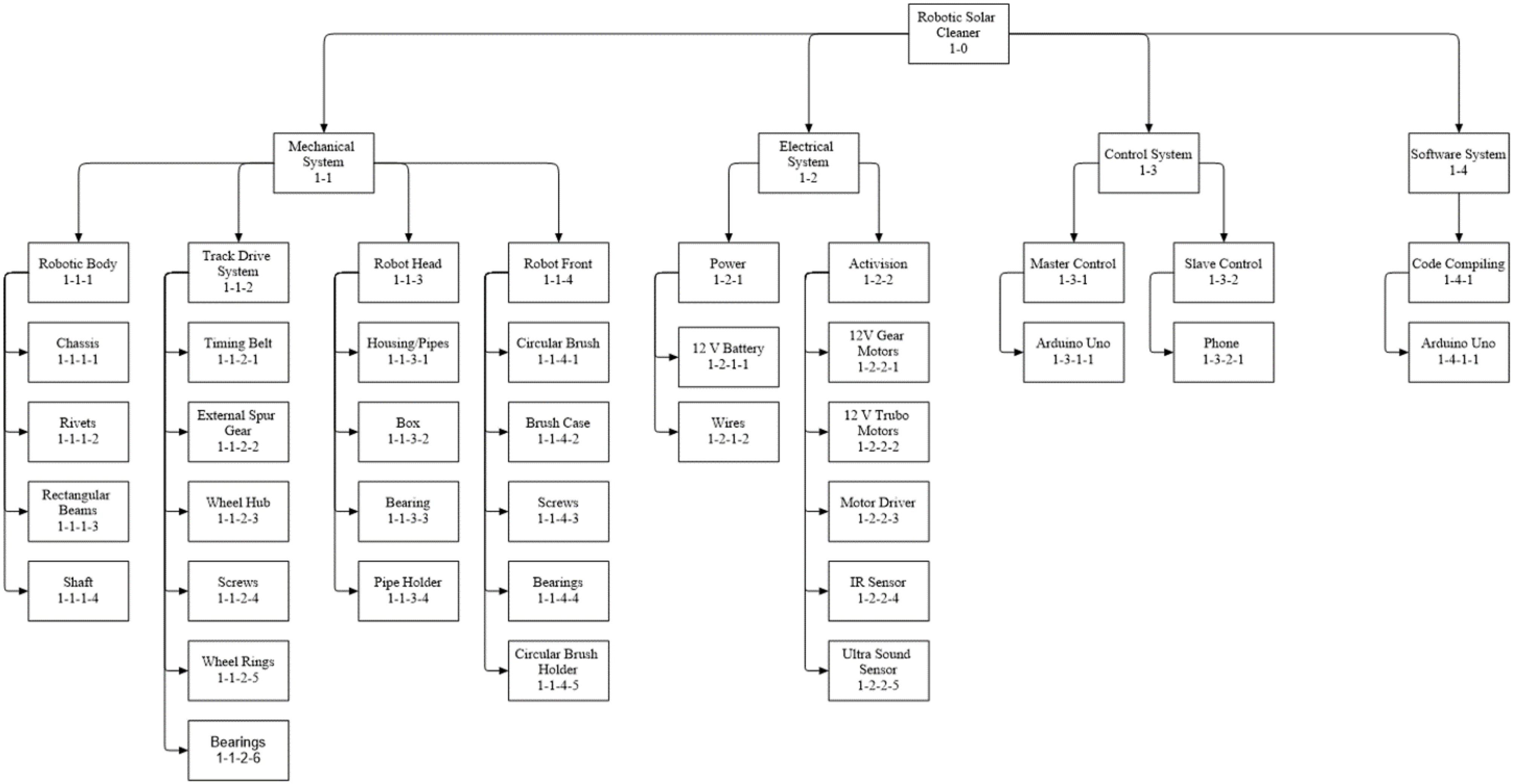

Figure 46. System Breakdown structure

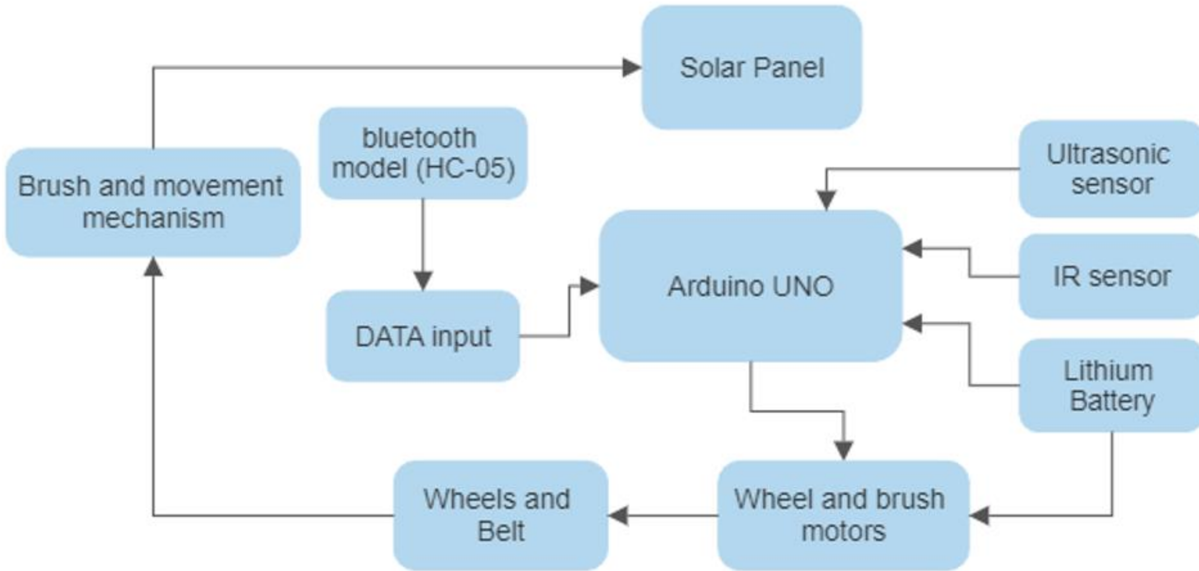

Figure 47. System layout diagram

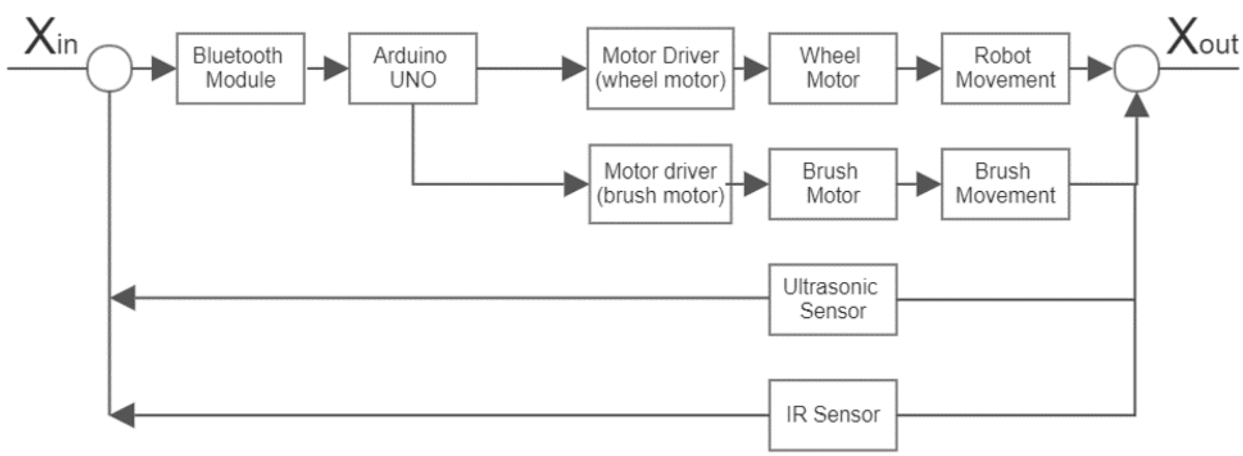

Figure 48. System block diagram

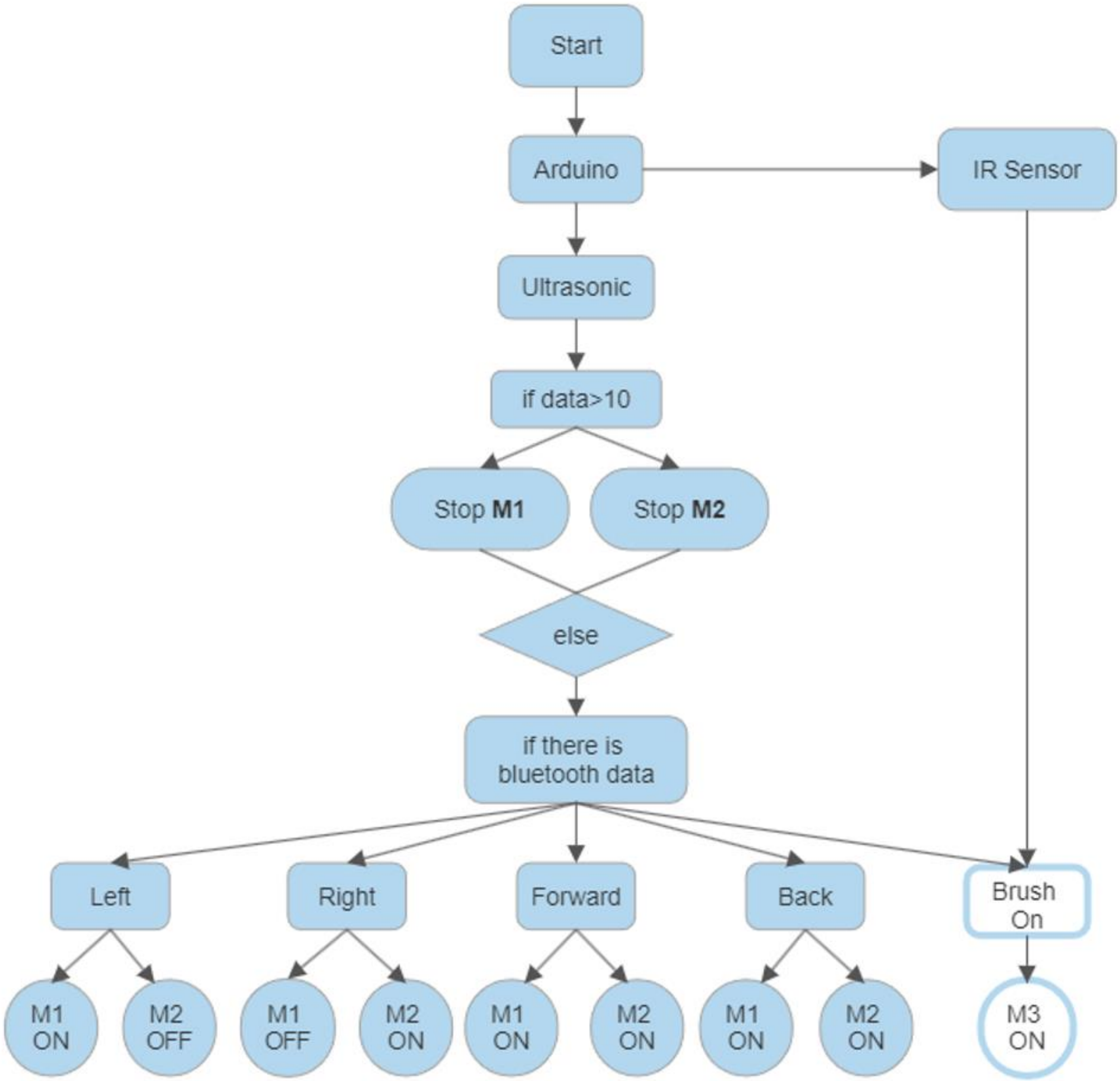

Figure 49. Program flowchart

The connections for the various components of a robotic solar panel cleaner to the Arduino Uno development board is done using a variety of cables and connectors. The DC motors that drive the wheels would be connected to the Arduino using a motor driver circuit. The motor driver circuit takes the digital signals from the Arduino and converts them into the high current signals needed to drive the motors. The motor driver circuit can be connected to the Arduino using a ribbon cable or other suitable connector. The ultrasonic sensor would be connected to the Arduino using a cable or connector that is compatible with one of the Arduino's analog input pins. This allows the Arduino to read the distance measurement from the sensor and use it to detect obstacles and adjust the robot's movement accordingly. The HC-O5 Bluetooth 0module can be connected to the Arduino using a serial communication interface. This can be done using a suitable connector. The Bluetooth module would be used to communicate with the robot wirelessly, enabling remote control and the transmission of sensor data. The battery would be connected to the Arduino using a suitable cable or connector. The battery will provide power to the Arduino and all of the connected components.

3.3 OTHER PROPOSED DESIGNS

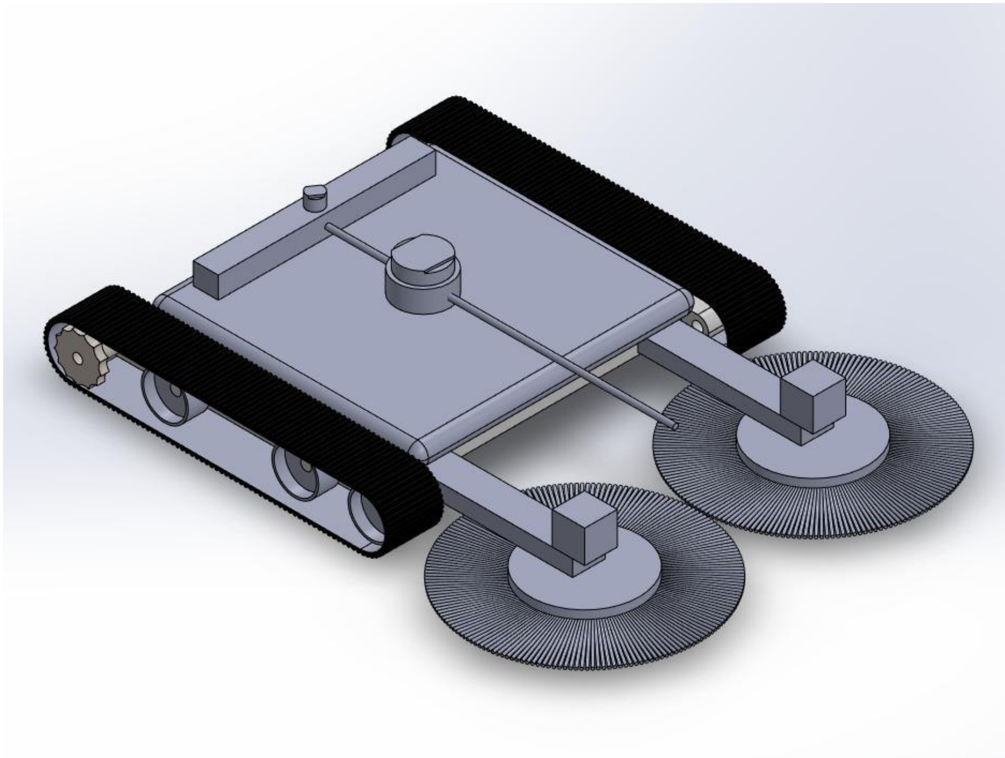

Figure 50. Isometric view of first design

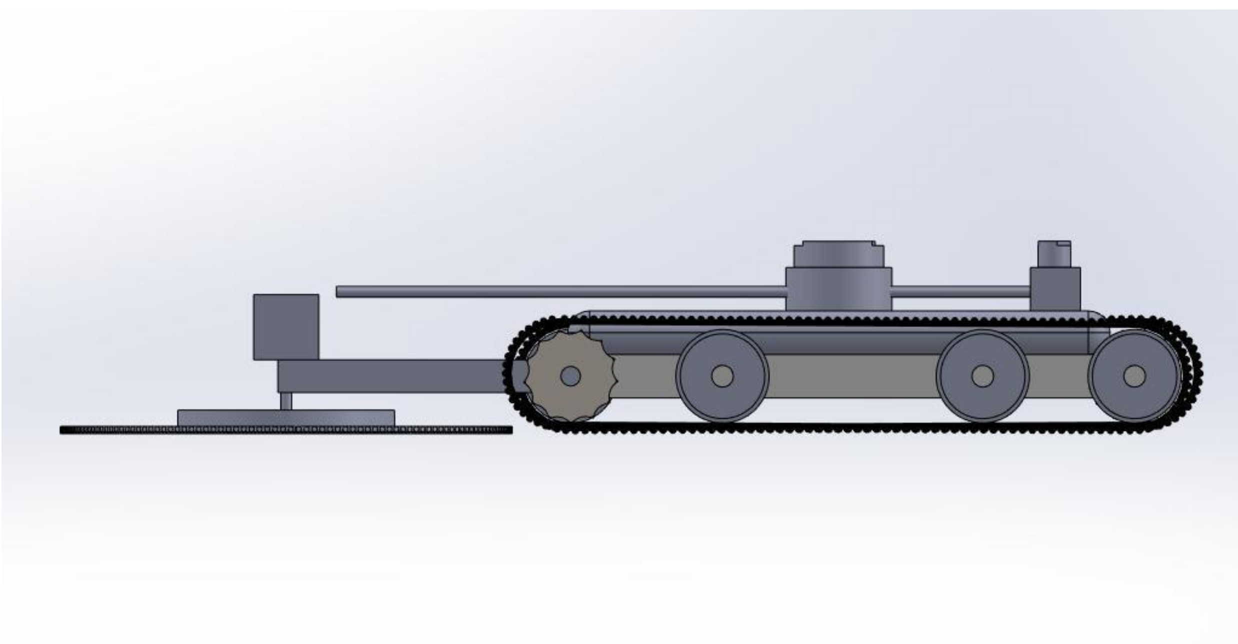

Figure 51. Side view of first design

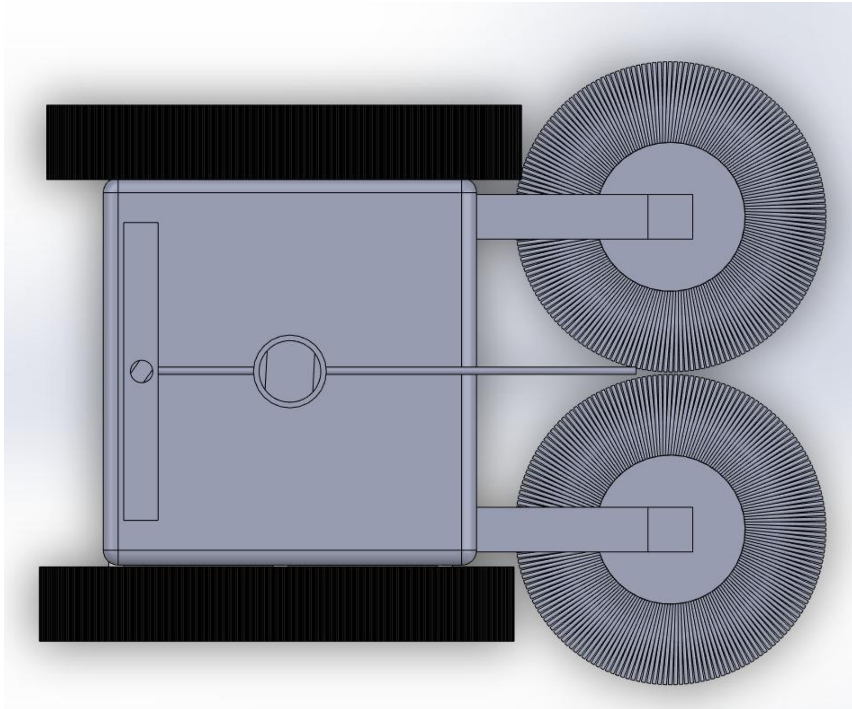

Figure 52. Top view of first design

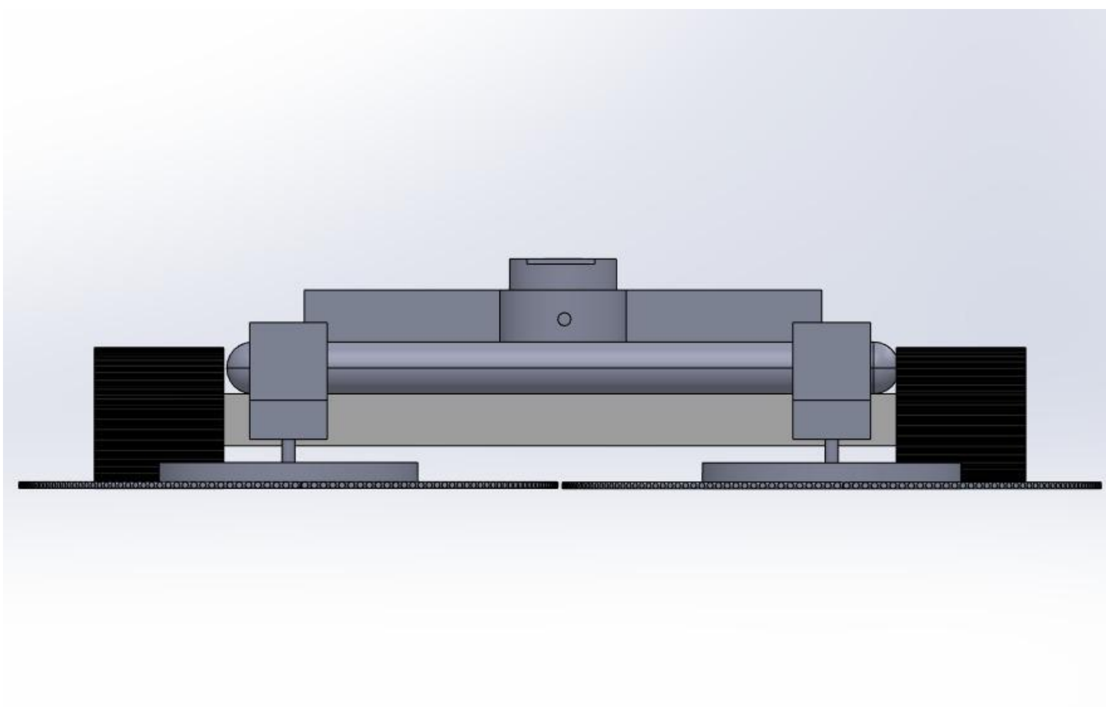

Figure 53. Front view of first design

The description for this design has been explained in section 3.1.1 of this chapter. Refer to the stated section for the description of this robotic system.

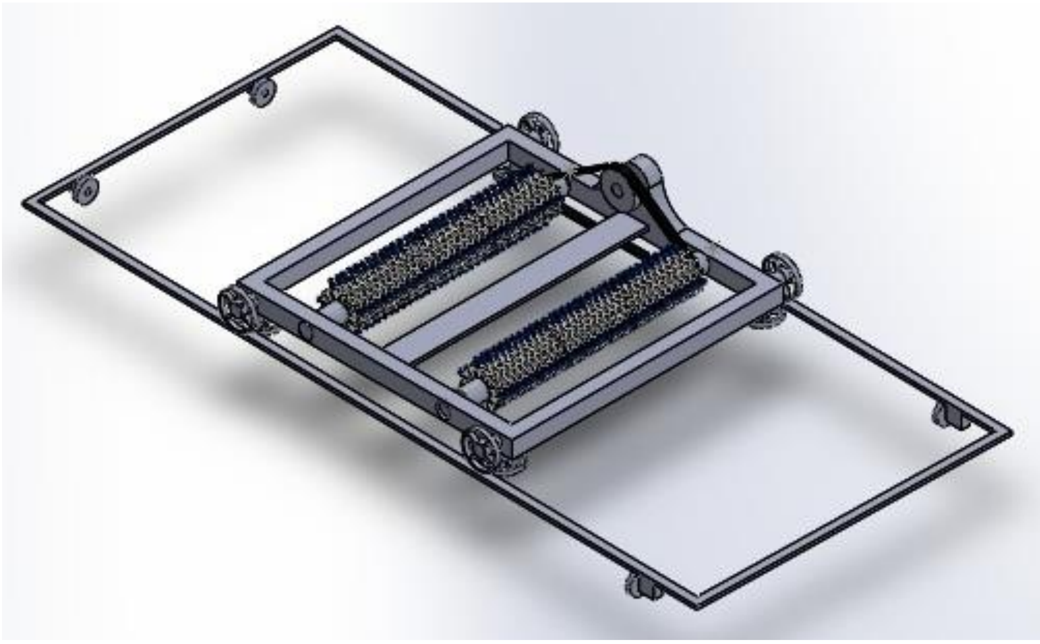

Figure 54. Proposed third design

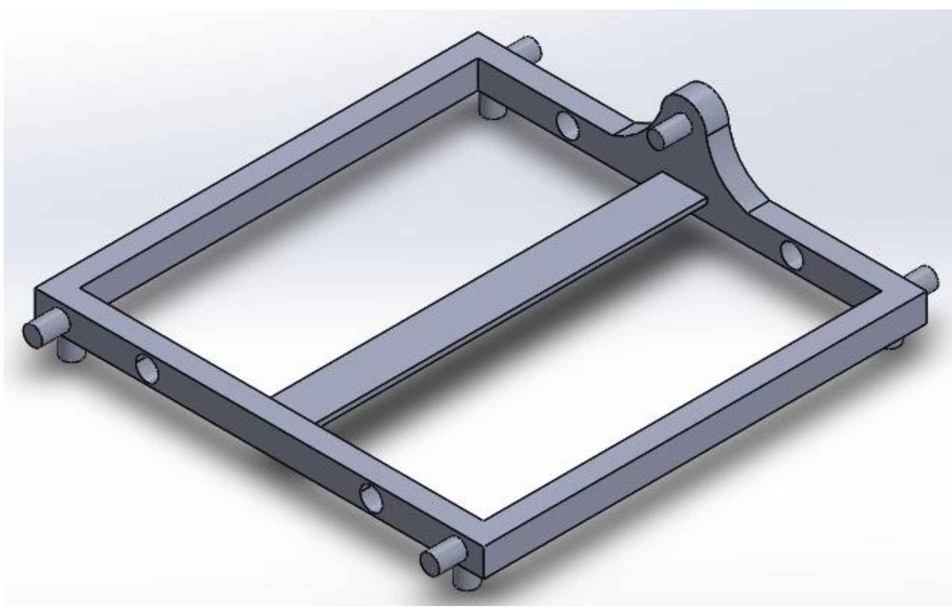

Figure 55. Frame structure of third design

The description for this design has been explained in section 3.1.1 of this chapter. Refer to the stated section for the description of this robotic system.

3.4. ENGINEERING STANDARDS

ELECTRICAL SUBSYSTEM

The engineering standards should be met by the electrical subsystem of the robotic cleaner such as the motors, circuit board, controller and sensors to ensure safety, reliability and ensure consistency. There are several engineering standards that apply to the electrical subsystem, depending on the components or part of the robotic cleaner. Some of the key standards are considered include:

Table 13. Engineering Standards for the Electrical Subsystem

STANDARD	**DEFINITION**
IEEE 802.15.4	This standard specifies the physical and media access control layers for low-rate wireless personal area networks (LR-WPANs). It is often used in robotic systems to enable wireless communication between the robot and other devices, such as sensors and controllers.
IEC 61131-3	This standard specifies the programming languages, programming systems, and user interfaces for programmable controllers. It is widely used in robotic systems to enable the control and automation of the robot's movements and functions.
ISO 10218	This standard specifies the safety requirements for industrial robots and robot systems. It covers the design, construction, installation, operation, and maintenance of robots and robot systems, with the aim of ensuring the safety of human workers and other people who may come into contact with the robot.

ISO/TS 15066	This standard specifies the safety requirements for collaborative robots, which are robots that are designed to work safely alongside humans in a shared workspace. It covers the design, construction, installation, operation, and maintenance of collaborative robots, with the aim of ensuring the safety of human workers and other people who may come into contact with the robot.
IEC 62443	This standard specifies the security requirements for industrial control systems, including robotic systems. It covers the design, construction, installation, operation, and maintenance of these systems, with the aim of ensuring their security against cyber threats.
ISO 9283	This standard specifies the performance evaluation of servo drives for electric traction drives. It is often used in robotic systems to ensure the accuracy and reliability of the robot's movements.
IEC 60909	This standard specifies the methods for the calculation of short-circuit currents in three-phase a.c. systems. It is often used in robotic systems to ensure the safety and reliability of the electrical subsystem, especially in cases where the robot is required to operate at high current levels.

MECHANICAL SUBSYSTEM

There are several engineering standards that are commonly used for the mechanical subsystem of robotic systems, including robotic solar cleaners. These standards provide guidelines and requirements for the design, construction, testing, and operation of mechanical components, such as gears, bearings, wheels, and mechanical connections. Some of the key engineering standards for the mechanical subsystem of robotic systems are listed below:

Table 14. Engineering Standards for the Mechanical Subsystem

STANDARD	**DEFINITION**
ISO 5593	This standard specifies the general requirements for the design and construction of gears and gearboxes. It covers the materials, dimensions, tolerances, and performance requirements of gears and gearboxes, and is relevant to the mechanical subsystem of a robotic solar cleaner that uses gears to transmit power and motion.
ISO 15243	This standard specifies the methods for the determination of the load capacity of rolling bearings. It is relevant to the mechanical subsystem of a robotic solar cleaner that uses bearings to support and guide the movement of rotating components, such as wheels and gears.
ISO 4672	This standard specifies the general requirements for the materials, dimensions, and tolerances of wheels and castors. It is relevant to the mechanical subsystem of a robotic solar cleaner that uses wheels or castors to move the robot over different surfaces.

ISO 898-1	This standard specifies the mechanical and physical properties of fasteners made of carbon steel and alloy steel. It is relevant to the mechanical subsystem of a robotic solar cleaner that uses bolts, screws, and other fasteners to connect and secure mechanical components.
ISO 12240-1	This standard specifies the general requirements for the design, materials, and testing of hydraulic hose assemblies. It is relevant to the mechanical subsystem of a robotic solar cleaner that uses hydraulic systems to power and control its movement.
ISO 965-1	This standard specifies the general requirements for the materials, dimensions, and tolerances of thread gauges. It is relevant to the mechanical subsystem of a robotic solar cleaner that uses threaded fasteners, as it provides guidelines for the measurement and inspection of these fasteners.
ISO 14689	This standard specifies the general requirements for the materials, dimensions, and tolerances of linear guides. It is relevant to the mechanical subsystem of a robotic solar cleaner that uses linear guides to support and guide the movement of mechanical components along a straight path.

3.5. Design Calculations

3.5.1. Force Analysis

The purpose of the calculation is to determine the minimum coefficient of friction required to prevent slipping of a robotic solar panel cleaner on an inclined PV panel. When the solar panel cleaner is operating on a tilted solar panel, there is a risk of it sliding or losing traction due to the gravitational force acting parallel to the surface. To prevent this, the friction between the rubber wheel mechanism and the solar panel surface needs to be sufficient to counteract the component of the gravitational force that tends to cause sliding. By modeling the forces involved and considering the static equilibrium condition, we can derive an inequality that relates the coefficient of friction (μ) to the angle of inclination (θ). The inequality states that the coefficient of friction must be equal to or greater than the tangent of the angle of inclination ($\mu \geq \tan\theta$) to prevent slipping. This calculation helps in determining the minimum requirement for the coefficient of friction to ensure that the robotic solar panel cleaner can effectively move upward on inclined solar panels without slipping, even under extreme operating conditions. It also emphasizes the importance of maintaining a suitable frictional force to avoid damage to the solar panel surface and preserve its integrity.

By understanding the relationship between the coefficient of friction and the angle of inclination or the tilt angle of the solar panel, engineers and designers can optimize the design of the robotic solar panel cleaner, choose appropriate materials, and implement strategies to enhance the frictional grip, ensuring the efficiency and safety of the cleaning operation.

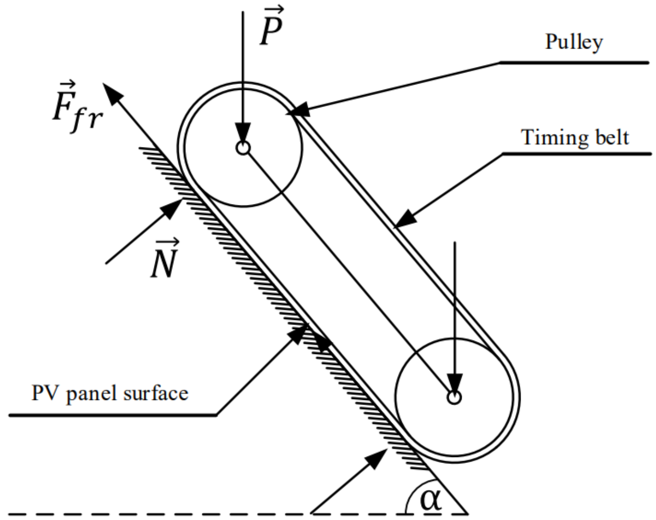

Figure 56. Force analysis in the static equilibrium state

(“Nguyen, M.T: Adhesive coefficient of rubber wheel crawler on wet tilted PV panel,” 2022)

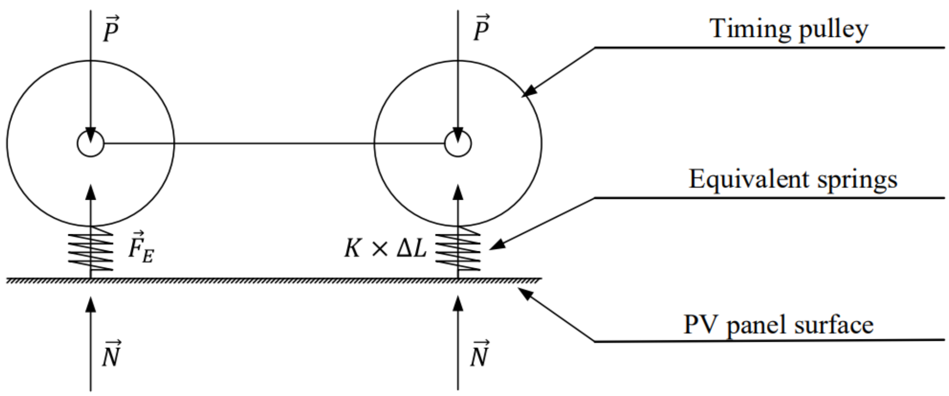

Figure 57. Equivalent model of rubber track mechanism

(“Nguyen, M.T: Adhesive coefficient of rubber wheel crawler on wet tilted PV panel,” 2022)

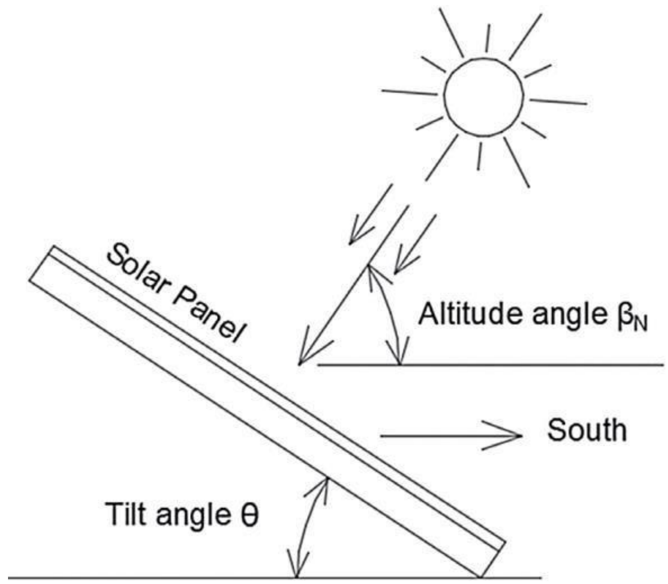

Figure 58. Tilt Angle of a Solar Panel

("Research Gate: South facing solar panel (PV module) with optimum tilt angle", 2017)

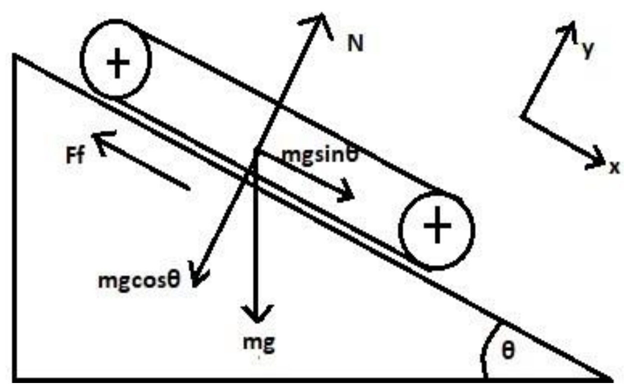

Figure 59. FBD analysis

In this analysis, we assume the following.

- No slippage between the pulley wheels and rubber belt
- Tensions on rubber belt are the same on both sides.
- Slip resistance is not affected by the motion of the brushes.

$\vec{N}$ = reaction force

$\vec{P}$ = gravity

$\vec{F}_{fr}$ = static friction force

mg = mass × gravity → weight

$mgsin\theta$ = horizontal component of weight

$mgcos\theta$ = vertical component of weight

θ = tilt angle of PV panel

$\vec{F}_E$ = elastic force

K = stiffness

ΔL = displacement

Based on the condition of dynamic equilibrium, the minimum static friction coefficient required depends on the slope of the PV array. This condition is proven below for our model with respect to figure.

summation of forces in the y-direction:

$$\sum F_x = 0 \qquad \text{(Equation 1)}$$

$$mgsin\theta - F_f = 0$$

$$mgsin\theta = F_f \qquad \text{(Equation 2)}$$

summation of forces in the x-direction:

$$\sum F_y = 0 \qquad \text{(Equation 3)}$$

$$N - mgcos\theta = 0$$

$$N = mgcos\theta \qquad \text{(Equation 4)}$$

Dividing both expressions

$$\frac{mgsin\theta}{mgcos\theta} = \frac{F_f}{N} = tan\theta \qquad \text{(Equation 5)}$$

$$\frac{F_f}{N} = \mu \qquad \text{(Equation 6)}$$

$$\text{Therefore } \mu = tan\theta \qquad \text{(Equation 7)}$$

The typical tilt angle of solar panels is from 30 to 45 degrees depending on geographical location of the solar panel.

By substituting the angles into equation 7

$\theta = 30°$

$\mu = \tan 30 = 0.58$

$\theta = 45°$

$\mu = \tan 45 = 1$

From this calculation we found that the required coefficient of friction to avoid slippage should be between 0.58 and 1, for angles 30 and 45 degrees. For a dry, clean rubber-on-glass contact, the coefficient of friction typically falls within the range of 0.6 to 1.0. Therefore, we are able to conclude that the robot is able to maneuver on solar panels with tilt angles between 30 and 45 degrees without slippage.

3.5.2. Gear wheel and Timing belt Calculations

To be able to design the gear wheels and timing belt mechanism, it was necessary to calculate the dimensions of the gear wheel which was to be 3D printed. We calculated these dimensions based on the circular pitch of the selected timing belt. The timing belts we selected were chosen based on their circumference and width. The circumference of the belt determined the wheelbase, that is the horizontal distance between the center of the front and rear wheels. We were then able to select the belt that gave a reasonable wheelbase. The width of the belt determined the face width of the gear wheel.

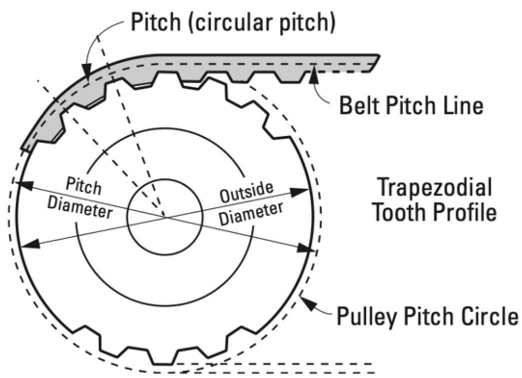

Figure 60. Belt and Wheel Mechanism

("Linear Motion Tips: Pulleys for synchronous belt drive systems", 2020)

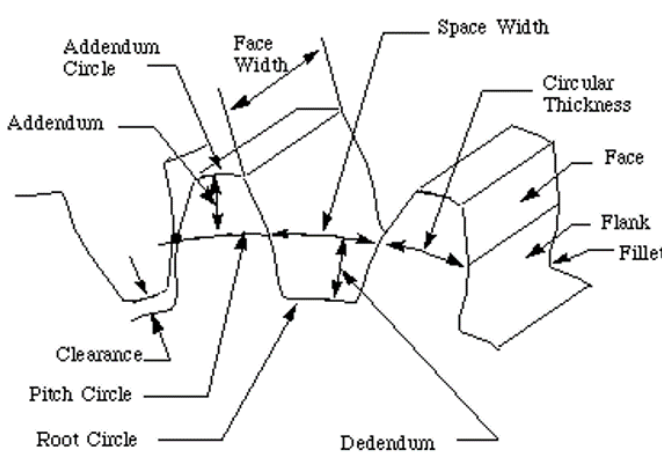

Figure 61. Gear Wheel Label

The dimensions of the gear wheel, that is the module, number of teeth, pitch diameter and outside diameter are shown below.

N.B: the outside diameter was fixed to 104.5 mm.

N.B: standard circular pitch of the timing belt = 7.4613 mm

CP = Circular Pitch, *PD* = Pitch diameter, *M* = Module, *N* = Number of teeth,

OD = Outside diameter

CP = M × 3.1416

$$M = \frac{CP}{3.1416} = \frac{7.4613}{3.1416} = 2.375$$

$$M = 2.375$$

$$OD = (N + 2) \times M \qquad \text{(Equation 8)}$$

$$\frac{OD}{M} = N + 2 \qquad \text{(Equation 9)}$$

$$N = \frac{OD}{M} - 2 \qquad \text{(Equation 10)}$$

$$N = \frac{104.5}{2.375} - 2 = 42$$

$$N = 42$$

$$M = \frac{PD}{N} \qquad \text{(Equation 11)}$$

$$PD = M \times N = 2.375 \times 42 = 99.75\text{mm}$$

$$PD = 99.75\text{mm}$$

3.5.3. Nozzle Volumetric Flow Rate Calculations

We calculated the water flow rate through the nozzles in the brush mechanism to be able to improve the cleaning efficiency of the brush mechanism as well as to ensure effective water usage. If the flow rate is too low, it may not provide enough water to effectively remove dirt and debris from the solar panels. On the other hand, if the flow rate is too high, it may lead to excessive water wastage or even damage to the panels. By optimizing the flow rate, we can ensure efficient cleaning while minimizing water consumption.

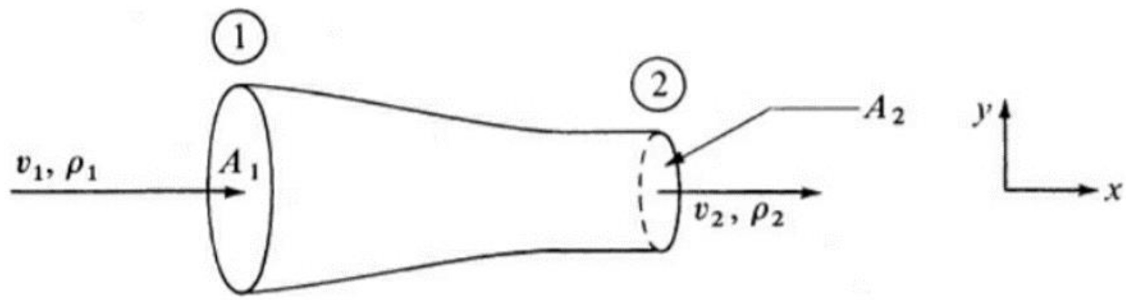

Figure 62. Illustration of water flow through a Nozzle

1. Assumptions:

   - Velocity of water inside the hose is 5m/s
   - The surface tension effects are negligible.
   - Water is assumed to be incompressible, ensuring a constant density throughout the system.
   - The water is assumed to be at a constant temperature, as variations in temperature can affect the fluid properties and flow behavior.
   - The flow calculation assumes ideal nozzle characteristics, neglecting any losses due to friction.

Volumetric Flow Rate Calculation:

Cross-sectional area of the hose and nozzle

A = πr^2 where is the radius of the hose.

The diameter of the hose is 13mm, r = 6.5mm = 0.0065m

A = $\pi(0.0065)^2 = 1.33 \times 10^{-4} m^2$

The diameter of the nozzle is 0.8mm, r = 0.0004m

A = $\pi(0.0004)^2 = 5.026 \times 10^{-7} m^2$

Nozzle Volumetric Flow rate

To calculate the nozzle flow rate, we firstly calculate for the hose flow rate

$$Q_{hose} = V_{hose} \times A_{hose} \qquad \text{(Equation 12)}$$

$$Q_{hose} = 5m/s \times 1.33 \times 10^{-4} m^2 = 6.65 \times 10^{-4} m^3/s$$

We then calculate the nozzle flow rate.

$$Q_{nozzle} = \frac{A_{nozzle}}{A_{hose}} \times Q_{hose} \qquad \text{(Equation 13)}$$

$$\frac{5.026 \times 10^{-7} m^2}{1.33 \times 10^{-4} m^2} \times 6.65 \times 10^{-4} m^3/s = 2.513 \times 10^{-6} m^3/s$$

$$Q_{nozzle} = 2.513 \times 10^{-6} m^3/s = 0.002513\ liters/s\ =\ 2.5ml/s\ per\ nozzle$$

$$Q_{nozzle} = 2.5ml/s \times 2\ nozzles = 5ml/s\ from\ both\ nozzles$$

We are then able to estimate the amount of water the robot uses per unit of time. We can do this by using the formula:

$$\text{Water used} = \text{Volumetric flow rate} \times \text{time} \qquad \text{(Equation 14)}$$

$$\text{Water used} = 5\text{ml/s} \times 60 \text{ seconds} = 300\text{ml}$$

We can therefore conclude that the robot uses 300ml of water for cleaning in one minute of operation.

3.5.4. Cleaning Efficiency Calculations

The efficiency calculation allows us to assess the effectiveness of the robotic solar panel cleaner in improving the power output of the solar panels. Efficiency calculations can also help to establish a maintenance schedule for cleaning the solar panels. By comparing the efficiency of different cleaning methods or technologies, we can also determine which approach yields the maximum power output of the solar panels.

To calculate the efficiency of a robotic solar panel cleaner, we compared the power output of a single PV panel before and after cleaning operation. Factors that could affect the power output such as shading, temperature, and time of day are assumed to remain constant during the comparison.

The efficiency is calculated as the ratio of the power output after the cleaning operation to the power output before the cleaning operation, multiplied by 100.

Below is the formula:

$$Efficiency = \left(\frac{Power\ output\ after\ cleaning}{Power\ output\ before\ cleaning}\right) \times 100\% \qquad \text{(Equation 15)}$$

Assuming a $1.7m^2$ photovoltaic solar panel rated at 330W with a power output of 300 Watts before cleaning and a power output of 320 Watts after cleaning.

$$Efficiency = \frac{320W}{300W} \times 100\% = 106.7\%$$

The estimated efficiency of the robotic solar panel cleaner for a dusty 1m by 1.7m 330W photovoltaic panel is about 107%. This indicates that the cleaning process increased the power output of the solar panel by around 7%.

3.6 COST ANALYSIS

Table 15. Cost Analysis

Items No.	Part Number	Part Name	Amount	Material	Source	Cost
1	1-1-1-1/1-1-1-3	Chassis/Main Body	4	Aluminum	Erhan yolcu Group Cyprus, Famagusta Tel:+905488610589	$ 31.25
2	1-1-1-2	Rivets	8	Steel	Genc Yapi Market Cyprus, Famagusta Tel: +90 392 444 43 62	$ 2.6
3	1-1-1-4	Shaft	1	Aluminum	Available	$ 0
4	-	3D printer	1	Various	AliExpress.com	$ 500
5	-	PLA+ Filament	2	PLA+	AliExpress.com	$5
6	1-1-2-2	External Spur Gear	4	PLA+	Available	$ 0

7	1-1-2-1	Timing Belt	2	Rubber	Zet Shop Cyprus, Famagusta Tel:+905338610874	$62.25
8	1-1-2-3	Wheel Hub	4	Steel	Robotistan Turkey www.robotistan.com	$26.5
9	1-1-2-4/ 1-1-4-3	Screws/Nut/ washers	50	Steel	Genc Yapi Market Cyprus, Famagusta Tel: +90 392 444 43 62	$5.2
10	1-1-2-6/ 1-1-3-3/ 1-1-4-4	Bearings	20	Steel	Arduino Engineering Center Basra, 4th of July, Basra, Iraq Tel: +964 770 316 1314	$3
11	1-1-2-5	Wheel Rings	4	PLA+	Available	$0
12	1-1-3-1	Pipes/Nozzle	2/2	Rubber/ Stainless Steel	Nizamoglu Shop Cyprus, Famagusta	$19

13	1-1-3-2	Box	1	Plexiglass	Hira CNC laser Cut Cyprus, Famagusta, Tel: +905488662474	$31
14	1-1-3-4	Pipe Holder	1	Plexiglass	Hira CNC laser Cut Cyprus, Famagusta, Tel: +905488662474	$10
15	1-1-4-1	Circular Brush	1	PLA+	Available	$0
16	1-1-4-2	Brush Case	1	Plexiglass	Hira CNC laser Cut Cyprus, Famagusta, Tel: +905488662474	$36.5
17	1-1-4-5	Circular Brush Holder	1	PLA+	Available	$0
18	1-2-1-1	AC/DC power Supply Battery	1	Various	Arduino Engineering Center Basra, 4th of July, Basra, Iraq Tel: +964 770 316 1314	$ 12

19	1-2-1-2	Wires	10	Various	Arduino Engineering Center Basra, 4th of July, Basra, Iraq Tel: +964 770 316 1314	$ 3
20	1-2-2-1	12V Gear Motors	2	Various	Arduino Engineering Center Basra, 4th of July, Basra, Iraq Tel: +964 770 316 1314	$19
21	1-2-2-2	12V Turbo Motors	2	Various	Arduino Engineering Center Basra, 4th of July, Basra, Iraq Tel: +964 770 316 1314	$20
22	1-2-2-3	Motor Driver	2	Various	Arduino Engineering Center Basra, 4th of July, Basra, Iraq Tel: +964 770 316 1314	$5

23	1-2-2-4	IR Sensor	2	Various	Arduino Engineering Center Basra, 4th of July, Basra, Iraq Tel: +964 770 316 1314	$3
24	1-2-2-5	Ultrasonic Sensor	1	Various	Robotistan Turkey www.robotistan.com	$2
25	1-3-1-1	Arduino Uno	1	Various	Arduino Engineering Center Basra, 4th of July, Basra, Iraq Tel: +964 770 316 1314	$ 25
26	1-3-2-1	Phone	1	Various	Available	$ 0
27	1-2-2-6	Bluetooth Module	1	Various	Robotistan Turkey www.robotistan.com	$2
Total						$824 + $100 Reserve

CHAPTER 4 - MANUFACTURING

4.1. Manufacturing Process Selection

Designing and developing the robotic solar panel cleaning system involves not only the integration of various engineering disciplines but also the careful selection of appropriate manufacturing processes. For the robotic system, various manufacturing processes were utilized to create different components of the system. The manufacturing processes are listed below:

4.1.1. CNC Machining

To create a robust and reliable chassis for the robotic solar panel cleaning system, a 3mm thick aluminum sheet was used due to its lightweight and corrosion-resistant properties. The aluminum chassis was then produced using CNC machining which is a precise and computer-controlled manufacturing process that ensured accurate cutting of the material. By utilizing CNC machining, the aluminum sheet was transformed into a precisely shaped and dimensioned chassis that could securely house the various components of the robotic system.

The box for housing the electrical components and the brush case of the robotic solar panel cleaning system were fabricated from plastic using CNC laser cutting. The result was a durable and functional box and brush case that meets the design requirements. CNC machining was opted as a suitable choice for creating these components based on the following reasons:

- ***Precision and Accuracy*****:** CNC machining offers a high degree of precision and accuracy, ensuring that the chassis is manufactured to the exact specifications of the 3D CAD model. This precision is important for ensuring the components of the robotic system fit seamlessly and that the system operates as intended.

- ***Complex Geometries*****:** CNC machining can create complex geometries and features, such as intricate patterns, shapes and curved surfaces that would be difficult to produce with other manufacturing processes.
- ***Material Versatility*****:** CNC machining can be used with a wide range of materials including metals, plastics, and composites, making it a flexible choice for various manufacturing applications.
- ***Consistency and Repeatability*****:** CNC machining produces consistent and repeatable parts ensuring that the chassis is manufactured to the same standard.

4.1.2. 3D Printing

3D printing, also known as additive manufacturing, is a process of creating three dimensional solid objects from a digital file. The creation of the three-dimensional parts is achieved by using additive processes as opposed to subtractive processes used in CNC machining. We opted for 3D printing to manufacture some parts for the robotic system based on the following parameters:

- ***Customization*****:** 3D printing allows for customization of parts, as it allows us to design and print the wheels of the robot to our exact specifications allowing specific features such as tread patterns, mounting holes and bearing, which are important for the proper functioning of the wheels
- ***Low setup cost*****:** 3D printing does not require expensive tooling, which means that the upfront costs of manufacturing are relatively low. This makes it an attractive option for small-scale production or prototyping.
- ***Reduced waste*****:** 3D printing produces minimal waste, as it only uses the material that is needed to create the part. This can help to reduce the environmental impact of manufacturing and save on material costs.

- ***Short lead times*****:** 3D printing allows us to produce parts on-demand, which means that we do not need to wait for parts to be shipped from a supplier. This can lead to shorter lead times and faster turnaround times for building the robot.

4.1.2.1. 3D Printing Process Selection

The 3D printing of parts of the solar panel cleaning robot involves the process of depositing ordered layers of materials to produce the desired parts which is designed with the aid of computer aided design (CAD). This method of manufacturing increases the freedom in design in terms of complex geometries. It also minimizes the total weight of the robot by altering some parameters like infill pattern and infill density. A decision matrix for the type of 3D printing process to use in the three-dimensional printing of the robot parts would be analyzed because there are several 3D printing processes available with each of them having their own benefits and limitations. In this section, it would be decided which 3D printing process to use by comparing different types and selecting the most suitable printing process for the robot solar panel cleaner parts. Before the comparison, a description of the types of available 3D printing processes would be highlighted in the following table.

Table 16. 3D printing processes

3D Printing Processes	Description
Stereolithography (SLA)	Producing parts with high level of detail, tight tolerance and smooth surface finish
Fused Deposition Modeling (FDM)	Quick method for producing physical models. Can be used for functional testing
Selective Laser Sintering (SLS)	Durable and suitable for functional testing. Suitable for parts quantities higher than other 3D processes
Digital Light Processing (DLP)	Can image an entire layer of the build all at once which results in faster build speeds. Suitable for low volume production.
Multi Jet Fusion (MJF)	Creates more consistent mechanical properties and an improved surface finish. MJF has accelerated build time resulting in lower production cost.

A comparison would be made for the most common and widely used 3D printing processes which are: Fused Deposition Modeling (FDM), Stereolithography (SLA), and Selective Laser Sintering (SLS). This would be used to determine the most suitable 3D printing process for the robot parts.

Table 17. Decision Matrix for 3D printing process

Criteria **Scale** **10 → Best** **1 → Worst**	**Priority**	**Requirement**	**FDM**	**SLA**	**SLS**
Cost	6	↓	7	5	8
Build Dimensions	4	↑	8	6	4
Accuracy & Tolerance	3	↑	7	9	9
Visual Characteristics	2	↑	7	9	8
Durability	5	↑	8	7	8
Speed	1	↑	7	8	7
Total			156	142	154

From the comparison of the three of the most established types of 3D printing processes, it is concluded that Fused Deposition Modeling (FDM) is the most suitable 3D printing process for the robot based on the specified criteria.

4.1.2.2. 3D Printing Material Selection

The right type of printing material should be selected for the 3D printing of the robot parts. The selected 3D printing process in the previous section was Fused Deposition Modeling (FDM). In Fused Deposition Modeling (FDM) 3D printing materials such as Acrylonitrile Butadiene Styrene (ABS), Polylactic acid (PLA), Polyethylene terephthalate (PET), Thermoplastic Polyurethane (TPU), Polycarbonate (PC), and nylon are the polymers used in the 3D printing. In this section, a comparison of the polymers used in Fused Deposition Modeling (FDM) would be done to decide the most suitable material to be used based on the specified criteria.

Table 18. Decision matrix for 3D printing materials

Criteria **Scale** **10 → High** **1 → Low**	**Priority**	**Requirement**	**PLA +**	**ABS**	**PET**	**TPU**	**PC**	**Nylon**
Visual quality	5	↑	7	5	5	3	5	5
Ease of printing	6	↑	9	3	7	1	3	5
Layer adhesion	4	↑	7	3	5	5	5	1
Impact Resistance	2	↑	1	5	5	9	5	7
Maximum Stress	3	↑	7	5	3	3	9	3
Cost	7	↓	6	6	5	4	3	2
Total			174	128	141	96	121	96

From the decision matrix based on the specified criteria, it was determined that Polylactic acid (PLA+) is the suitable material for the 3D printing of the robot parts. Polylactic Acid (PLA) is a good choice of material because it allows for easy printing, good visual quality and a high maximum stress. Additionally, it was selected as the material for the 3D printing because it has a higher maximum printing speed, lower layer heights, demonstrates less part warping, sharper printed corners, and an affordable pricing. One of the goals of the manufacturing process is to use environmentally friendly materials so it is a good choice to use Polylactic Acid (PLA+) because they degrade faster than normal plastic-based materials and it is also a common material used in 3D printing.

4.1.3. Drilling

Drilling is an essential process in manufacturing the robotic solar panel cleaning system. This process is used to create holes of varying sizes and shapes on the robotic components like the chassis, brush case, etc. The process involves the use of various types of drill bits and equipment which were also dependent on the type of material being drilled. High-speed steel (HSS) drill bits were used for drilling the aluminum while carbide-tipped bits were used for drilling plastic. The choice of drill bit was also dependent on the size and shape of the hole required. As for the drilling equipment, drilling machines such as bench drill press and hand drills were used for the drilling process.

4.1.4. Joining Assembly

In the manufacturing process of the robotic solar panel cleaning system, the joining method of different parts is an important process that has a significant impact on the performance, durability, and effectiveness of the robotic system. Therefore, it was essential to carefully evaluate different joining methods to determine the most suitable method for developing the robotic system. Several joining methods can be used for different parts such as the chassis, brush case, and other components. Bolting with threaded fasteners and Adhesive bonding with silicon were used to join components of the robotic system like the brush case, motors, wheels, etc. The main focus in this section is on the chassis since it is the main frame that holds the robotic system. Four joining methods were considered for the aluminum chassis which includes welding, riveting, bolting, and adhesive bonding. These methods were compared based on specified criteria to enable us to make the best choice for joining the chassis. A tabular representation of this comparison is provided below which includes the criteria and weighing scale.

Table 19. Decision Matrix for Chassis Assembly

		Weighing Scale 1 → 10 1 = Low 10 = High					
Joining Methods	**Description**	**Strength**	**Durability**	**Cost Effectiveness**	**Ease of Assembly**	**Aesthetics**	**Total**
Welding	A process that uses heat to melt and fuse metals together	8	8	5	5	5	31
Bolting	A method that uses nuts and bolts to fasten two pieces together	7	7	7	8	6	35
Riveting	A process that uses a rivet gun to fasten two pieces together with a metal pin and a rivet	8	9	9	7	8	41
Adhesive Bonding	A method that uses adhesives to bond two surfaces together	6	6	7	8	7	34

Based on the criteria and weighing scale, riveting is the best choice for the aluminum chassis because it provides a good balance between strength, durability, cost-effectiveness, ease of assembly, and aesthetics.

4.1.5. Bending Operation

Following the selection of riveting as the joining method for the chassis assembly, the aluminum chassis underwent a bending process to shape the part to the desired form specified in the robotic system's design. The bending operation was done by a bending machine to achieve the desired shape for the chassis.

4.2. Detailed Manufacturing Process

These detailed manufacturing processes highlight the various steps involved in creating essential components for the robotic solar panel cleaner, including the brush, brush case, chassis, plexiglass box and gear wheels. Each process combines design, material selection, fabrication techniques, and post-processing to produce functional and customized parts that contribute to the overall efficiency and effectiveness of the robotic solar panel cleaner.

4.2.2. CNC Machining and Assembly for the Chassis

The manufacturing process of the robotic solar panel cleaning system was initialized by making the chassis. This is the main frame of the robotic system where other components and parts would be attached. A 3mm thick aluminum sheet is used to make the chassis. This is done by a CNC milling machine to produce the desired shape specified in the design of the part.

Figure 63. Aluminium sheet

The CNC machining process involves first preparing the detailed CAD model of the chassis, specifying the desired dimensions and features. The CNC program for CAD model is generated which includes instructions for tool path, cutting depth, and feed rates.

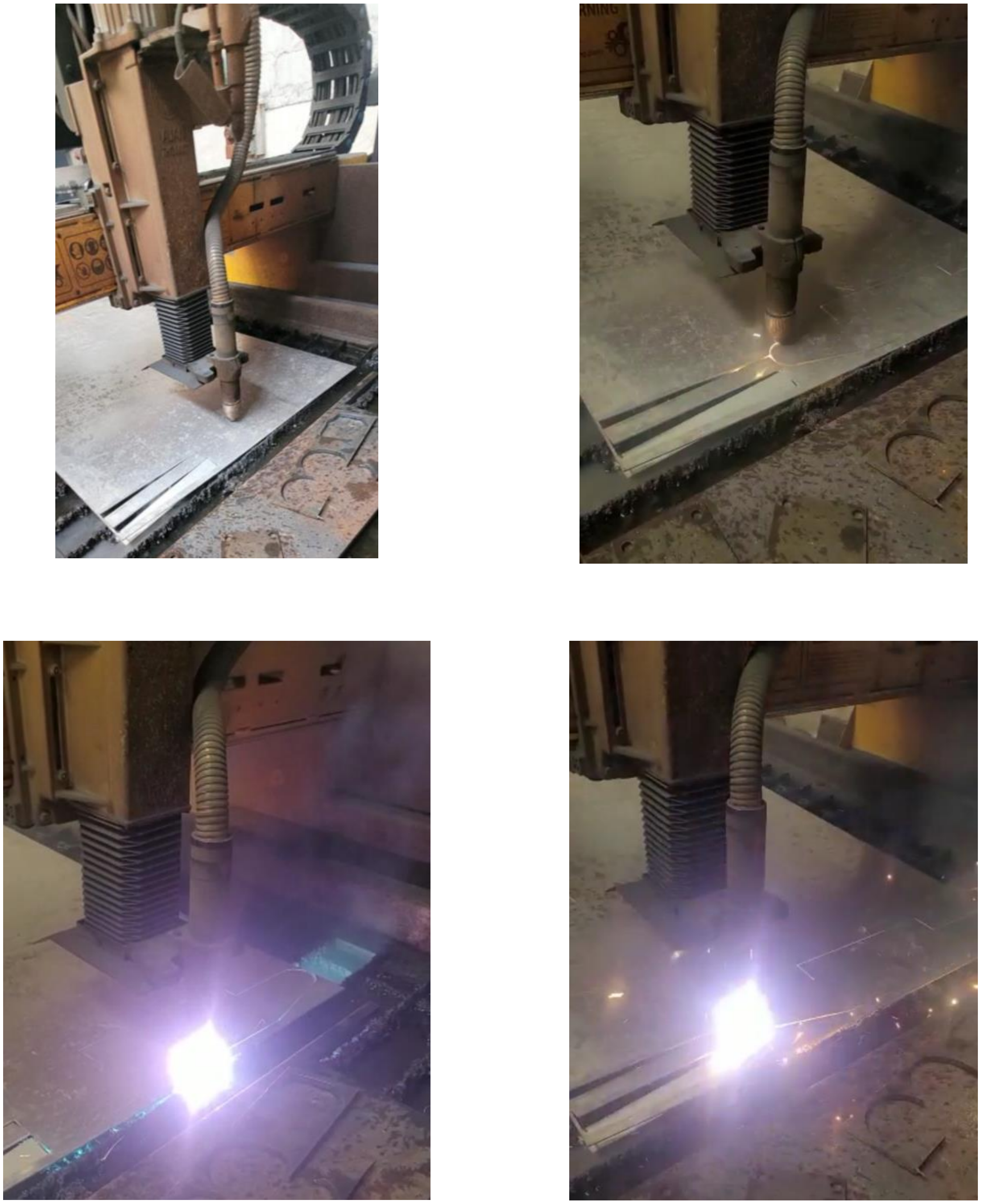

Figure 64. CNC Machining of Aluminium sheet

Following the CNC machining of the aluminum sheet, the parts go through a bending operation to produce the desired shape of the chassis. The bending machine was set up with the required tooling and programmed with the specific bending angles and dimensions. The aluminum parts were carefully positioned and clamped in the bending machine. The bending machine accurately bent the parts at the predetermined locations, creating the desired shape and structure for the chassis. The Chassis has two identical parts which are secured firmly together by a 3mm thick aluminum beam which was also cut from the CNC process. The beam runs across the two parts of the chassis and is held firmly to the chassis by a riveting process using 5mm blind rivets.

Figure 65. Chassis Parts from CNC and Bending Operations

Figure 66. Rivets

Figure 67. Riveting of Chassis

Figure 68. Robot Chassis

Drilling holes on the chassis of the robotic system was an important step in the assembly process to bearings, shafts, motors screws, brackets, etc. Optimal locations for holes were determined and specialized drilling equipment was used to create holes. Hand drills were used to make small holes and larger holes were done with bench drill presses. Bearing and shafts are placed in the holes, providing rotational movement and support for moving parts. Motors are securely mounted onto the chassis from the holes and screws are utilized to fasten and secure components.

Figure 69. Drilling holes on the chassis

4.2.3. 3D Printing of Components

Components such as the gear wheels, gear wheel rings, brush shaft, brush holder, etc. were 3D printed using the Creality CR-1OS Pro 3D Printer, using a Fused Deposition Modeling (FDM) technique and Polylactic Acid (PLA) filaments. This offers a versatile and efficient means of producing high-quality robotic parts. The step-by-step 3D printing process is described below.

Figure 70. Creality CR-10 Smart 3D Printer

Figure 71. PLA+ Filament

Step 1: Designing and Preparing the Model

The initial stages involve creating the design of the robotic parts using CAD software such as Solid works. Once the design is complete, it is converted into a printable file format - STL.

Step 2: Slicing and Preparing for Printing

The STL file is imported into the UltiMaker CURA slicing software where it is divided into layers and prepared for printing. In the stage, various printing parameters are set. These settings determine the strength, resolution, and overall quality of the printed part.

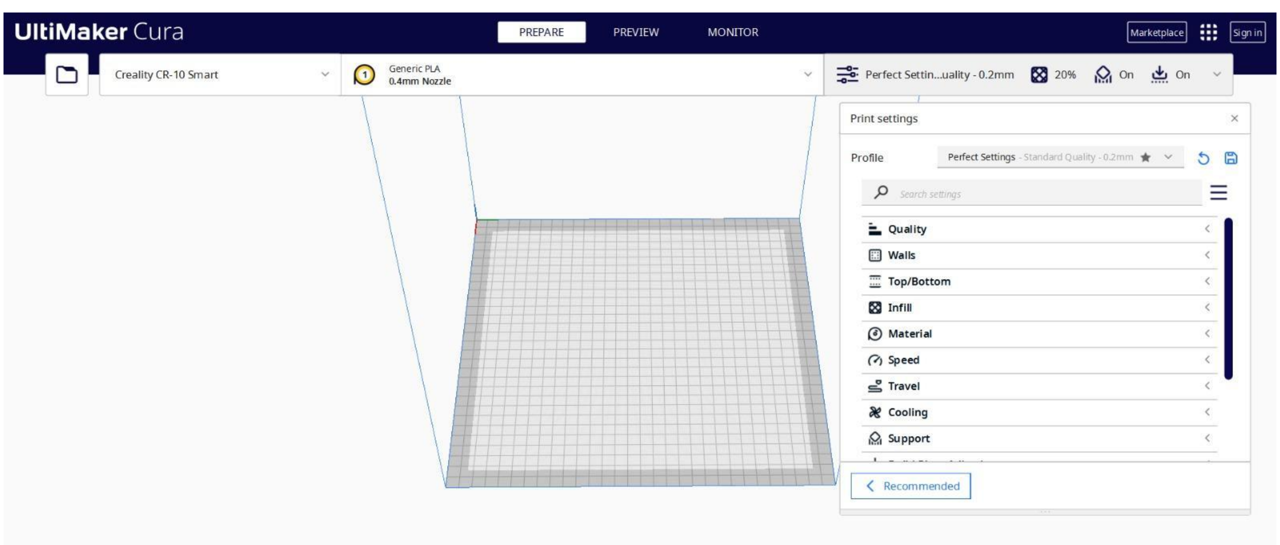

Figure 72. UltiMaker CURA Software

The most important settings used in 3D printing the robot’s part from the software are as follows:

- Standard quality: 0.2 mm
- Layer height: 0.2mm
- Initial layer Height: 0.28 mm
- Wall thickness: 1.2 mm
- Infill Density: 20%
- Infill Pattern: Gyroid
- Printing Temperature: 205℃
- Printing Temperature Initial Layer: 210℃
- Bed Temperature: 60℃
- Print Speed: 50 mm/s
- Infill Speed: 55 mm/s
- Retraction Distance: 5 mm
- Retraction Speed: 45 mm/s

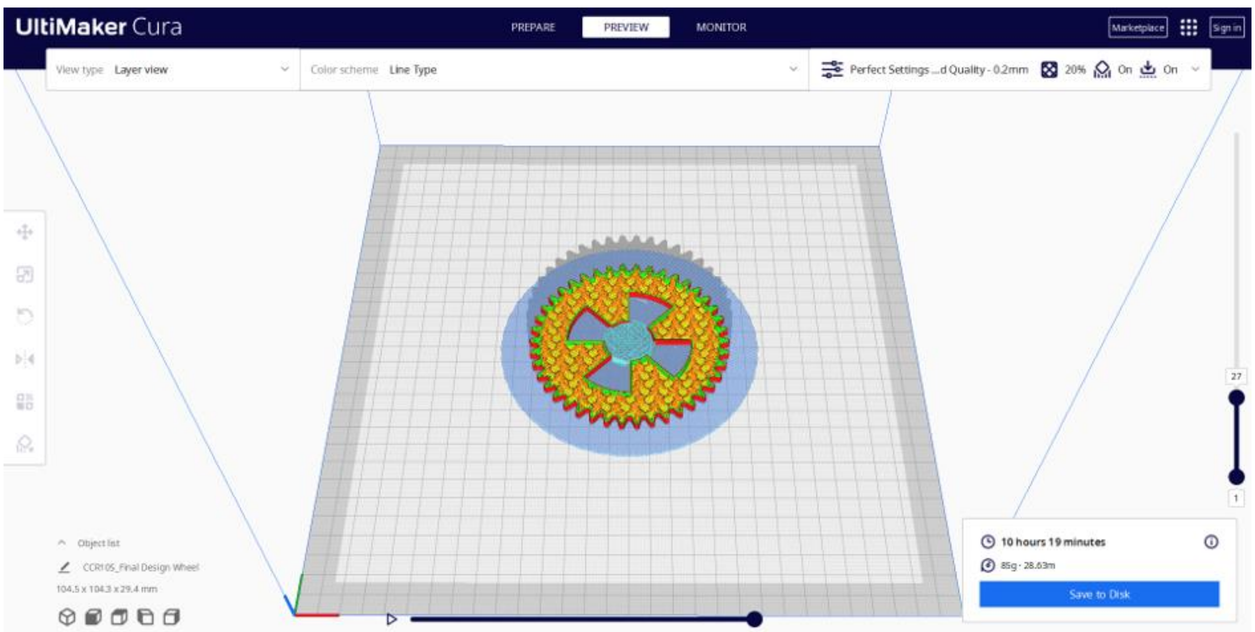

Figure 73. Slicing and Printing Previews for Gear Wheel (a)

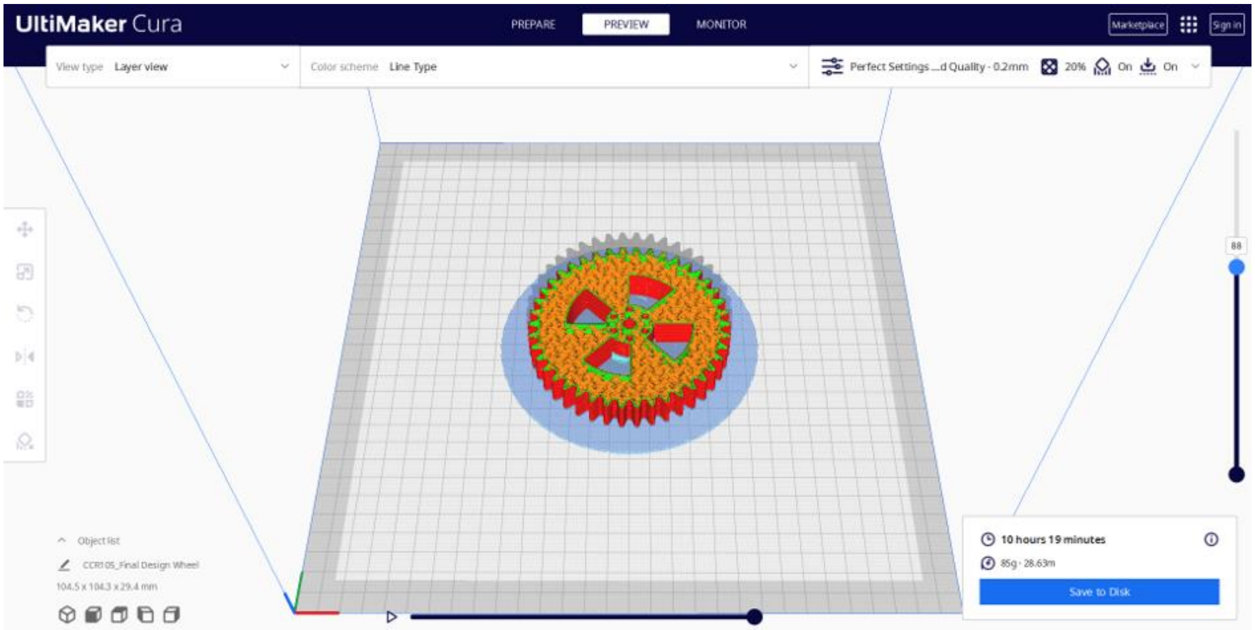

Figure 74. Slicing and Printing Previews for Gears Wheel (b)

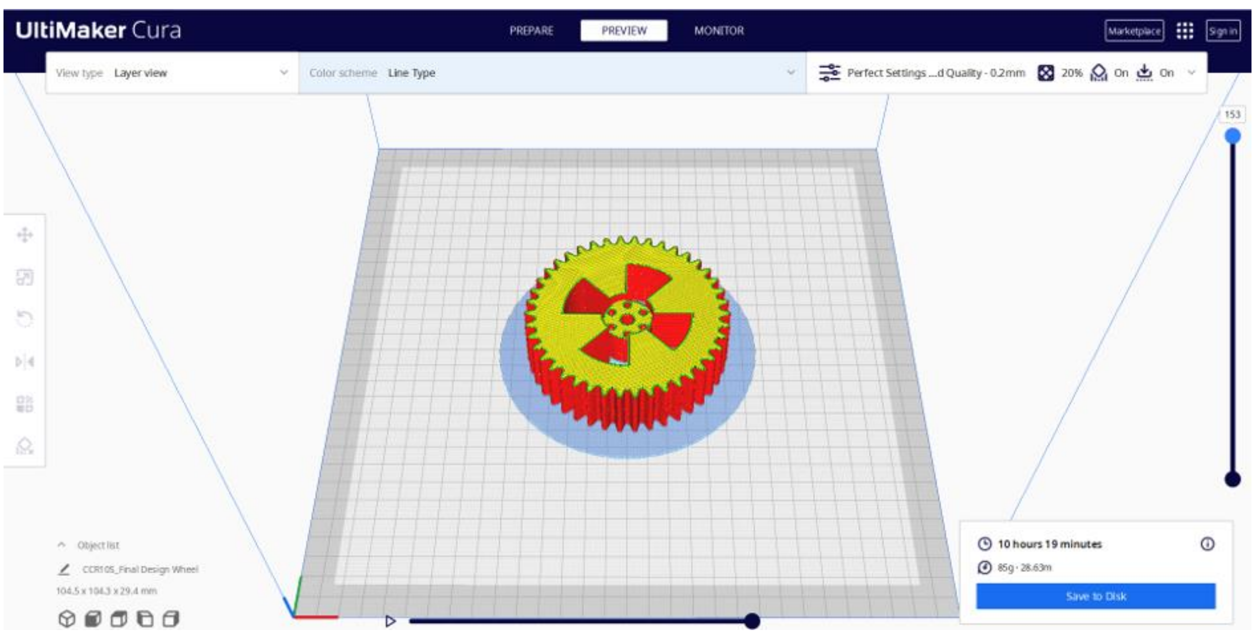

Figure 75. Slicing and Printing Preview for Gear Wheel (c)

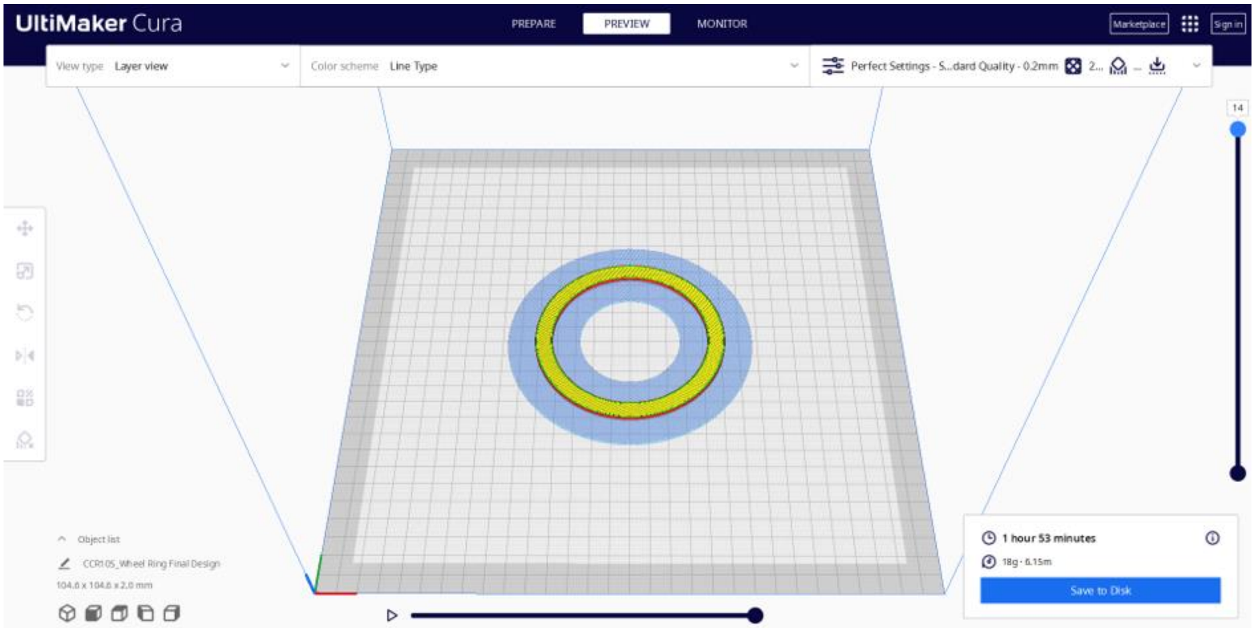

Figure 76. Slicing and Printing Preview for Wheel Ring

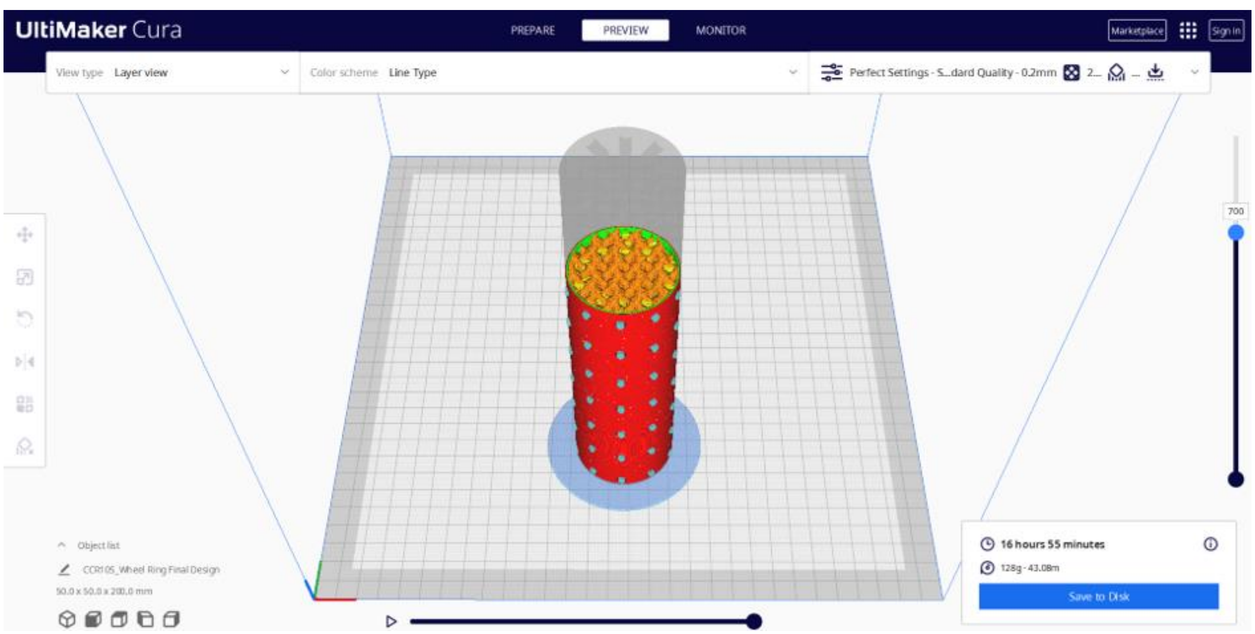

Figure 77. Slicing and Printing Preview for Brush Shaft (a)

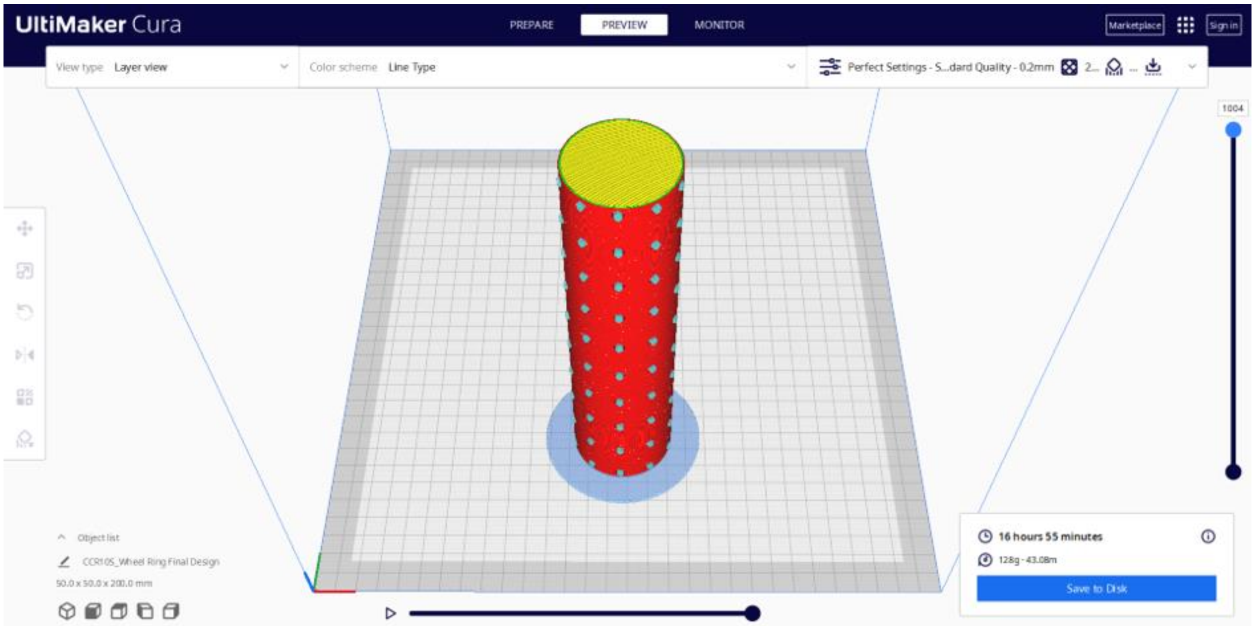

Figure 78. Slicing and Printing Preview for Brush Shaft (b)

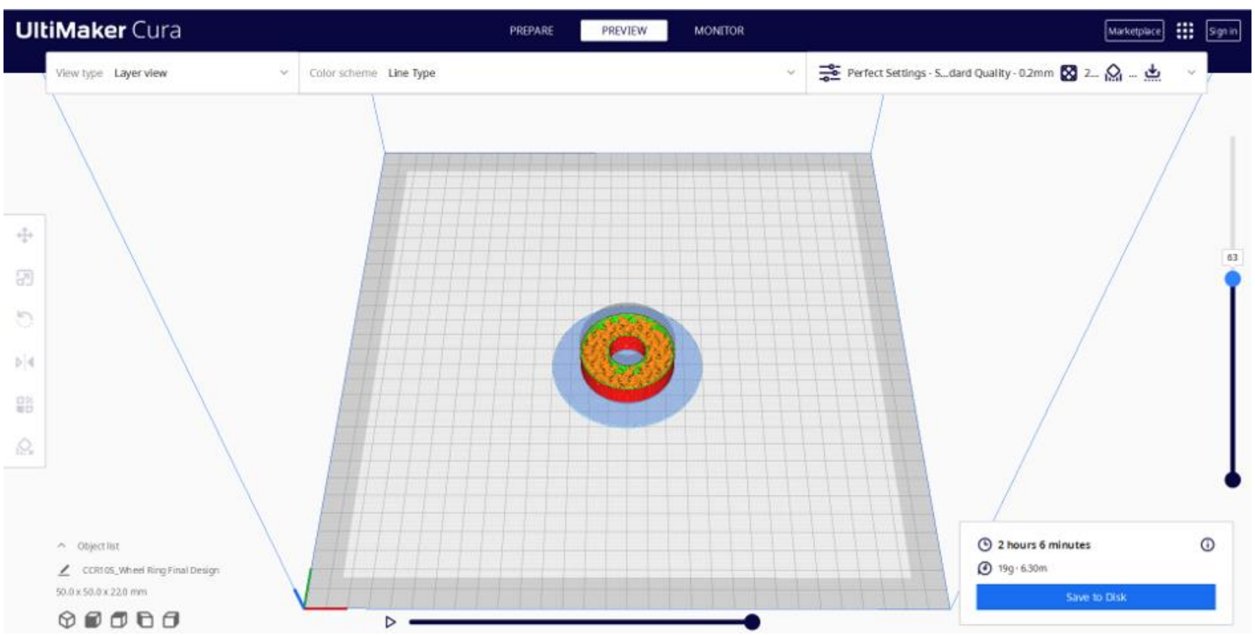

Figure 79. Slicing and Printing Preview for Brush Holder (a)

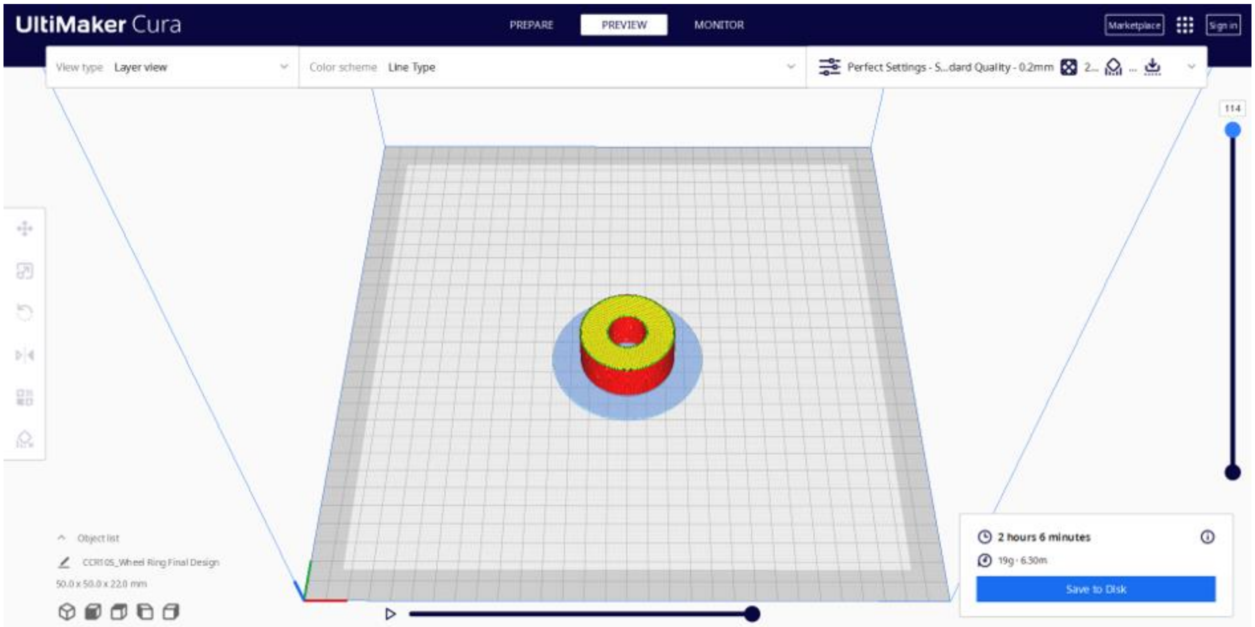

Figure 80. Slicing and Printing Preview for Brush Holder (b)

Step 3: Setting Up the Printer

The 3D printer is prepped for printing. The printing bed is leveled, ensuring proper adhesion and a level printing surface. The printer's extruder is heated to the appropriate temperature to melt the PLA+ filament.

Step 4: Loading and Extruding PLA+ Filament

The PLA+ filament is loaded into the printer's filament holder. The filament is fed through the printer's extruder, which heats and melts it. The extruder then deposits the melted filaments in a precise manner, layer by layer, according to the slicing software's instructions.

Step 5: Printing the Parts

With the printer properly set up, the actual printing process begins. The extruder moves along the X, Y, and Z axes depositing the melted filaments to build the part in layers.

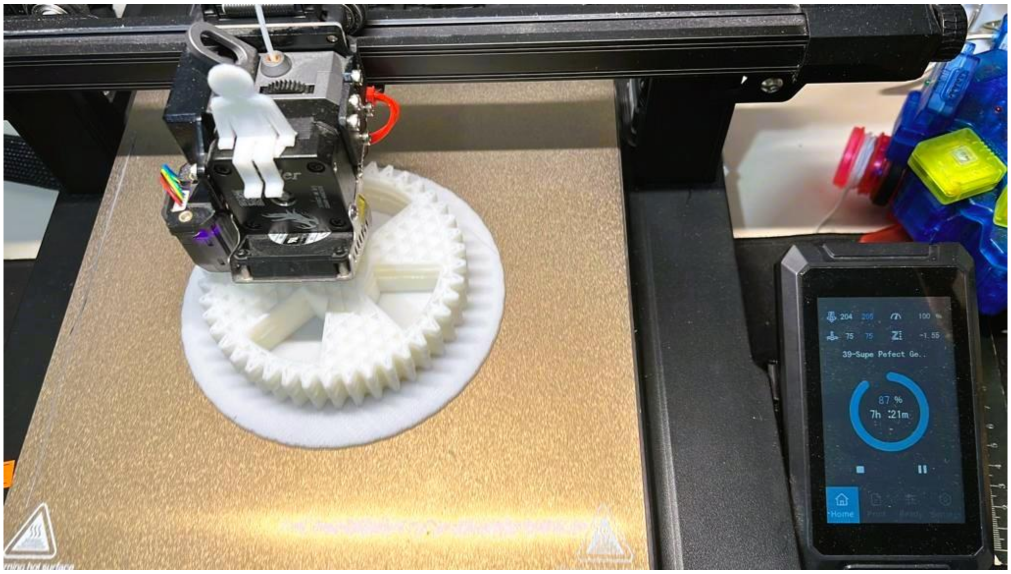

Figure 81. 3D Printing of Wheel Gears

Step 6: Cooling and Solidification

Once the printing is complete, the printed part cools to solidify the PLA+ material and enhance its structural integrity. The support structures are also removed.

Figure 82. 3D Printed Gear Wheels

Figure 83. 3D Printed Wheel Rings

Figure 84. 3D Printed Brush Shaft

The wheel rings are attached to the edges of the wheel gears and their purpose is to prevent the belts from slipping out of the wheels. To create the brush bristles for the robotic solar panel cleaning system, we took bristles from a broom or similar material. The brush bristles were cut to the desired length for optimal cleaning performance. Adhesives, such as glue or epoxy, was applied to the holes or slots on the 3D printed brush shaft. The bristles were then carefully inserted into the holes, ensuring proper alignment and distribution along the shaft. The adhesive was allowed to cure, securely attaching the brush hairs to the brush shaft.

4.2.4. CNC Laser Cutting for Brush Case and Box

The brush case and the box were fabricated from plastic, specifically plexiglass (acrylic) using CNC laser cutting technology with varying thickness. The box has a thickness of 5mm while the brush case has a thickness of 3mm. Plexiglass is a plastic material which is a suitable lightweight alternative to glass. The CNC laser cutting provides a precise and efficient way to make these components. The design of the brush case and box was done using CAD software. The CAD file is then made into a format that is compatible with the CNC laser cutting machine. The CNC laser machine uses a high-power laser beam to precisely cut through the plastic material. The cut pieces of plexiglass were prepared for assembly. Silicone adhesive was applied along the edges of the plexiglass pieces to create a secure and watertight bond structure for the brush case and box. The pieces were carefully aligned and joined together, ensuring proper positioning and alignment. Pressure or clamps were applied to hold the pieces in place while the adhesive cured.

Figure 85. Plexiglass (Acrylic) Box

Figure 86. Pre-Alignment of Brush Mechanism

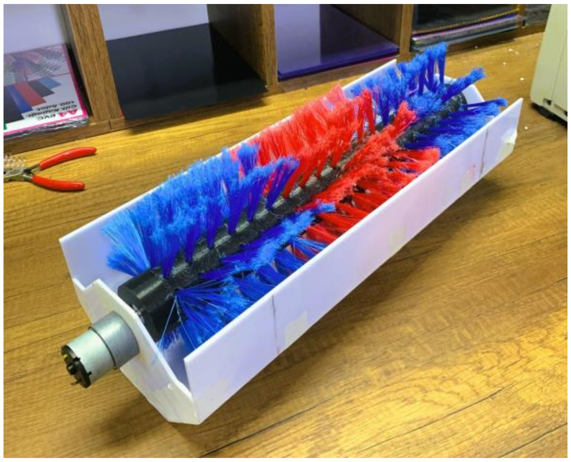

Figure 87. Brush Mechanism

Figure 88. Brush Assembly

Figure 89. Pre-Alignment of Brush Mechanism with the Chassis

4.2.5. Assembly of the robotic solar panel cleaning system

The assembly process of the robotic system involves the systematic integration of the components of the robotic system. During the assembly process of the robotic system, extra measures such as testing, spray painting, and modifications were taken to produce an aesthetically pleasing and fully functional system that can perform its task of properly cleaning solar panels in order to improve its efficiency and performance. Throughout the assembly process, the components were carefully inspected to ensure they meet the required specifications and quality standards. Attention is also paid to proper wiring and connection of electrical components to ensure efficient and reliable operation of the robotic solar panel cleaning system.

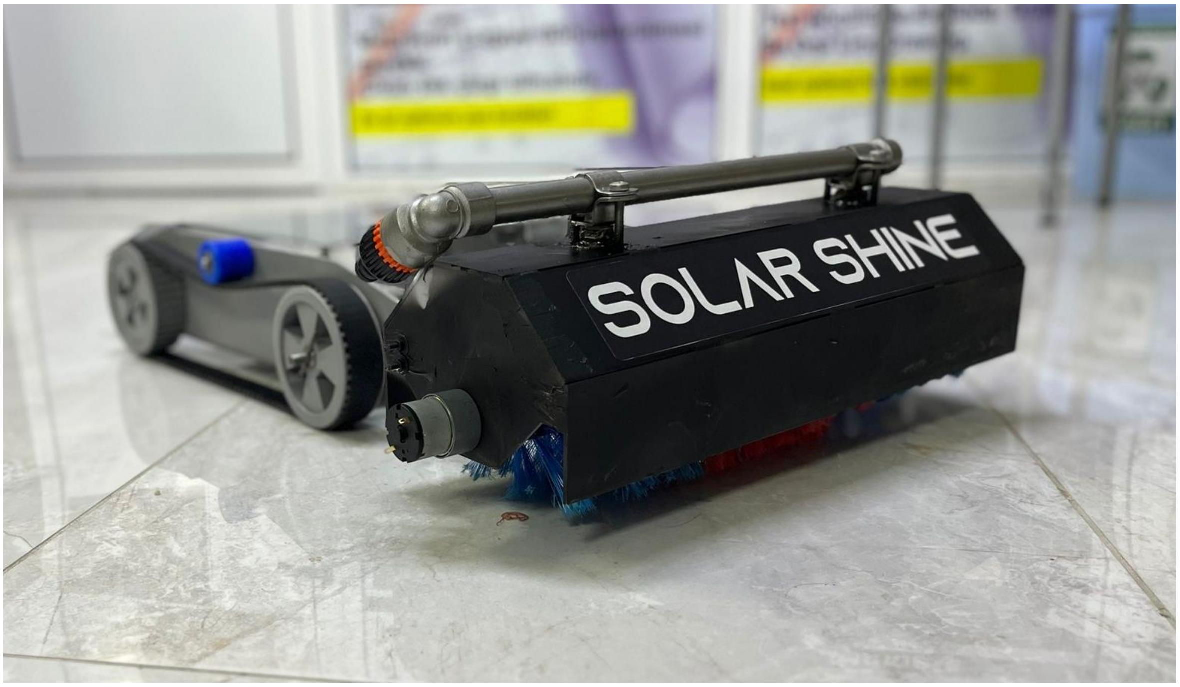

Figure 90. Solar Shine robotic cleaning system

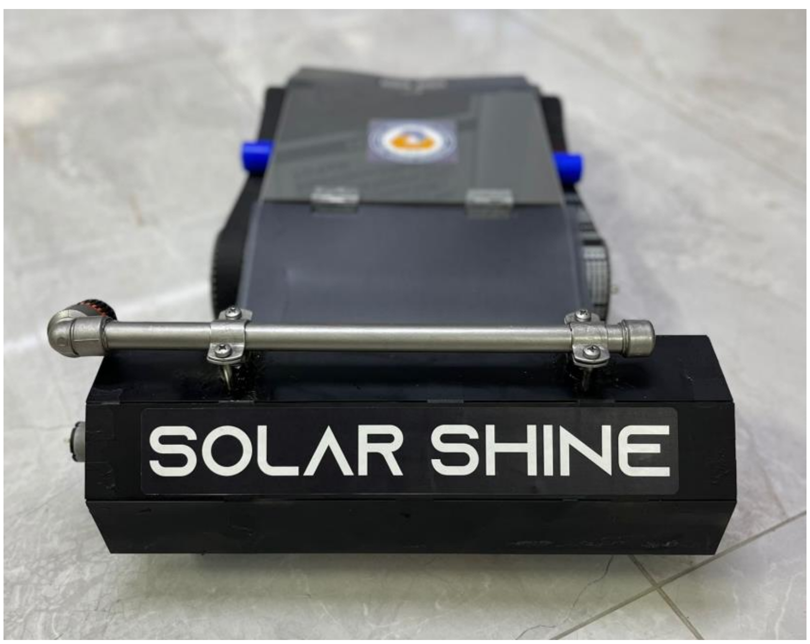

Figure 91. Front view of the assembled robot

Figure 92. Top view of assembled robot

Figure 93. Rear view of assembled robot

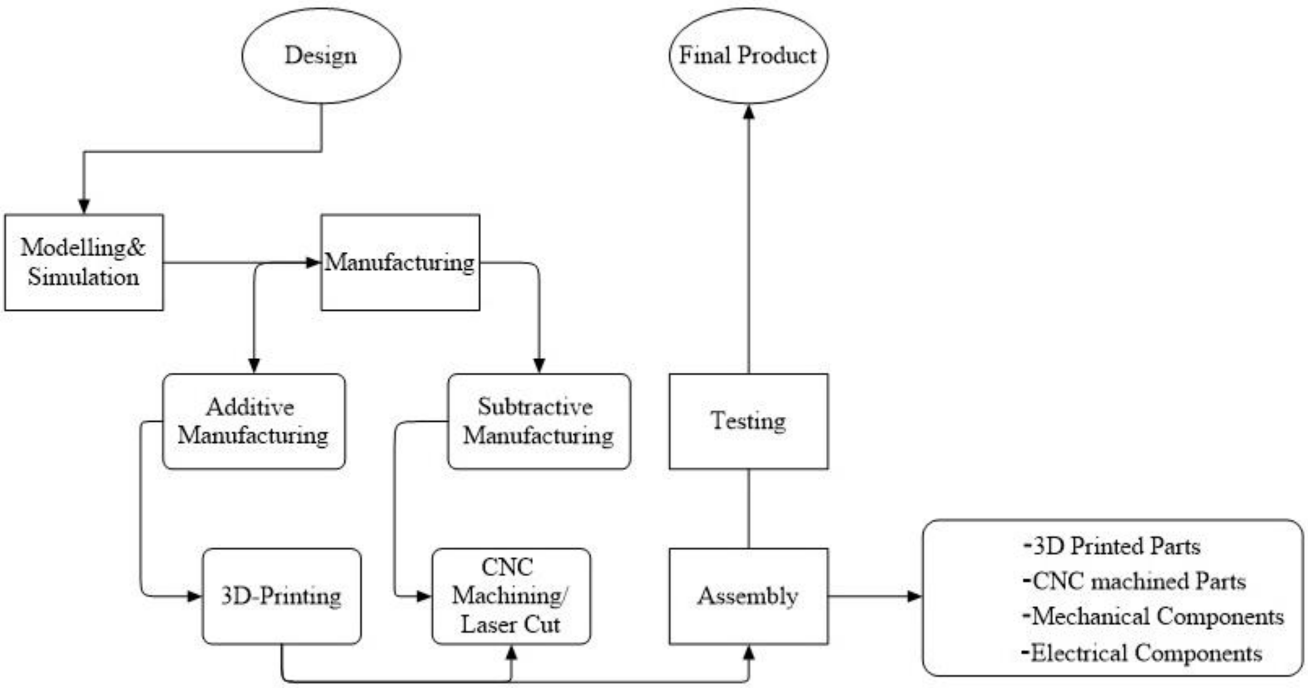

Figure 94. Manufacturing Process Flow Chart

4.3. Detailed Description of the Manufactured Robotic Solar Panel Cleaner

The Solar Shine ™ robot is a robotic solar panel cleaner designed majorly for large scale cleaning of vast arrays of solar panels. It can also be used for small scale cleaning operations. It offers a scalable solution to meet the challenges of maintaining large arrays of solar panels. As the demand for clean energy surges and solar farms continue to expand, the need for effective and efficient maintenance is important. Manual cleaning is both labor intensive and time-consuming, making it insufficient to keep with the maintenance demands of solar panel installations. Designed with sustainability and scalability in mind, the Solar Shine robotic solar panel cleaner addresses the challenges head-on making it an ideal system for efficient solar panel cleaning.

Figure 95. Array of Solar Panels

(“New Atlas: Rooftop solar array”, 2014)

As engineers, we conducted comprehensive research and extensively analyzed the limitations of solar panels to ensure their long-lasting durability and prevent any potential damage. One critical aspect we focused on was the weight-bearing capacity of the panels. To address this concern, our design team meticulously investigated the issue and discovered that standard solar panels have a weight tolerance of 22 kilograms per square meter, with a maximum load capacity of 34 kilograms, as indicated by Chris in the solar gear guide. Consequently, to mitigate the risk of damage to the solar panels, we developed a robotic solar cleaner with a significantly reduced weight, totaling only 4.5 kilograms.

Furthermore, when it comes to cleaning solar panels, it is crucial to utilize a brush specifically designed for this purpose to prevent any potential harm. To address this requirement, our design team created a non-abrasive brush that prevents scratching or wearing off the protective coatings on the solar panels. Using abrasive brushes can compromise the panels' efficiency and longevity, which is why it is essential to select brushes that are specifically engineered to be gentle on the panel surfaces.

By considering the weight-bearing capacity of solar panels during the design phase and developing non-abrasive cleaning brushes, we can ensure the optimal performance and extended lifespan of the panels, contributing to the overall efficiency and reliability of solar energy systems.

Table 20. Technical Data of the robot

Technical Data	
Robot length (without brush)	0.62m
Robot length (with brush)	0.78m
Brush length	0.31m
Brush width	0.16m
Brush bristle material	Nylon bristles
Box width	0.25m
Box height	0.15m
Robot turning radius	0.62m
Robot speed	0.238m/s
Cleaning time (2m x 1m solar panel)	4.2seconds per meter
Battery running time (rechargeable)	5 hours

Table 21. Mass Distribution

Component	Quantity	Weight	Total
Brush / Brush Case	1	900g	900g
Wheels	4	50g	200g
Chassis	1	2300g	3000g
Box	1	300g	500g
Arduino Uno	1	24g	24g
Motors	3	150g	450g
Motor Driver	2	24g	48g
Battery	1	300g	300g
Ultrasonic Sensor	2	8g	16g
Total			5438g

Table 22. Power Distribution

Component	Quantity	Required Power	Total
Arduino Uno	1	0.1A	0.1A
Gear Wheel Motors	2	0.2	0.4A
Motor Driver	2	0.036A	0.072A
Brush Motor	1	0.2	0.2A
Ultrasonic Sensor	2	0.015A	0.03A
IR Sensor	1	0.02	0.02A
Total			0.822A = 822mA

Table 23. Comparison with other standard robots

	SolarCleano F1	SolarCleano M1	SolarCleano B1	hyCLEANER SOLAR facelift	Solar Shine
					
Total weight (kg)	80	37	-	83	5.538
Dimensions (m) (LxWxH)	1.45x1.3x0.35	0.80x0.86x0.35	5.95x1.74x3.51	1.2x0.9x0.5 (Without brush)	0.62x0.31x0.15 0.78x0.45x0.15
Brush size (m)	1.7	0.8	4.4	1.1x0.3x1.3	0.45x0.16x0.2
Remote control range (m)	200	200	-	-	30
Brush diameter (m)	0.17	0.17	0.38	0.3	0.18
Gradeability (°)	25	-	0 - 34	25	45

POWER CONSUMPTION/ROBOT SPEED

The speed of the robot is 0.238 m/s

So, it will cut a distance of 0.238m(238cm) in 1 sec, or we can say it needs 4.2 sec to cut 1m distance.

And it will take an average of (4.2+4.2+10) =18.4sec to cover an 2mx1m solar panel, 4.2 sec to cut the first 1m, 10 sec to rotate, and finally 4.2 sec to cover the other 1 m width.

The battery discharging duration:

In this case, the discharge rate is given by the battery capacity (in Ah) divided by the number of hours it takes to charge/discharge the battery. In our case, a battery capacity of 4.5Ah, and the electrical components take about 822mA, so the battery lasts for t=4.5Ah/0.822A=5.4745 hours which equals to 5h 28.5 min.

Table 24. Design for Assembly

(DFA) Design For Assembly		
Assembly Evaluation for: Robotic Solar Panel Cleaner		1→ Bad 10→ Very good
	OVERALL ASSEMBLY	
1	Overall part count minimized	6
2	Minimum use of separate fasteners	6
3	Base part with fixturing features (locating surfaces and holes)	7
4	Repositioning required during assembly sequence	5
5	Assembly sequence efficiency	6
	PART RETRIEVAL	
6	Characteristic that complicates handling (tangling, flexibility) have been avoided	6
7	Parts have been designed for a specific feed approach (belt mechanism)	5
	PART HANDLING	
8	Parts with end-to-end symmetry	5
9	Parts with symmetry about the axis of insertion	4
10	Where the symmetry is not possible, parts are clearly asymmetric	4
	PART MATING	
11	Straight-line motions of assembly	6
12	Chamfers and features that facilitate insertion and self-alignment	4
13	Maximum part accessibility	6

CHAPTER 5 - PRODUCT TESTING

5.1. Verification of the objectives of the project

The overall objective of our project was to design a Robotic Solar Panel Cleaner that will achieve the removal of dust from PV panels, such that the performance and efficiency of the PV panel is not compromised.

To verify this objective, the testing procedure involves evaluation of the performance of the PV panel before the cleaning process and after the cleaning process. The cleaning efficiency of the Robotic Solar Panel Cleaner will be determined by the achieved performance of the PV panel after the cleaning process.

Design for Cost - To design a cost-effective robot cleaning system we carried out an extensive cost analysis, this involved a review in the sourcing of mechanical components, electrical components and services in the manufacturing of the robot. This enabled us to select inexpensive and readily available materials and components as well as economical manufacturing processes. This technique allowed us to minimize the cost of developing the cleaning system without limiting the robot's performance or deviating from the main objectives.

Design for Manufacturability – We implemented an extensive review into the suitable manufacturing processes that are accessible, available and well suited for our design. In an aim to design a cleaning system that is manufacturable using readily available materials while also outsourcing required components. This allowed us to carry out an economical manufacturing process for the design of the cleaning system.

Design for Safety – We designed a cleaning system that is safe to operate by the users and is also safe in the work environment. By carrying out a thorough review into the failure of all systems components and the effects of the failure of these components to the user and work environment during the operation and use of the cleaning system. This allowed us to reduce the possibility of causing harm to the user and damage to the solar panels as well as damage to the cleaning system itself. Sensors to enable the robot to compute its position on the solar panel, preventing it from tipping over the panel and damaging the robot. All electrical wires are insulated and covered properly to avoid short circuiting with the water system. Smoothing, chamfering and fileting of sharp edges on the body of the robot prevent harm to the user during handling of the robot.

Design for Sustainability - To develop a sustainable cleaning system for the use and operation over a long-life span, we selected durable components and parts that are easily replaceable with minimal technical skill. To ensure long-lasting operation and use of the cleaning system, we devised a maintenance plan that requires the cleaning of the system after daily operation. This reduces the accumulation of dirt and dust particles in the moving components and parts of the cleaning system, ensuring a long-life span.

Design for Environment – We designed the cleaning system to be environmentally friendly by selecting components and parts that have hardly any carbon footprint, throughout the use of the cleaning system. Implementing proper disposal of components such as the battery, plastic components and electrical components is advised after the end of life of the system or after replacement of components to reduce harmful emission of waste products. Recyclable plastic will also be used in the manufacturing of the components of the system where possible.

5.1.1. DC MOTOR TESTING

To ensure functionality, reliability, and safety of our robotic solar panel cleaner, it was important to test the DC motors. Ensuring that the motors will operate to the required performance. We followed the steps below to make sure the motors perform their intended task.

1. Visual Inspection: The 12V Worm DC motors were opened and visually inspected for any physical damage, loose connections, or misalignments. The lubrication condition of the gears in the motors was inspected, and no issues were found.
2. Resistance Testing: A multi-meter was used to measure the resistance across the motor terminals. The measured resistance was verified to be within the specified range, indicating proper electrical continuity.
3. Voltage Testing: A 12V DC power supply was connected to the motor, and the voltage across the motor terminals was measured while the motor was running. The measured voltage matched the specified rating of 12V, confirming correct voltage supply.
4. Current Testing: The current drawn by the motor was measured using a multimeter. The measured current was compared with the motor's rated current, and it was found to be within the acceptable range, indicating proper electrical performance.
5. Load Testing: An appropriate load, such as a small propeller or a fan blade, was attached to the motor. The motor's performance under load conditions was observed, and it was found to handle the load without stalling or overheating, demonstrating its capability to withstand applied loads.
6. Speed and Torque Testing: The motor's rotational speed was measured using an encoder. The measured speed was within the specified range, ensuring the motor's adherence to the desired speed requirements. The motor's torque was measured by attaching a torque sensor, and it met the required specifications.

7. Efficiency Testing: The input power (voltage multiplied by current) and output power (torque multiplied by angular speed) of the motor were measured and calculated. The motor's efficiency was calculated by comparing the measured input and output power. It was found to operate within the desired efficiency level, indicating effective conversion of electrical power into mechanical power.
8. Endurance Testing: The motor was run continuously for an extended period, emulating its expected usage. The motor's performance was monitored, and its durability was assessed. No significant issues were observed during the prolonged operation, indicating that the motor could withstand continuous use without experiencing any noticeable degradation or malfunctions.

5.1.2. ARDUINO UNO TESTING

To ensure proper functionality, compatibility, and control of the robotic cleaner, it was important that a series of tests were performed on the Arduino Uno. To verify that the board operates as expected, enabling successful operation of our overall system, the following tests were carried out.

1. Visual Inspection: The Arduino Uno circuit board was inspected for any physical damage, loose connections, or soldering issues. All components were verified to be properly seated and securely attached. No visible defects or abnormalities were found.
2. Power Supply Testing: A suitable power source was connected to the Arduino Uno board, ensuring that the voltage and current rating aligned with the board's requirements. It was verified that the board received power and functioned properly.
3. Bluetooth Connectivity Testing: The Bluetooth module was installed and configured on the Arduino Uno board. It was paired with a compatible device, such as a smartphone or

computer. A stable and reliable Bluetooth connection was established between the Arduino Uno and the control device.

4. Control Signal Testing: A simple code or program was written for the Arduino Uno to interpret incoming Bluetooth commands. The control signals were tested by sending various commands (e.g., forward, backward, left, right) from the control device. It was verified that the Arduino Uno received and processed the commands correctly, resulting in appropriate movement of the robot.
5. Sensor Integration Testing: HC-SR04 Ultrasonic sensors were connected to the Arduino Uno board as per the circuit design. It was verified that the Arduino Uno could read data from the ultrasonic sensors accurately. The integration of sensor data with the control commands received via Bluetooth was successfully tested.
6. Power Efficiency Testing: The power consumption of the Arduino Uno board was measured during different operational modes, such as forward, backward, and cornering. The power efficiency was evaluated, and areas for optimization were identified if necessary.
7. Endurance Testing: The Arduino Uno board and the robot were run under typical usage conditions for an extended period. The board's performance and stability were monitored over time. No significant issues were identified during prolonged operation, confirming its endurance and reliability.

5.1.3. WATER SYSTEM TESTING

To ensure effective cleaning performance of the robot as well as to mitigate possible leakages, it was important to test the water system. Ensuring the system is functional and that it provides reliable pressure for cleaning of dust as required and to avoid possible damage to the electrical components in case of a short circuit.

1. Leakage Testing: The water system components, including pipes, valves, and nozzles, were connected. The system was filled with water, and a thorough inspection was conducted to identify any visible leaks at the connections and joints. The system was monitored over a specified period, and no signs of water leakage, such as drips, puddles, or wet areas, were observed.
2. Insulation and Gasket Testing: Proper insulation and rubber gaskets were installed between the water system and its connection to the overall system. It was verified that the insulation and gaskets effectively sealed the connection, preventing water leakage.
3. Pressure Testing: The water system's ability to handle the required pressure was tested. Specified pressure was applied to the system, and it remained stable without any noticeable pressure drops or fluctuations during operation. All components, including pumps and valves, functioned properly under the designated pressure.
4. Flow Rate Testing: The flow rate of water from the nozzles or spray heads was measured. The measured flow rate was compared to the desired specifications, and it was found to meet the requirements. Consistent and uniform water distribution across the solar panels was ensured.
5. Spray Pattern Testing: The spray pattern of the water system was evaluated and inspected. The angle, coverage, and dispersion of the water spray onto the solar panels were observed

and evaluated. It was verified that the spray pattern effectively cleaned the panels without causing excessive water wastage or uneven cleaning.

6. Reliability and Endurance Testing: The water system was operated for an extended period to simulate its expected usage. The system's performance and reliability were monitored over time, and it proved to be durable, exhibiting resistance to wear, corrosion, and degradation.
7. Safety Testing: The water system was tested for compliance with safety standards and regulations. It was verified that there were no risks of electrical hazards or short circuits due to water leakage, ensuring the safety of the overall system.

5.1.4. BRUSH SYSTEM/MECHANISM TESTING

Testing the brush mechanism/system in a robotic solar panel cleaner is important to ensure effective cleaning, uniformity, dust handling, compatibility with the water system, durability, safety, ease of maintenance, optimization, and performance enhancement. Testing verifies that the mechanism/system efficiently removes dust, covers the entire surface evenly, handles and contains dust properly, integrates smoothly with the water system, operates reliably, and meets safety standards. It allows for adjustments, identifies weaknesses, enhances usability, and promotes optimal energy generation.

1. Visual Inspection: The brush mechanism was inspected for any physical damage, loose connections, or wear. It was verified that the brush was securely attached to the motor shaft and the brush cover. No visible defects or abnormalities were found in the brush and the brush cover.

2. Functional Testing: The DC motor was switched on to spin the brush. It operated smoothly without any unusual noise or vibrations. The brush rotation was evaluated and found to be even and consistent.
3. Compatibility with Water System: Proper alignment and connection between the brush and the water spray were ensured. It was verified that the brush and water spray worked together effectively, providing efficient dust cleaning without interference.
4. Dust Cleaning Efficiency Testing: A controlled amount of dust or debris was applied to a test surface representing solar panels. The brush mechanism was activated, and its ability to remove dust effectively was observed. The cleanliness of the test surface after the brush mechanism operated was assessed and found to be satisfactory.
5. Dust Cleaning Uniformity Testing: The brush mechanism's ability to clean dust uniformly across the surface was evaluated. The test surface was inspected for any areas showing inconsistent cleaning or residue build-up. It was verified that the brush covered the entire surface evenly and left no areas untouched.
6. Durability and Reliability: The brush mechanism was run for an extended period, simulating typical cleaning operations. The motor's performance was monitored, and it remained stable and reliable over time. The brush's durability and resistance to wear were evaluated, and it retained its cleaning effectiveness.
7. Safety Considerations: The brush mechanism's safety features and potential risks were evaluated. It was ensured that the mechanism did not pose any hazards to the solar panels, the robotic system, or personnel. The brush mechanism operated safely in conjunction with the water system, minimizing risks of water leakage or electrical malfunctions.

8. Maintenance and Ease of Use: The ease of maintenance and user-friendliness of the brush mechanism were evaluated. The accessibility of components for cleaning, replacement, or adjustment was assessed. It was verified that the brush mechanism could be easily integrated and maintained within the overall robotic solar panel cleaner system. The use of screws for installation and assembly facilitated ease of removal of the system.

Table 25. FMEA Analysis

FMEA	Failure Mode and Effect Analysis								
	Product Name: Robotic Solar Panel Cleaner								
Item Number	**Item**	**Process Step**	**Potential Failure Mode**	**Potential Failure Effect**	**Severity**	**Occurrence**	**Detection**	**RPN**	**Risk Mitigation**
1-1-2-2	External Spur Gear	3D printed	Stringing and Oozing	Poor Quality material finish	9	8	4	288	Increase retraction speed
1-1-2-5	Wheel Rings		Layer shifting	Mechanical characteristic failure					Reduce the printing speed
1-1-4-1	Circular Brush		Dimensional inaccuracy	Part mating failure					Print the design with higher dimensions
1-1-4-5	Circular Brush Holder								
1-1-1-1/1-1-1-3/1-1-3-2/ 1-1-4-2	Chassis/Beams /Brush Case/ Box	CNC Machining	Dimensional Inaccuracy	Part mating failure	9	8	4	288	Machine the design with higher dimensions
1-1-2-1	Timing Belt	-	Improper Belt tension	Belt slippage	9	7	2	126	Place both Gears in a way that timing belt not too much in

									tension
1-1-1-2/1-1-2-4/1-1-2-6/ 1-1-3-3/1-1-4-4/1-1-4-3	Screws/ Bearing	-	Fatigue/Mechanical Failure	Vibration/ Excessive noise	9	6	2	126	selecting the correct fastener and understanding the preload necessary
1-1-4-1	Circular Brush	-	Wear due to high friction	Inefficient cleaning of solar panels	5	6	1	30	Use of high-quality brushes and avoid using synthetic brushes
1-2-1-1	12V /4.5A Lead Battery	-	Over heating	Battery life is reduced	6	8	3	144	Use of suitable batteries that can handle supplying power to the robot
			Expansion	Explosion of the battery	9	5	7	315	Use of high-quality Lead acid rechargeable batteries
1-2-1-2	Wires	-	Overheating	Poor Power Supply	5	7	6	210	Use of high-quality wires and cables
			Short Circuit	Damaging of electronic components	6	9	4	216	

			Entanglement	Loosening of wire connection	2	3	4	24	
1-2-1-1/ 1-2-2-2	12V Motors	-	Over heating	Damage of motor	5	10	3	150	Put usage limitation
			Winding and cable failure	Motor will not function	6	5	9	270	Use of high-quality motors
	12V Turbo Motors		Bearing Failure	Vibration and excessive noise	7	7	3	147	Use of high-quality bearings
1-3-1-1	Arduino Uno	-	Overload	Damage of electronic Components	8	7	3	168	Never connect numerous electronic components to one controller
			Short Circuit	Damage of electronic Components	6	7	4	168	Use of specific battery voltage
1-3-2-1	Phone Controller	-	Failure to connect	Losing slave control on the Robot	3	7	2	42	Use of stronger range and fast Bluetooth modules
1-4-1-1	Arduino Code	-	Software complications	Unexpected movements of the robot	5	5	1	25	Check for errors during coding

1-2-2-3	Motor Driver	-	Voltage imbalance	Robot will not move	8	2	8	128	Use proper Voltage which is 12 V
1-2-2-4	IR Sensor	-	failure of the transmitter	Unexpected movements of the robot	9	1	8	72	Cover the sensors to avoid water leakage
1-2-2-5	Ultrasonic Sensor	-	hardware failures of the ultrasound transducer	Unexpected movements of the robot	9	1	8	72	Cover the sensors to avoid water leakage

Table 26. FMEA scale for severity

(Scale of 1 [least severe] to 10[most severe])

Rating	Effect	Description
1	Minor	Unreasonable to expect minor nature of this failure will have any noticeable effect on item or system performance or subsequent process or assemble operation
2-3	Low	Slight deterioration of item or system performance or a slight inconvenience with a subsequent process or assembly operation
4-6	Moderate	Item or system performance deterioration. May result in unscheduled rework/repair/and/or damage to equipment
7-8	High	Inoperable item or system. May result in serious disruption to subsequent processing or assembly operation and/or require major rework.
9-10	Very High	Failure affects safety. May endanger machine or assembly operators. (9 with warning, 10 without warning)

Table 27. FMEA scale for Occurrence

(Scale of 1 [least frequent] to 10[most frequent])

Rating	**Effect**	**Description**
1	Remote	Failure unlikely. No failure ever associated with processes or identical processes.
2	Very low	Only isolated failures associated with this process or almost identical processes.
3-5	Low	Isolated failures associated with similar processes
6-7	Moderate	This process has occasional failures, but not in major proportions.
8-9	High	This process or similar processes have often failed
10	Very high	Failure is almost inevitable

Table 28. FMEA scale for Detection

(Scale of 1 [always detected] to 10[never detected])

Rating	Effect	Description
1-2	Very high	Certain to detect the failure mode
3-4	High	Good chance of detecting failure modes, process automatically detects failure mode.
5-6	Moderate	May detect the existence of failure mode
7-8	Low	Poor chance of detecting the existence of failure mode
9	Very low	Probably will not detect the existence of failure mode
10	Absolutely no detection	Will not or cannot detect the existence of failure.

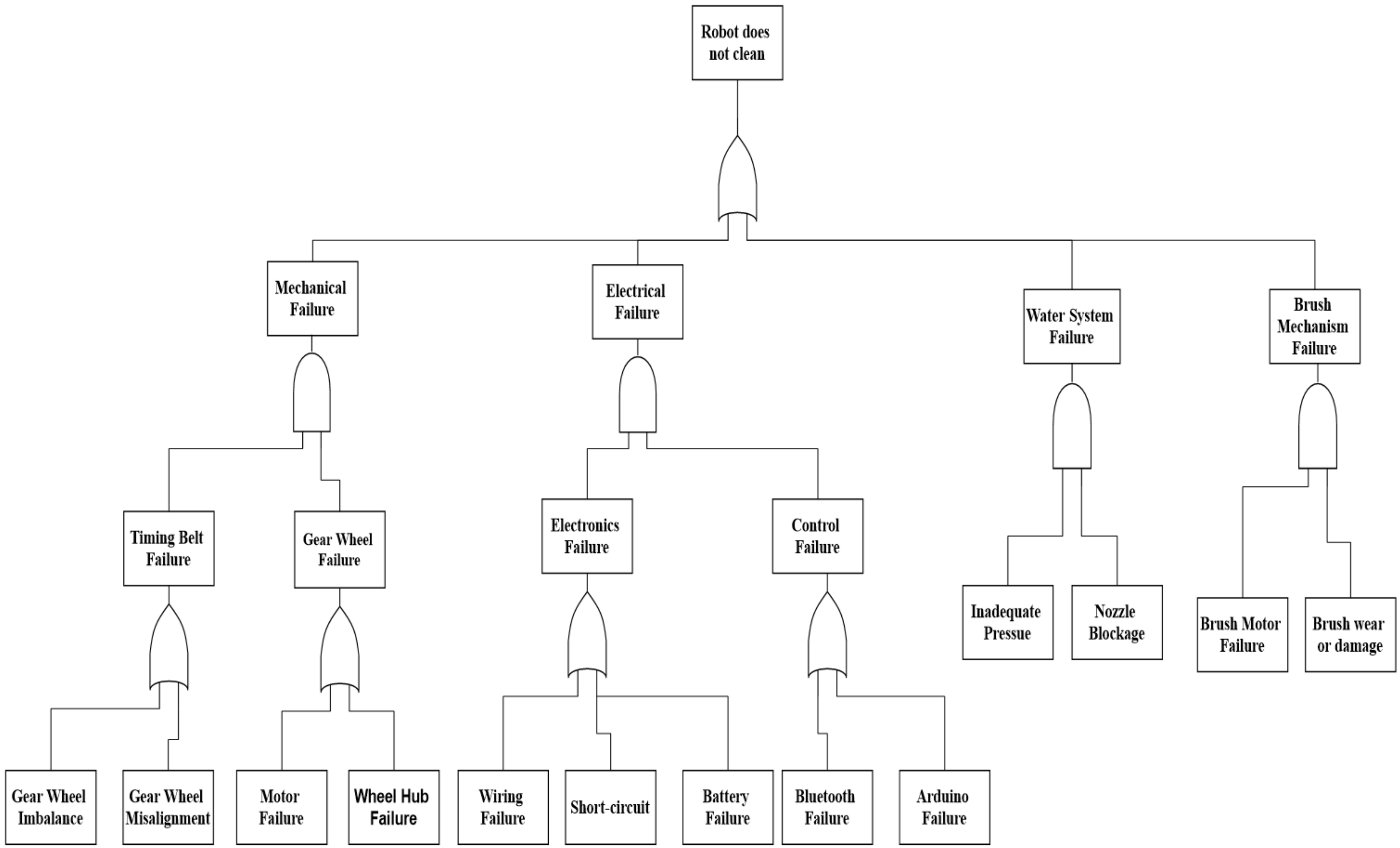

Figure 96. Fault Tree Analysis

5.2. Verification of the applied engineering standards

In the development of the robotic solar panel cleaner project, several engineering standards were applied across various aspects of the project, including design, manufacturing, testing, safety, and assembly. These standards played a crucial role in ensuring quality, safety, and adherence to industry best practices.

ISO 9001: The project implemented the guidelines outlined in ISO 9001 for the establishment of a quality management system. This standard ensured that quality processes were followed throughout the project, including design, manufacturing, testing, and documentation. By implementing ISO 9001, the project aimed to achieve consistent quality.

ISO 12100: The principles of risk assessment and risk reduction, as outlined in ISO 12100, were applied to the project. This standard guided the identification and mitigation of potential hazards in the design and manufacturing processes of the robotic solar panel cleaner. By adhering to ISO 12100, the project ensured the safety of operators and maintenance personnel.

ISO 13849: The safety requirements and design principles specified in ISO 13849 were followed in the control systems of the robotic solar panel cleaner. This standard ensured that safety-related control systems were designed and implemented correctly, minimizing risks and protecting against potential hazards.

IEC 60529: The project referred to IEC 60529 to select appropriate levels of protection for the components and enclosures of the robotic solar panel cleaner. This standard helped determine the degree of protection against solid objects, dust, water, and environmental factors, ensuring the durability and reliability of the system.

ANSI/RIA R15.06: The safety requirements outlined in ANSI/RIA R15.06 for industrial robots were considered during the development of the robotic solar panel cleaner. This standard provided guidelines for the safe design, installation, operation, maintenance, and training associated with industrial robots. By adhering to these safety requirements, the project ensured the safe operation of the robotic system.

ISO 9283: This standard guided the evaluation of performance criteria for industrial robots. It provided criteria and test methods to assess the performance of the robotic system, including accuracy, repeatability, and other essential characteristics.

EN 12975-2: This standard defined test methods for evaluating the performance of solar collectors. It was relevant to the project, as the robotic solar panel cleaner incorporated solar collectors.

ISO 9060: This standard pertained to instruments used for measuring hemispherical solar and direct solar radiation. It provided specifications and classifications for instruments used in solar energy measurement. It ensured accurate measurement of solar radiation in the project.

ISO/TR 23482-1:2020: This standard focused on safety-related test methods for robotics. It provided guidance on evaluating the safety aspects of the robotic solar panel cleaner and ensuring compliance with relevant safety standards.

CHAPTER 6 - RESULTS AND DISCUSSION

6.1. The Results

The project focused on designing and manufacturing an efficient and reliable robotic solar panel cleaner. Throughout the manufacturing and testing phases, the team encountered several challenges and implemented various improvements to enhance the robot's performance and reliability.

The robot was designed to move along the length of the panel, covering a width of 40 cm, and then rotate at the end to cover another 40 cm of width. A box located in the middle of the robot contained the battery, Arduino UNO, and motor driver. Additionally, two ultrasonic sensors were installed at the foreground of the robot to detect the edges of the panel. When the robot detected an edge, it gave an alert and then rotated to make a second cleaning pass.

To evaluate the towing ability of the robot, its movement speed and towing capacity were tested at a 15∘ incline to determine the optimal speed and towing capability for optimal performance.

The cleaning technique utilized an electromechanical system for solar panel cleaning. This system underwent careful inspection and refinement to ensure optimal effectiveness. Importantly, as the external system was not connected to the panels, it did not affect the true performance of the solar photovoltaic (SPV) system. However, the efficiency improvement value was relatively low in the tests conducted on 50 W SPV panels. It was noted that if the tests were performed on SPV modules with higher wattage ratings while maintaining the same surface area, the increase in efficiency would have been significantly greater.

To confirm the operational capabilities of the robot, a series of experimental testing scenarios were conducted. The tests focused on assessing the robot's effectiveness in both static and dynamic modes. Initially, the solar panel was intentionally covered with varying amounts of sand to replicate the process of dust accumulation. The robot was then deployed to clean the panel's surface. After two cleaning passes, the robot successfully removed over 80% of the accumulated dust on the panel. Subsequent tests yielded similar results, indicating consistent performance. However, due to the use of short brushes, some dust remained on the panel as the brushes did not cover the entire width of the surface.

The robot's capability to operate on panels with varying degrees of tilt was also evaluated. The maximum angle at which the robot remained effective was determined by placing the robot on a panel equipped with a tilt sensor and manually tilting the panel while the robot was in operation. It was found that the robot is capable of cleaning solar panels at tilt angles ranging from 0∘ to 40∘.

6.1.1. Discussion

During the project, the team encountered significant challenges related to 3D printing. The process proved to be time-consuming and resulted in a lack of accuracy for some printed parts, particularly the wheels. The lack of balance in the 3D printed wheels caused vibrations and instability during operation, compromising the overall performance of the robotic solar cleaner. To address this issue, the team redesigned the wheels, incorporating a larger wheel hub that provided a stronger connection to the motor shaft. This modification minimized wobbling and enhanced stability during movement.

The lack of balance in the wheels also affected the alignment and tension of the timing belts. The uneven weight distribution caused the timing belts to move off-track as the wheels rotated, impacting the accuracy and performance of the robotic solar cleaner. To mitigate this issue, the team added rings on the sides of the wheels to act as guides, keeping the timing belts aligned and preventing them from slipping off the wheels.

In addition to the 3D printing challenges, the project faced supply chain and component availability issues. The unavailability of rubber tank treads specifically designed for the robotic solar cleaner led the team to use timing belts sourced from cars as an alternative solution. This adaptation required additional design considerations and modifications to ensure compatibility and functionality.

To mitigate filament shortage and power cuts during the 3D printing process, the team focused on proper inventory management of filament supplies and implemented backup power solutions to minimize disruptions and maintain manufacturing efficiency.

These challenges and their corresponding solutions show the iterative nature of the manufacturing process and the need for continuous improvement. The issues faced with 3D printing accuracy, wheel balancing, and timing belt alignment prompted redesigns, modifications, and the introduction of additional components such as rings for improved performance. The adaptability and problem-solving skills of the project team played a crucial role in overcoming these challenges and ensuring the overall reliability and functionality of the robotic solar cleaner.

6.2 The Engineering Standards

As previously stated, ISO 17212:2004 outlines the standard procedures for preparing component surfaces prior to bonding for both laboratory evaluation and construction purposes.

In accordance, ISO 45001 Occupational Health and Safety standard was used during testing and assembly with this standard, protective gloves and safety goggles were used to ensure maximum compliance with safety regulations.

The plastic filament utilized in the project adhered to engineering standards, including ISO 9001:2015 for Quality Management Systems. Since all of the filament used was recycled material, compliance with this standard ensured the efficient application of the system.

ISO 17295:2023

Additive manufacturing — General principles — Part 1 positioning, coordinates and orientation

ISO 17296-2:2015

Additive manufacturing — General principles — Part 2: Overview of process categories and feedstock

ISO 17296-3:2014

Additive manufacturing — General principles — Part 3: Main characteristics and corresponding test methods

6.3. The Constraints

During the project, several constraints were encountered:

- **Economic limitations:** as all parts had to be procured within the financial budget allocated for the project.
- **Availability:** due to low production of parts for ultrasonic metal welding, some parts were either out of stock or unavailable. This issue was resolved by switching to ultrasonic plastic welding.
- **Supply Chain Challenges and Customs Regulations:** as most of the parts were ordered overseas, there were delays in their arrival due to customs regulations in both Turkey and the TRNC.
- **Safety:** This was also a top priority, and all necessary precautions were taken to ensure a safe workshop environment.
- **Environmental:** concerns were taken into account, and all waste produced during the project was disposed of in a safe and environmentally friendly manner, also 3D printing can be tricky, which is why using recycled materials and minimizing waste is important. It's crucial to be careful when consuming plastic filament to avoid unnecessary waste and minimize the impact on the environment in case of design errors.
- **Manufacturability:** the project was limited on using 3D printing and making the chassis from aluminum.

CHAPTER 7 - CONCLUSION AND FUTURE WORKS

7.1. The Conclusion

In conclusion, the robotic solar cleaner project has successfully designed and manufactured an efficient and reliable device for cleaning solar panels. Throughout the manufacturing and testing phases, the project team encountered various challenges and implemented several improvements to enhance the performance and reliability of the robot.

The project addressed the challenge of 3D printing accuracy by redesigning the wheels with a larger wheel hub, minimizing vibrations and instability during operation. Additionally, the team introduced rings on the sides of the wheels to keep the timing belts aligned, overcoming the issue of off-track movement.

Supply chain and component availability issues were overcome by adapting timing belts sourced from cars as an alternative solution to unavailability of rubber tank treads. The team made necessary design considerations and modifications to ensure compatibility and functionality.

The project also focused on proper inventory management of filament supplies and implemented backup power solutions to mitigate filament shortage and power cuts during the 3D printing process, ensuring manufacturing efficiency.

The robot's operational capabilities were confirmed through experimental testing scenarios, demonstrating its effectiveness in both static and dynamic modes. The robot successfully removed over 80% of accumulated dust on the panel following two cleaning passes, indicating consistent performance. However, improvements could be made to the brush design to cover the entire width of the surface, reducing remaining dust.

The robot showcased its capability to clean solar panels at tilt angles ranging from 0° to 40°, ensuring its versatility and effectiveness on panels with varying degrees of tilt.

Future works for the robotic solar cleaner project include enhancements to the mechanical system, electrical system, control system, and other relevant systems. These include further optimization of the cleaning mechanism, integration of weather sensors for adaptive cleaning, development of self-diagnostic capabilities for maintenance, and implementation of data logging and analysis for performance optimization.

Overall, the project's iterative design process, adaptability, and problem-solving approach played a crucial role in overcoming challenges and enhancing the performance and reliability of the robotic solar cleaner. By addressing various issues, the project team has ensured the effectiveness of the device in cleaning solar panels, contributing to improved efficiency and sustainability in the field of solar energy.

7.2. The Future Works

The robotic solar panel cleaner project has achieved significant progress in designing and manufacturing an efficient device for cleaning solar panels. However, there are several areas where further improvements can be made to enhance the mechanical system, electrical system, control system, and other relevant systems. Here are some potential areas for future development:

7.2.1. Mechanical System Improvements

Enhanced Brush Design: The existing short brushes used in the cleaning mechanism may leave some dust on the panel surface. Future work can focus on developing longer brushes or alternative cleaning mechanisms that cover the entire width of the panel, ensuring more thorough cleaning.

Lightweight and Balanced Design: To improve stability and performance, efforts can be made to optimize the weight distribution of the robot, reduce unnecessary components, and explore lightweight materials for the chassis and other structural elements.

Interchangeable Components: Introducing modular design principles can facilitate easier maintenance and replacement of components, allowing for quick repairs and upgrades as needed.

7.2.2. Electrical System Improvements

Power Optimization: Investigate energy-efficient components and power management techniques to maximize the robot's operating time and minimize energy consumption. This can involve optimizing the battery capacity, improving power conversion efficiency, and implementing smart power management algorithms.

Remote Monitoring and Control: Incorporate remote monitoring and control capabilities to enable real-time status monitoring, diagnostics, and remote operation of the robot. This could involve integrating wireless communication modules and a user-friendly interface for remote access.

7.2.3. Control System Improvements:

Sensor Fusion and Advanced Navigation: Explore sensor fusion techniques, such as combining ultrasonic sensors with other sensors like LiDAR or cameras, to enhance the robot's perception capabilities and enable more precise navigation and obstacle avoidance.

Autonomous Operation: Develop advanced control algorithms and artificial intelligence techniques to enable autonomous operation of the robot. This can involve path planning, localization, and decision-making algorithms to optimize cleaning routes, adapt to varying panel configurations, and handle dynamic environmental conditions.

Improved Edge Detection: Refine the edge detection system using ultrasonic sensors or other suitable technologies to enhance the accuracy and reliability of identifying panel edges, reducing false alerts, and ensuring complete coverage during cleaning operations.

Weather and Environmental Adaptability: Consider integrating weather sensors to enable the robot to adapt its cleaning operations based on weather conditions. For example, the robot could automatically adjust its cleaning schedule or intensity during rainy or dusty periods.

Maintenance and Self-Diagnosis: Develop self-diagnostic capabilities to detect system faults or abnormalities and provide proactive alerts or troubleshooting guidance to ensure timely maintenance and minimize downtime.

Data Logging and Analysis: Implement data logging capabilities to collect performance metrics, cleaning efficiency, and environmental data for analysis. This data can be used to optimize cleaning strategies, track panel performance over time, and identify patterns or trends related to dust accumulation.

Future Work: Autonomous Robot Mechanism

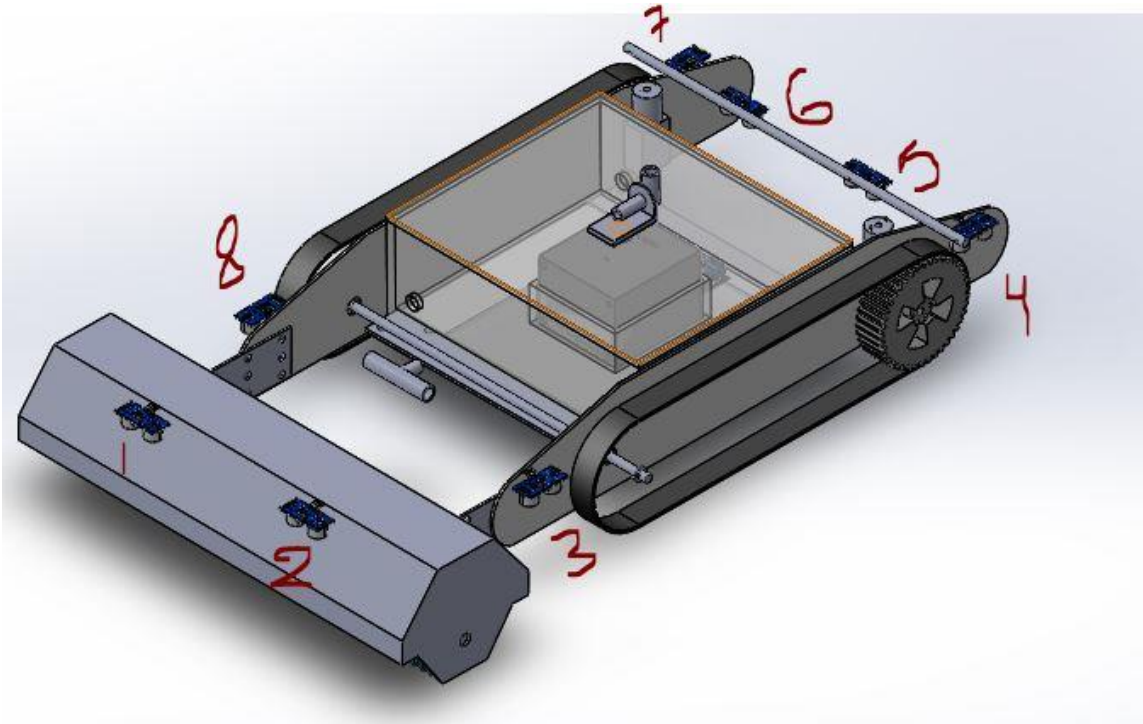

Use waterproof sensor

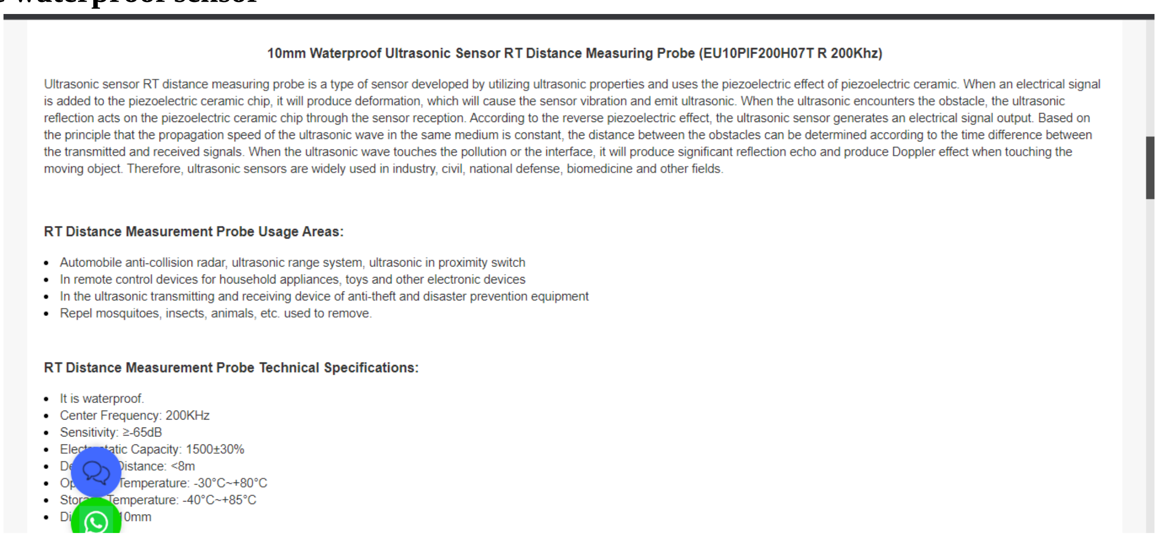

10mm Waterproof Ultrasonic Sensor RT Distance Measuring Probe (EU10PIF200H07T R 200Khz)

Ultrasonic sensor RT distance measuring probe is a type of sensor developed by utilizing ultrasonic properties and uses the piezoelectric effect of piezoelectric ceramic. When an electrical signal is added to the piezoelectric ceramic chip, it will produce deformation, which will cause the sensor vibration and emit ultrasonic. When the ultrasonic encounters the obstacle, the ultrasonic reflection acts on the piezoelectric ceramic chip through the sensor reception. According to the reverse piezoelectric effect, the ultrasonic sensor generates an electrical signal output. Based on the principle that the propagation speed of the ultrasonic wave in the same medium is constant, the distance between the obstacles can be determined according to the time difference between the transmitted and received signals. When the ultrasonic wave touches the pollution or the interface, it will produce significant reflection echo and produce Doppler effect when touching the moving object. Therefore, ultrasonic sensors are widely used in industry, civil, national defense, biomedicine and other fields.

RT Distance Measurement Probe Usage Areas:

- Automobile anti-collision radar, ultrasonic range system, ultrasonic in proximity switch
- In remote control devices for household appliances, toys and other electronic devices
- In the ultrasonic transmitting and receiving device of anti-theft and disaster prevention equipment
- Repel mosquitoes, insects, animals, etc. used to remove.

RT Distance Measurement Probe Technical Specifications:

- It is waterproof.
- Center Frequency: 200KHz
- Sensitivity: ≥-65dB
- Elec[illegible]tatic Capacity: 1500±30%
- De[illegible]Distance: <8m
- Op[illegible] Temperature: -30°C~+80°C
- Stor[illegible] Temperature: -40°C~+85°C
- Di[illegible]10mm

Use arduino mega since we need a lot of input and output pins, then :
connect ultra s.1 trig , echo to 2,3 .
connect ultra s.1 trig , echo to 4,5
connect ultra s.1 trig , echo to 6,7
connect ultra s.1 trig , echo to 8,9
connect ultra s.1 trig , echo to 10,11
connect ultra s.1 trig , echo to 12,13
connect ultra s.1 trig , echo to 14,15
connect ultra s.1 trig , echo to 16,17

CODE:

```
void setup() {
  int trigpin1=2;
  int echopin1=3;
  int trigpin2=4;
  int echopin2=5;
  int trigpin3=6;
  int echopin3=7;
  int trigpin4=8;
  int echopin4=9;
  int trigpin5=10;
  int echopin5=11;
  int trigpin6=12;
  int echopin6=13;
  int trigpin7=14;
  int echopin7=15;
  int trigpin8=16;
  int echopin8=17;
  int enA=18;
  int in1=19;
  int in2=20;

  int enB=21;
  int in3=22;
  int in4=23;
  int speed=255;
}

void loop() {
  long duration1 , distance1,duration1 , distance2,duration2 , distance3,duration3 ,
distance4,duration4 , distance5,duration5 , distance6,duration6 , distance7,duration7 ,
distance8,duration8;
  digitalWrite(trigpin1,HIGH);
  delayMicroseconds(1000);
  digitalWrite(trigpin1,LOW);
  duration1=pulseIn(echopin1,HIGH);
  distance1=(duration1/2)/29.1;

  digitalWrite(trigpin2,HIGH);
  delayMicroseconds(1000);
  digitalWrite(trigpin2,LOW);
  duration2=pulseIn(echopin2,HIGH);
  distance2=(duration2/2)/29.1;

digitalWrite(trigpin3,HIGH);
  delayMicroseconds(1000);
  digitalWrite(trigpin3,LOW);
  duration3=pulseIn(echopin3,HIGH);
  distance3=(duration3/2)/29.1;

digitalWrite(trigpin4,HIGH);
  delayMicroseconds(1000);
  digitalWrite(trigpin4,LOW);
  duration4=pulseIn(echopin4,HIGH);
```

```
  distance4=(duration4/2)/29.1;

  digitalWrite(trigpin5,HIGH);
  delayMicroseconds(1000);
  digitalWrite(trigpin5,LOW);
  duration5=pulseIn(echopin5,HIGH);
  distance5=(duration5/2)/29.1;

  digitalWrite(trigpin6,HIGH);
  delayMicroseconds(1000);
  digitalWrite(trigpin6,LOW);
  duration6=pulseIn(echopin6,HIGH);
  distance6=(duration6/2)/29.1;

  digitalWrite(trigpin7,HIGH);
  delayMicroseconds(1000);
  digitalWrite(trigpin7,LOW);
  duration7=pulseIn(echopin7,HIGH);
  distance7=(duration7/2)/29.1;

  digitalWrite(trigpin8,HIGH);
  delayMicroseconds(1000);
  digitalWrite(trigpin8,LOW);
  duration8=pulseIn(echopin8,HIGH);
  distance8=(duration8/2)/29.1;
  delay(10);

if   (distance1>10 and distance2>10 ){
  foward();
}
else if (distance1 <10 and distance1<10){
if (distance2>10 and distance2>10){
  left();
  else{
    right();
  }

}

}

}
void forward(){

  analogWrite(enA,speed);
  digitalWrite(in1,HIGH);
  digitalWrite(in2,LOW);

  analogWrite(enB,speed);
  digitalWrite(in3,HIGH);
  digitalWrite(in4,LOW);

}
void backward()
```

```
{
  analogWrite(enA,speed);
  digitalWrite(in1,LOW);
  digitalWrite(in2,HIGH);

  analogWrite(enB,speed);
  digitalWrite(in3,LOW);
  digitalWrite(in4,HIGH);
}
void left(){

  analogWrite(enA,speed);
  digitalWrite(in1,LOW);
  digitalWrite(in2,HIGH);

  analogWrite(enB,speed);
  digitalWrite(in3,HIGH);
  digitalWrite(in4,LOW);
}
void right(){
  analogWrite(enA,speed);
  digitalWrite(in1,HIGH);
  digitalWrite(in2,LOW);

  analogWrite(enB,speed);
  digitalWrite(in3,LOW);
  digitalWrite(in4,HIGH);
}
void stop(){
    analogWrite(enA,0);
    digitalWrite(in1,LOW);
    digitalWrite(in2,LOW);

    analogWrite(enB,0);
    digitalWrite(in3,LOW);
    digitalWrite(in4,LOW);
}
```

After finishing the movement, the whole pathway will be scanned and evaluated.

Table 29. Robot Physiology

Waste level	Low	Moderate	High
Brush level	At the surface	Little force	High force
Motor speed	High	Moderate	low
Brush motor speed	Moderate	Moderate	High
Battery consumption	Low	Moderate	High
Water pressure	Low	Low	High

Figure 97 Industrial Solar Panels

Moreover, for more accurate scanning and more accurate cleaning IR sensor is replaced by camera implemented with image processing technology which can analyze the image and tell the percentage of dirtiness, so the robot will respond on these data. After scanning the whole area and analyzing the data , the algorithm in the robot will find the best route which can finish the cleaning in less power and more efficient . This technology will help a lot in saving power and having higher efficiency because in this technology you will use high technology algorithm which will calculate the best route for more better cleaning and after this route is chosen it will have the ability to save it. so, you can let the robot clean in the night when there is no sun, this will be a perfect timing for cleaning.

For this technology we have done many researches on the implementation so first of all need for our project we need a good processor and a perfect camera quality for us raspberry pi camera will be good with a jatson nano processor and a big memory will be required, after having the components ,the step of machine learning will be the next step , so a big data set required like almost 2000 pictures or higher, the much higher the much better and the efficiency of the robot will be much higher, after that the this images should be annotated and the target should be separated in each picture , then these images should be used with proper python code , after the iteration will finish , we will have a ready dust and soil detector module.

There are many ready modules to use in roboflow website we can just use it and may update it with more larger data set this will help in improving the recognition.

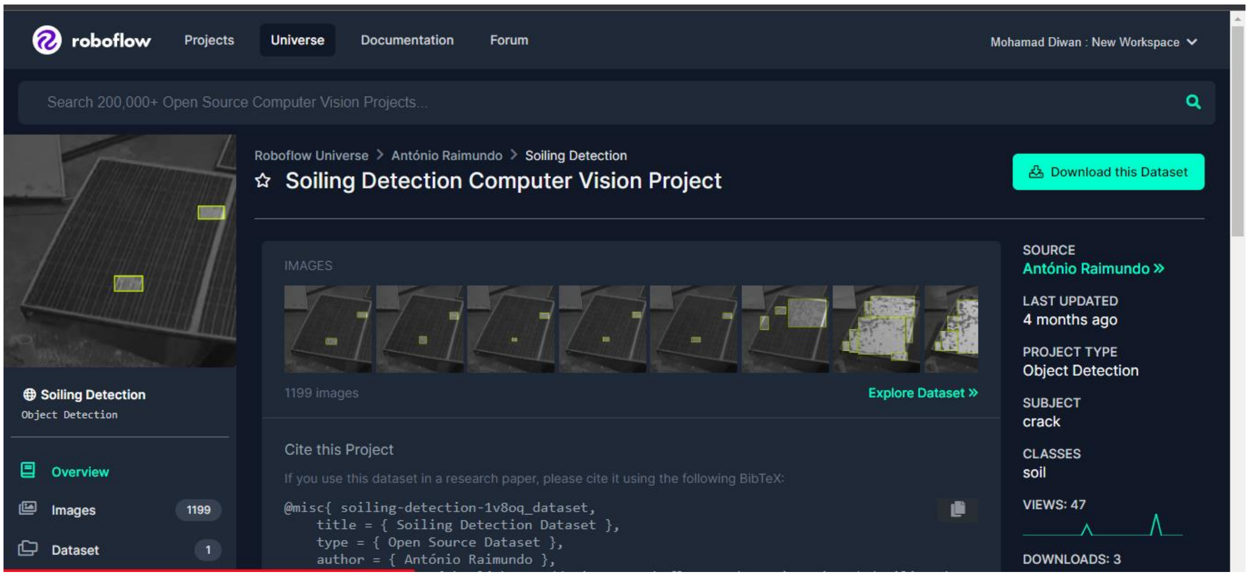

Figure 98. Soiling detection module.

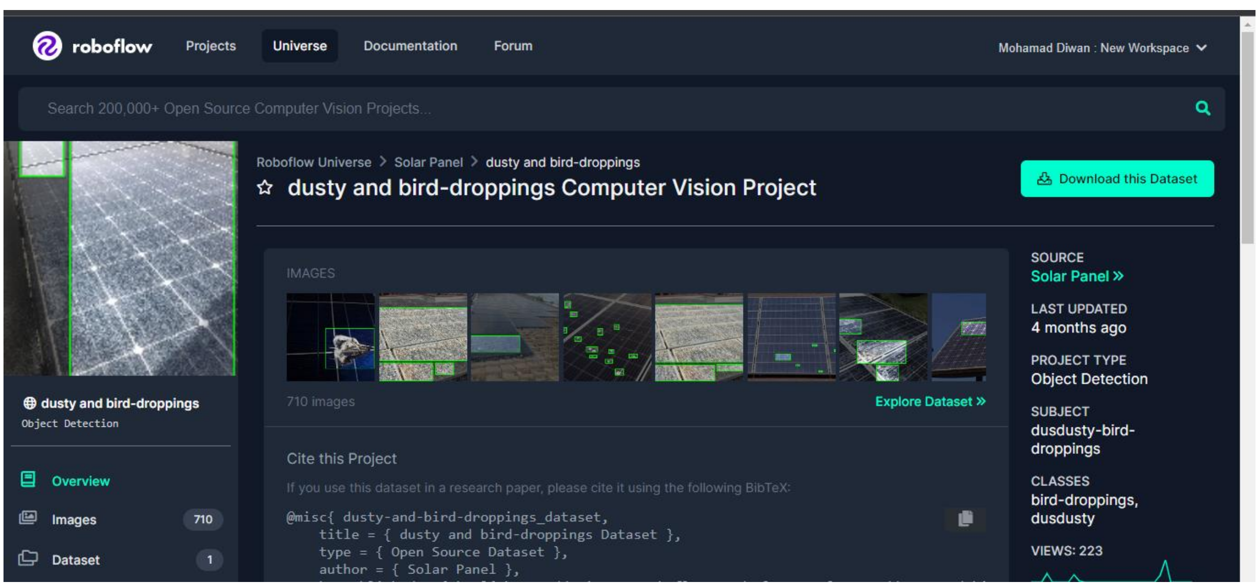

Figure 99. dusty and bird dropping detection.

Figure 100. raspberry pi camera

Figure 101. Jatson nano.

Future Work: Automated Brush Case:

Not all the areas in the panels have the same percentage of wastes so sometimes it is not necessary to have a high pressure brush on the panel, and some other times when the waste is sticky, it may need a higher pressure with slower movement for this feature the robot will have the ability to save some energy and to have a perfect cleaned panel at the same time.

The mechanism can be done by the help of stepper motor and two gears and belt. the stepper motor will control the level of orientation, and this stepper motor will be controlled by the Arduino.

This is an example of how it should be implemented:

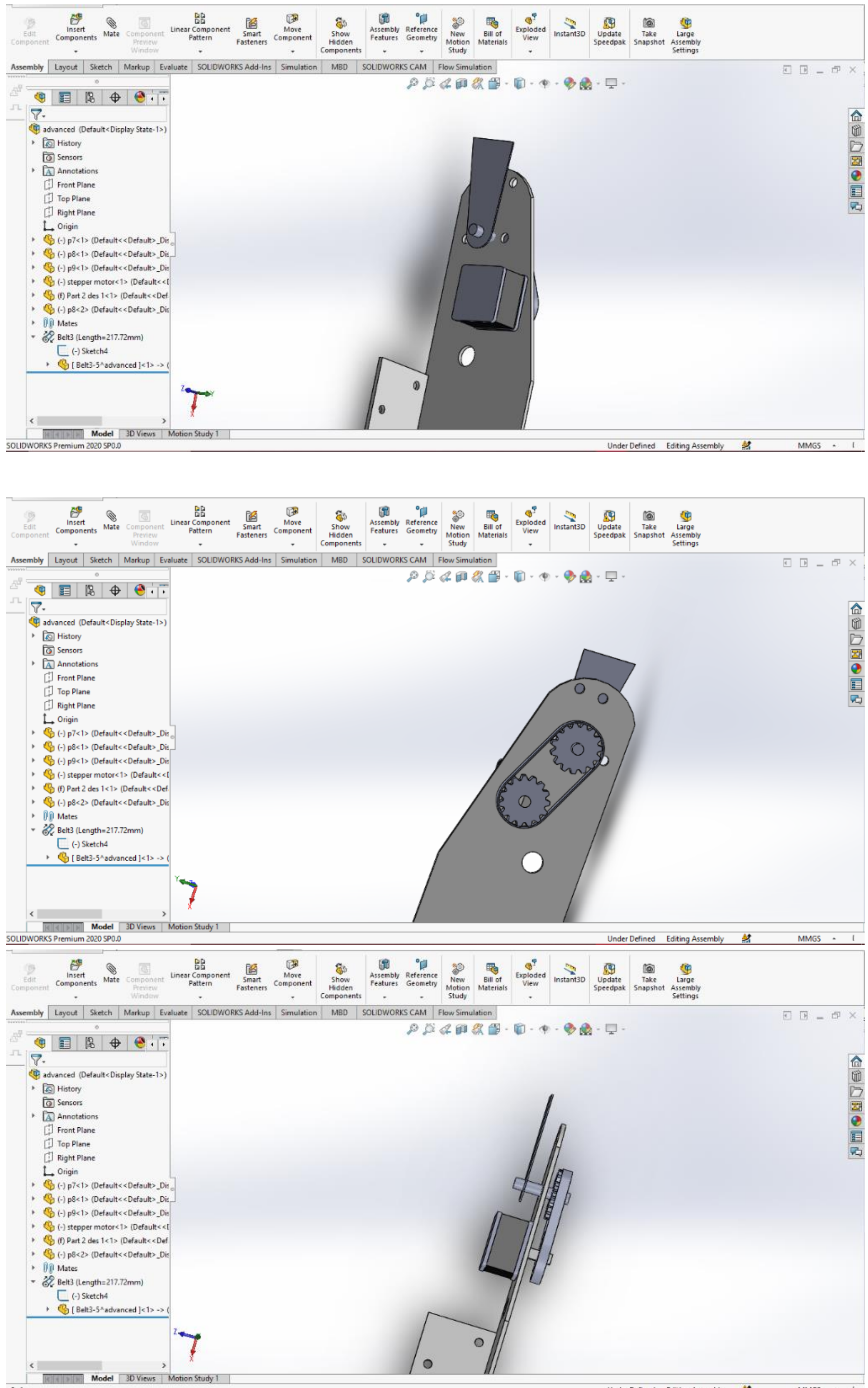

Figure 102. solid work drawing of the autonomous brush

REFERENCES

1. Arduino Cloud. (n.d.). Retrieved December 31, 2022, from https://create.arduino.cc/projecthub/Aboubakr_Elhammoumi/real-time-data-acquisition-of-solar-panel-using-arduino-2c4705

2. Bentork. (2022). *Solar Panel Cleaning Robots Battery Manufacturers Pune India & Suppliers.* https://bentork.com/robotics-batteries-solar-panel-cleaning-robot/

3. Botland. (n.d.). *Buy aluminium mounting hub 8mm M3*. https://botland.store/adapters-for-motors/9611-aluminium-mounting-hub-8mm-m3-2pcs-pololu-5904422372422.html

4. Clean Solar Solutions Ltd. (2020, September 30). *Solar panel cleaning robots*. https://cleansolar.solutions/specialist-solutions/solar-panel-cleaning-robots/

5. Collins, D. (2020, June 17). *How to specify pulleys for synchronous belt drive systems*. Linear Motion Tips. https://www.linearmotiontips.com/how-to-specify-pulleys-for-synchronous-belt-drives/

6. Ecoppia. (n.d.). Robotic Solar Panel Cleaning Services for Utility-Scale PV Sites | Ecoppia. https://www.ecoppia.com/

7. Electrosal. (n.d.). *Automatic solar panel cleaning robot using Arduino*. https://www.electrosal.com/product/automatic-solar-panel-cleaning-robot-using-arduino/

8. GmbH, L. (n.d.). *Flat fan nozzles | Lechler US*. https://www.lechlerusa.com/en/products/product-by-type/flat-fan-nozzles

9. Gupta, U. (2022, November 1). *Affordable robotic cleaning solution for solar panels*. https://www.pv-magazine.com/2022/11/01/affordable-robotic-cleaning-solution-for-solar-panels/

10. Hanim, Faridah & Yaakub, Muhamad & Mohd Nordin, Ili Najaa Aimi & Sahari, Norain & Zambri, Aira & Sy Yi, Sim & Saibon, Muhammad. (2020). Development of solar panel cleaning robot using Arduino. Indonesian Journal of Electrical Engineering and Computer Science. 19. 1245. 10.11591/ijeecs.v19.i3.pp1245-1250.

11. IEEE xplore. (n.d.). *Design and implementation of automatic robot for floating* https://ieeexplore.ieee.org/abstract/document/9402482/

12. IEEE Xplore. (n.d.). *Rooftop solar panel cleaning robot using Omni wheels*. https://ieeexplore.ieee.org/abstract/document/8448530/

13. IEEE (n.d) *A fully portable robot system for cleaning solar panels*. Retrieved December 31, 2022, from https://ieeexplore.ieee.org/abstract/document/7373479/

14. International Organization for Standardization. (2012a). Robots and robotic devices — Safety requirements for industrial robots — Part 1: Robots.

15. International Organization for Standardization. (2012b). Robots and robotic devices — Vocabulary.

16. IRJET. (n.d.). *Design of Robotic Cleaning System for Industrial Solar Panel Arrays*. IRJET- International Research Journal of Engineering and Technology. https://www.irjet.net/archives/V7/i11/IRJET-V7I11141.pdf

17. ISO - Standards. (n.d.). https://www.iso.org/standards.html

18. Khadka, Nasib & Bista, Aayush & Adhikari, Binamra & Shrestha, Ashish & Bista, Diwakar. (2020). Smart solar photovoltaic panel cleaning system. IOP Conference Series: Earth and Environmental Science. 463. 012121. 10.1088/1755-1315/463/1/012121.

19. KG, n. N. (n.d.). *Tension pulleys | norelem*. https://www.norelem.com/us/en/Products/Product-overview/Systems-and-components-for-machine-and-plant-construction/22000-Drive-technology/Toothed-belt-pulleys-Splined-shaft-Timing-belts/22102-Tension-pulleys.html

20. KU Leuven. (n.d.). *The development of a cleaning robot for PV panels*. Kegeleers. https://iiw.kuleuven.be/onderzoek/eavise/mastertheses/kegeleers.pdf

21. Michele Gabrio Antonelli, Pierluigi Beomonte Zobel, Andrea De Marcellis, Elia Palange,

    Autonomous robot for cleaning photovoltaic panels in desert zones, https://doi.org/10.1016/j.mechatronics.2020.102372.

22. Natarajan, K. (2020, January 1). *Fault detection of solar PV system using SVM and thermal image processing*. International Journal of Renewable Energy Research. https://www.academia.edu/73290415/Fault_Detection_of_Solar_PV_System_Using_SVM_and_Thermal_Image_Processing

23. Natarajan, K. (2020, January 1). *Fault detection of solar PV system using SVM and thermal image processing*. International Journal of Renewable Energy Research. Retrieved December 31, 2022, from

24. Nevon Projects. (2021, August 2). *Solar panel cleaning robot*. https://nevonprojects.com/solar-panel-cleaning-robot/

25. New Atlas. (2014, April 4). *Jaguar installs UK's largest rooftop solar array*. https://newatlas.com/uk-largest-solar-array-jaguar-land-rover/31503/

26. Nguyen, M.T.; Truong, C.T.; Nguyen, V.T.; Duong, V.T.; Nguyen, H.H.; Nguyen, T.T. Research on Adhesive Coefficient of Rubber Wheel Crawler on Wet Tilted Photovoltaic Panel. Appl. Sci. 2022, 12, 6605. https://doi.org/10.3390/ app12136605

27. Occupational Safety and Health Administration. (2012). Hazard Communication.

28. Owano, N. (2013, December 2). *Robot with brush, water, wiper tackles solar panel cleaning*. Phys.org. Retrieved December 28, 2022, from https://phys.org/news/2013-12-robot-wiper-tackles-solar-panel.html

29. *Photovoltaic solar panel cleaning brush for robot*. Anhui Dasion Brush Co.,Ltd. (n.d.). https://www.dasionbrush.com/photovoltaic-solar-panel-cleaning-brush-for-robot_p24.htm

30. Qdah, K. , Abdulqadir, S. , Harbi, N. , Soqyyah, A. , Isa, K. , Alharbi, M. and Binsaad, N. (2019) Design and Performance of PV Dust Cleaning System in Medina Region. *Journal of Power and Energy Engineering*, **7**, 1-14. doi: 10.4236/jpee.2019.711001.

31. ResearchGate. (n.d.). *Development of solar panel cleaning robot using Arduino*. https://www.researchgate.net/publication/344027601_Development_of_solar_panel_cleaning_robot_using_Arduino

32. ResearchGate. (n.d.). *Smart solar photovoltaic panel cleaning system*. https://www.researchgate.net/publication/340490331_Smart_solar_photovoltaic_panel_cleaning_system

33. SCIRP Open Access. (2019, November 12). *Design and performance of PV dust cleaning system in Medina region*. https://www.scirp.org/html/1-1770660_96319.htm

34. Smart Prototyping. (n.d.). *Dual H-bridge motor driver L298N*. https://www.smart-prototyping.com/L298N-Dual-H-bridge-Motor-Driver-Board

35. SolarCleano. (n.d.). *F1 | SolarCleano*. https://solarcleano.com/en/products/solar-panel-cleaning-robot-f1

36. *Solar panel brushes save time on big cleaning jobs*. J. Racenstein Company, LLC. (n.d.). Retrieved December 31, 2022, from https://www.jracenstein.com/learn/expert-

37. Solar Panel Cleaning Robots. (n.d.). Retrieved December 31, 2022, from https://www.portescap.com/en/industries-supported/motors-for-robotics/solar-panel-cleaning-robots

38. Solarduino. (2020, January 12). *Infrared (IR) sensor module with Arduino*. A blog about DIY solar and arduino projects. https://solarduino.com/infrared-ir-sensor-module-with-arduino/

39. Svarc, J. (2022, December 12). *Best solar battery systems 2022*. CLEAN ENERGY REVIEWS. https://www.cleanenergyreviews.info/blog/best-solar-battery-systems#

40. Taylor & Francis. (2021). *A self-powered solar panel automated cleaning system: Design and testing analysis*. https://www.tandfonline.com/doi/full/10.1080/15325008.2021.1937400

41. The American Society of Mechanical Engineers. (2004). Unified Inch Screw Threads (UN and UNR Thread Form).

42. *The components for solar panel cleaning robot (1. Brush, 2. wheels, 3* ... (n.d.). https://www.researchgate.net/figure/The-components-for-solar-panel-cleaning-robot-1-brush-2-wheels-3-support-wheel-4_fig1_336867266

43. Verma, D. (2022, January 9). *Android phone controlled robot using Arduino*. Engineers Garage. https://www.engineersgarage.com/android-phone-controlled-robot-using-arduino/

44. Wikimedia Foundation. (2022, December 29). *Solar panel*. Wikipedia. https://en.wikipedia.org/wiki/Solar_panel

45. Taylor & Francis. (2021). A self-powered solar panel automated cleaning system: Design and testing analysis. https://www.tandfonline.com/doi/full/10.1080/15325008.2021.1937400

46. The American Society of Mechanical Engineers. (2004). Unified Inch Screw Threads (UN and UNR Thread Form).

47. The components for solar panel cleaning robots (1. Brush, 2. wheels, 3 ... (n.d.). https://www.researchgate.net/figure/The-components-for-solar-panel-cleaning-robot-1-brush-2-wheels-3-support-wheel-4_fig1_336867266

48. Verma, D. (2022, January 9). Android phone-controlled robot using Arduino. Engineers Garage. https://www.engineersgarage.com/android-phone-controlled-robot-usingarduino/

49. Wikimedia Foundation. (2022, December 29). Solar panel. Wikipedia. https://en.wikipedia.org/wiki/Solar_panel

APPENDIX A: ELECTRONIC MEDIA

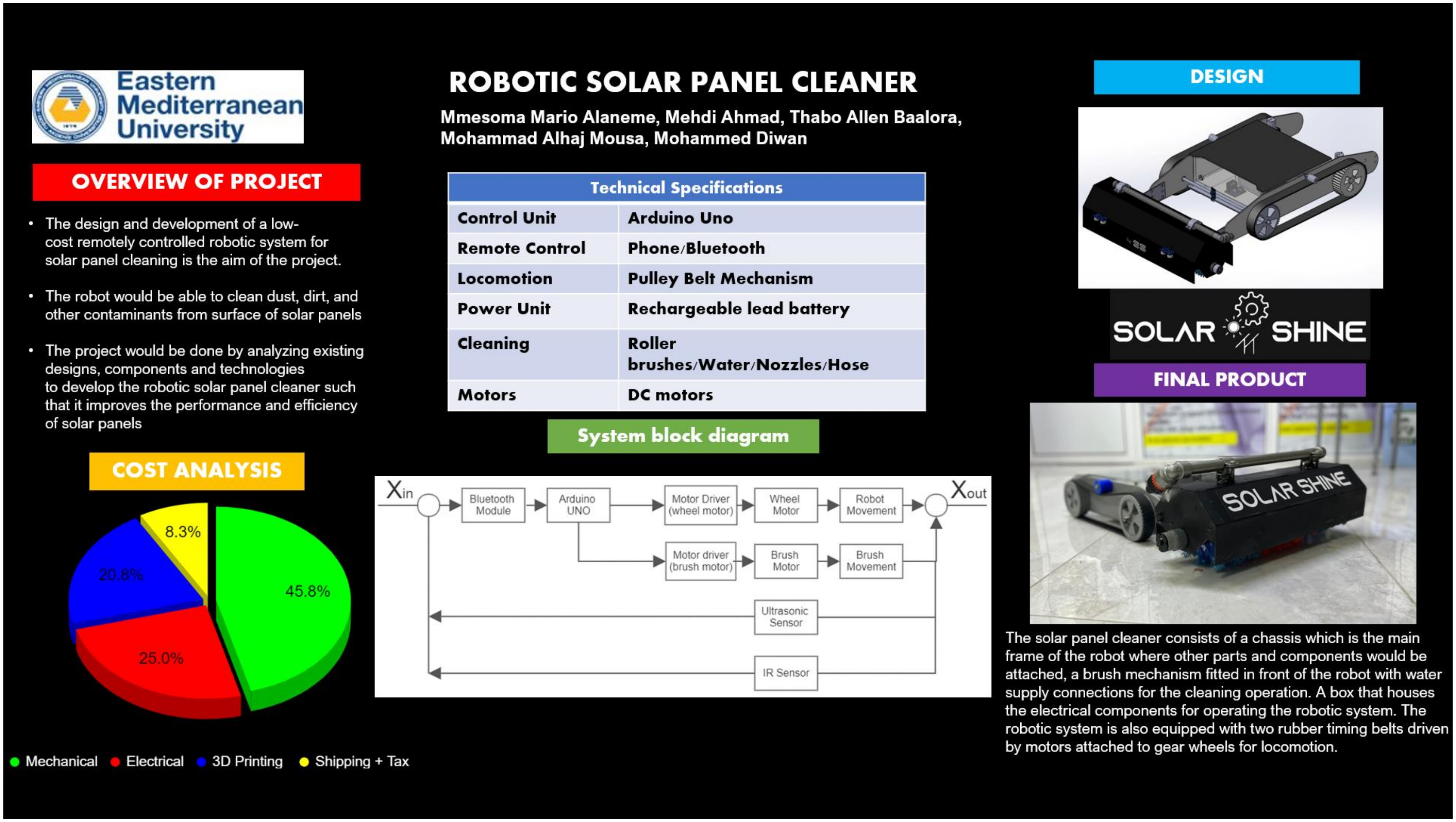

More information can be found on our website: http://www.solarshineprojectemu.com/

APPENDIX B: STANDARDS

ISO 8373:2012: Robots and robotic devices — defines terms used in relation with robots and robotic devices operating in both industrial and non-industrial environments.

ISO 9283: This standard specifies the performance evaluation of servo drives for electric traction drives. It is often used in robotic systems to ensure the accuracy and reliability of the robot's movements.

ISO 9787:2013: Robots and robotic devices — Coordinate systems and motion nomenclatures

ISO/TS 15066: This standard specifies the safety requirements for collaborative robots, which are robots that are designed to work safely alongside humans in a shared workspace. It covers the design, construction, installation, operation, and maintenance of collaborative robots, with the aim of ensuring the safety of human workers and other people who may come into contact with the robot.

ISO/DIS 10218-2 ROBOTICS — Safety requirements for robot systems in an industrial environment — PART 2: Robot systems, robot applications and robot cells integration.

ISO 5593: This standard specifies the general requirements for the design and construction of gears and gearboxes. It covers the materials, dimensions, tolerances, and performance requirements of gears and gearboxes, and is relevant to the mechanical subsystem of a robotic solar cleaner that uses gears to transmit power and motion.

IEC 61131-3: This standard specifies the programming languages, programming systems, and user interfaces for programmable controllers. It is widely used in robotic systems to enable the control and automation of the robot's movements and functions.

IEC 62443: This standard specifies the security requirements for industrial control systems, including robotic systems. It covers the design, construction, installation, operation, and maintenance of these systems, with the aim of ensuring their security against cyber threats.

ASTM D2303-20e1: Standard Test Methods for Liquid-Contaminant, Inclined-Plane Tracking and Erosion of Insulating Materials

ISO/TR 20218-2:2017 International organization of standardization - Safety design for industrial robot systems

ISO/CD 10218 International organization of standardization – safety requirements for industrial robots

IEC 60909: This standard specifies the methods for the calculation of short-circuit currents in three-phase a.c. systems. It is often used in robotic systems to ensure the safety and reliability of the electrical subsystem, especially in cases where the robot is required to operate at high current levels.

ASTM F2792: Standard Guide for Additive Manufacturing of Polymer Products

ISO/ASTM 52900: Additive manufacturing – General principles -Terminology and definitions

APPENDIX C: CONSTRAINTS

Constraints	**Yes**	**No**
Cost	X	
Time	X	
Manufacturability	X	
Sustainability	X	
Safety	X	
Environmental Factors	X	

APPENDIX D: PROJECT PLAN

LOGBOOK

TEAM MEMBER	STUDENT ID	DEPARTMENT
Mmesoma Mario Alaneme	18701377	Mechanical Engineering
Mehdi Ahmad	20910981	Mechanical Engineering
Thabo Allen Baalora	19700189	Mechanical Engineering
Mohammed Diwan	19700715	Mechatronics
Mohammed Haj Mousa	19700713	Mechatronics

Report Writing	Written by
Report Editing	Mmesoma Mario Alaneme Mehdi Ahmad
Report Format	Mmesoma Mario Alaneme
Abstract	Thabo Allen Baalora
Chapter 1	Mmesoma Mario Alaneme
Chapter 2	Mehdi Ahmad Thabo Allen Baalora Mmesoma Mario Alaneme Mohammed Diwan
Chapter 3	Mmesoma Mario Alaneme Mohammed Haj Mousa Thabo Allen Baalora Mehdi Ahmad
Chapter 4	Mmesoma Mario Alaneme Mehdi Ahmad
Chapter 5	Thabo Allen Baalora Mehdi Ahmad
Chapter 6	Mohammed Haj Mousa Thabo Allen Baalora
Chapter 7	Thabo Allen Baalora

References	Team
Appendix A	Mmesoma Mario Alaneme
Appendix B	Mmesoma Mario Alaneme
Appendix C	Mmesoma Mario Alaneme
Appendix D	Mmesoma Mario Alaneme Mehdi Ahmad
Appendix E	Mohammed Diwan
Appendix F	Mmesoma Mario Alaneme
Appendix G	Mohammed Diwan
Appendix H	Mohammed Diwan

ID	Name
1	1. Conceptual Design
2	1.1 Objective of the Robot
3	1.2 Reviewing previous designs
4	1.3 Multiple design plans
5	2. preliminary design of the robot
6	2.1 Designing different concepts
7	2.2 Discussion and report drafting
8	3. Detail design of solar cleaner robot
9	3.1 Selection of parts
10	3.2 detailed CAD drawings
11	3.3 completion of Robot design
12	3.4 Manufacturing plan
13	3.5 testing plan for all parts
14	3.6 Updating the draft
15	4. Prototype development
16	4.1 Procuration of components
17	4.1.1 DC Motor
18	4.1.2 Electronics Components
19	4.1.3 Picking some materials
20	4.1.4 Getting the 3-D printer and filaments
21	4.2 CNC manufacturing of the chassis
22	4.3 3-D Printing of the wheels
23	4.4 riveting of the robot chassis
24	4.5 Assembly of the movement mechanism
25	4.6 plugging the electrical components
26	4.7 Test of the robot (first test)
27	5. Manufacturing of the brush and brush chassis
28	5.1 Designing of the brush mechanism
29	5.2 Manufacturing of the brush mechanism
30	5.3 Testing of the mechanism
31	6.water mechanism
32	6.1 Design the water mechanism
33	6.2 manufacturing of water mechanism
34	6.3 Testing
35	6.4 Fixing some issues (leakage,...)
36	7. Validation and testing of Robot
37	7.1 Assembly of the whole robot
38	7.2 Testing
39	7.3 Resolving some Problems
40	7.4 Testing again
41	8.Report updating and submitting

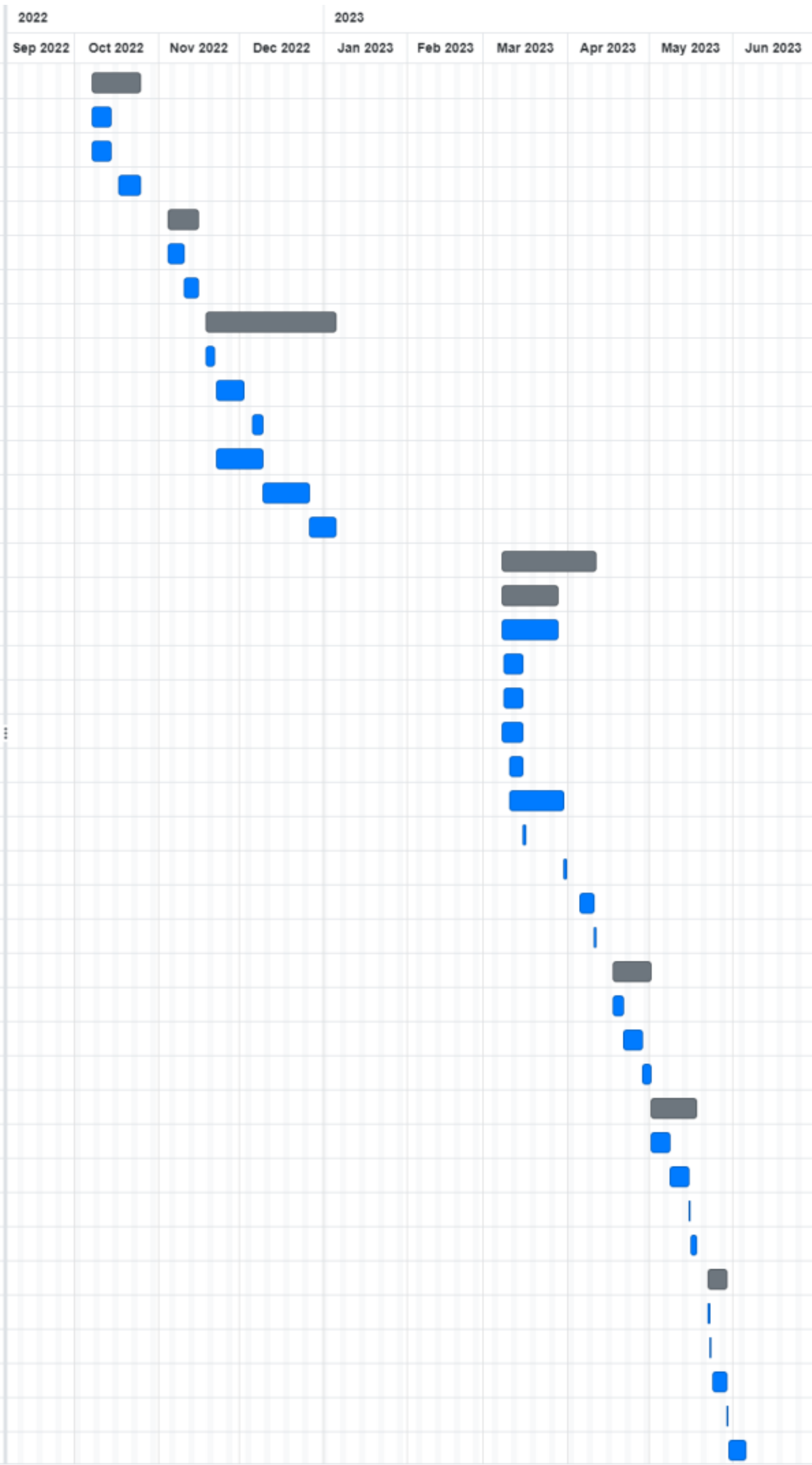

ID	Name	Start Date	End Date	Duration
1	1. Conceptual Design	Oct 07, 2022	Oct 25, 2022	13 days
2	1.1 Objective of the Robot	Oct 07, 2022	Oct 14, 2022	6 days
3	1.2 Reviewing previous designs	Oct 07, 2022	Oct 14, 2022	6 days
4	1.3 Multiple design plans	Oct 17, 2022	Oct 25, 2022	7 days
5	2. preliminary design of the robot	Nov 04, 2022	Nov 15, 2022	8 days
6	2.1 Designing different concepts	Nov 04, 2022	Nov 10, 2022	5 days
7	2.2 Discussion and report drafting	Nov 10, 2022	Nov 15, 2022	4 days
8	3. Detail design of solar cleaner robot	Nov 18, 2022	Jan 05, 2023	35 days
9	3.1 Selection of parts	Nov 18, 2022	Nov 21, 2022	2 days
10	3.2 detailed CAD drawings	Nov 22, 2022	Dec 02, 2022	9 days
11	3.3 completion of Robot design	Dec 05, 2022	Dec 09, 2022	5 days
12	3.4 Manufacturing plan	Nov 22, 2022	Dec 09, 2022	14 days
13	3.5 testing plan for all parts	Dec 09, 2022	Dec 26, 2022	12 days
14	3.6 Updating the draft	Dec 26, 2022	Jan 05, 2023	9 days
15	4. Prototype development	Mar 07, 2023	Apr 11, 2023	26 days
16	4.1 Procuration of components	Mar 07, 2023	Mar 28, 2023	16 days
21	4.2 CNC manufacturing of the chassis	Mar 10, 2023	Mar 15, 2023	4 days
22	4.3 3-D Printing of the wheels	Mar 10, 2023	Mar 30, 2023	15 days
23	4.4 riveting of the robot chassis	Mar 15, 2023	Mar 16, 2023	2 days

ID	Name	Start Date	End Date	Duration
23	4.4 riveting of the robot chassis	Mar 15, 2023	Mar 16, 2023	2 days
24	4.5 Assembly of the movement mechanism	Mar 30, 2023	Mar 31, 2023	2 days
25	4.6 plugging the electrical components	Apr 05, 2023	Apr 10, 2023	4 days
26	4.7 Test of the robot (first test)	Apr 10, 2023	Apr 11, 2023	2 days
27	▼ 5. Manufacturing of the brush and brush chassis	Apr 17, 2023	May 01, 2023	11 days
28	5.1 Designing of the brush mechanism	Apr 17, 2023	Apr 21, 2023	5 days
29	5.2 Manufacturing of the brush mechanism	Apr 21, 2023	Apr 28, 2023	6 days
30	5.3 Testing of the mechanism	Apr 28, 2023	May 01, 2023	2 days
31	▼ 6.water mechanism	May 01, 2023	May 18, 2023	14 days
32	6.1 Design the water mechanism	May 01, 2023	May 08, 2023	6 days
33	6.2 manufacturing of water mechanism	May 08, 2023	May 15, 2023	6 days
34	6.3 Testing	May 15, 2023	May 15, 2023	1 day
35	6.4 Fixing some issues (leakage,...)	May 16, 2023	May 18, 2023	3 days
36	▼ 7. Validation and testing of Robot	May 22, 2023	May 29, 2023	6 days
37	7.1 Assembly of the whole robot	May 22, 2023	May 23, 2023	2 days
38	7.2 Testing	May 23, 2023	May 23, 2023	1 day
39	7.3 Resolving some Problems	May 24, 2023	May 29, 2023	4 days
40	7.4 Testing again	May 29, 2023	May 29, 2023	1 day
41	8.Report updating and submitting	May 30, 2023	Jun 05, 2023	5 days

APPENDIX E: ENGINEERING DRAWINGS

The engineering drawings for the robotic system are shown in the following pages

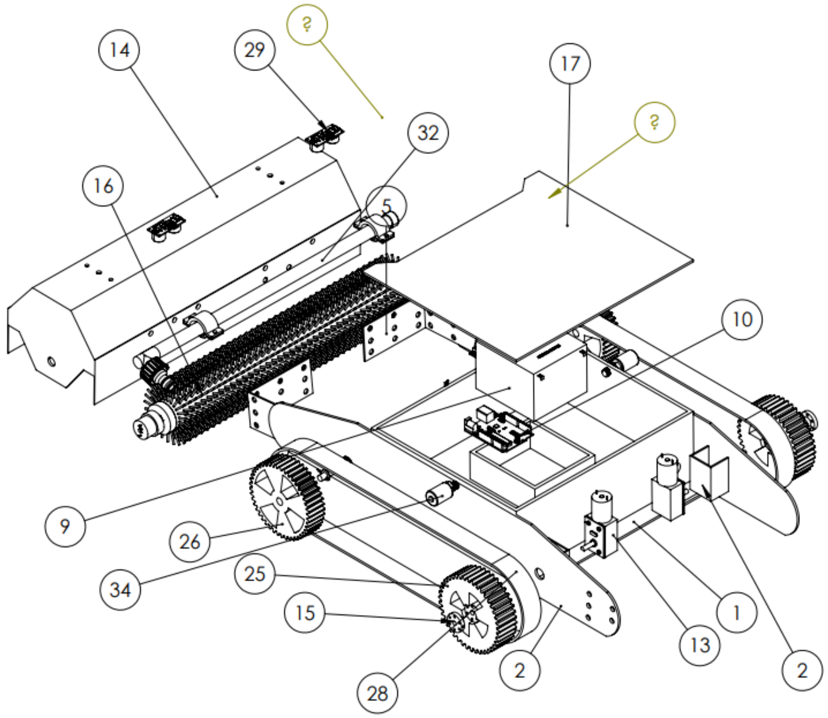

ITEM NO.	PART NUMBER	QTY.
1	Chassis Frame	2
2	Chassis Beam	2
3	rivets	8
4	Box	1
5	brackets	2
7	wheel shaft	1
8	wheel shaft washer	2
9	BATTERY	1
10	ARDUINO UNO R3	1
11	L298N Stepper Motor Driver	2
12	cotter pin	2
13	real motor	2
14	brush chase	1
15	wheel hub	2
16	Brush	1
17	box cover	1
18	brush motor	1
22	wheel hub brush motor	1
25	Rear wheels	2
26	front wheels	2
27	Belt 1	1
28	Belt 2	1
29	ultrasonic sensor	2
30	water nozzle	2
31	motor insulation	2
32	WATER PIPE	1
33	IR Controller	1
34	pulley	2

	NAME	SIGNATURE	DATE	EMU
DRAWN	Mohmmad Diwan	M.D	20/12/2022	Mechanical Enginnering Department
CHK'D	Assist. Prof. Dr. OMID SHEKOOFA		23/12/2022	
Scale: 1:5	Title : Main assembly			PART NO : Explode view

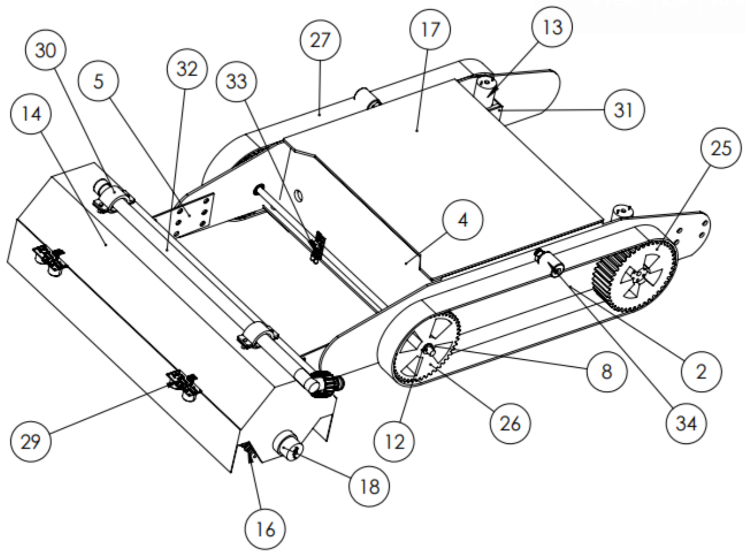

ITEM NO.	PART NUMBER	QTY.
1	Chassis Frame	2
2	Chassis Beam	2
3	rivets	8
4	Box	1
5	brackets	2
7	wheel shaft	1
8	wheel shaft washer	2
9	BATTERY	1
10	ARDUINO UNO R3	1
11	L298N Stepper Motor Driver	2
12	cotter pin	2
13	real motor	2
14	brush chase	1
15	wheel hub	2
16	Brush	1
17	box cover	1
18	brush motor	1
22	wheel hub brush motor	1
25	Rear wheels	2
26	front wheels	2
27	Belt 1	1
28	Belt 2	1
29	ultrasonic sensor	2
30	water nozzle	2
31	motor insulation	2
32	WATER PIPE	1
33	IR Controller	1
34	pulley	2

	NAME	SIGNATURE	DATE	EMU
DRAWN	Mohmmad Diwan	M.D	20/12/2022	Mechanical Enginnering Department
CHK'D	Assist. Prof. Dr. OMID SHEKOOFA		23/12/2022	
Scale: 1:5	Title : Main assembly			PART NO :

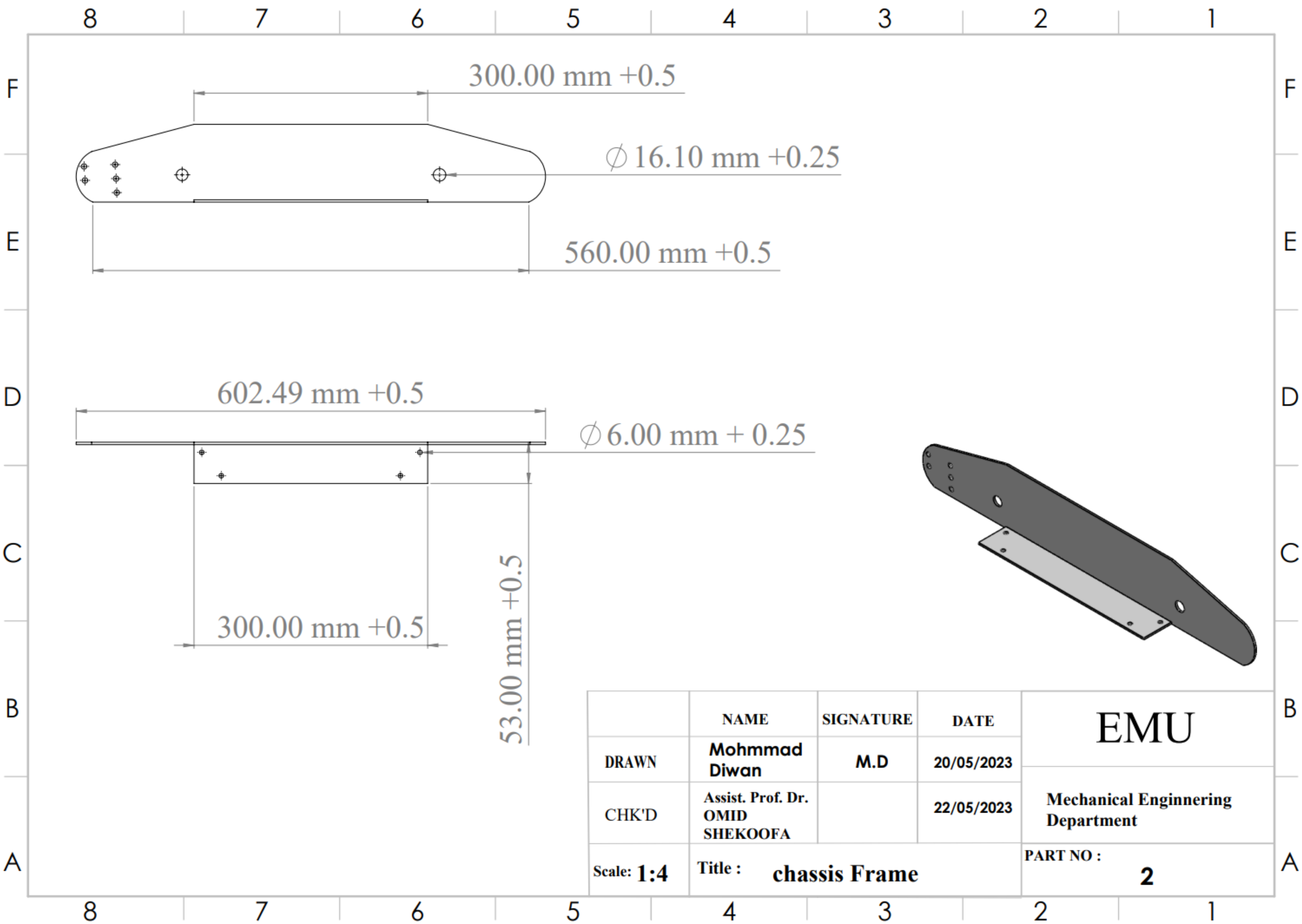
300.00 mm +0.5
∅ 16.10 mm +0.25
560.00 mm +0.5
602.49 mm +0.5
∅ 6.00 mm + 0.25
300.00 mm +0.5
53.00 mm +0.5
NAME
SIGNATURE
DATE
EMU
DRAWN
Mohmmad Diwan
M.D
20/05/2023
CHK'D
Assist. Prof. Dr. OMID SHEKOOFA
22/05/2023
Mechanical Enginnering Department
Scale: 1:4
Title : chassis Frame
PART NO : 2

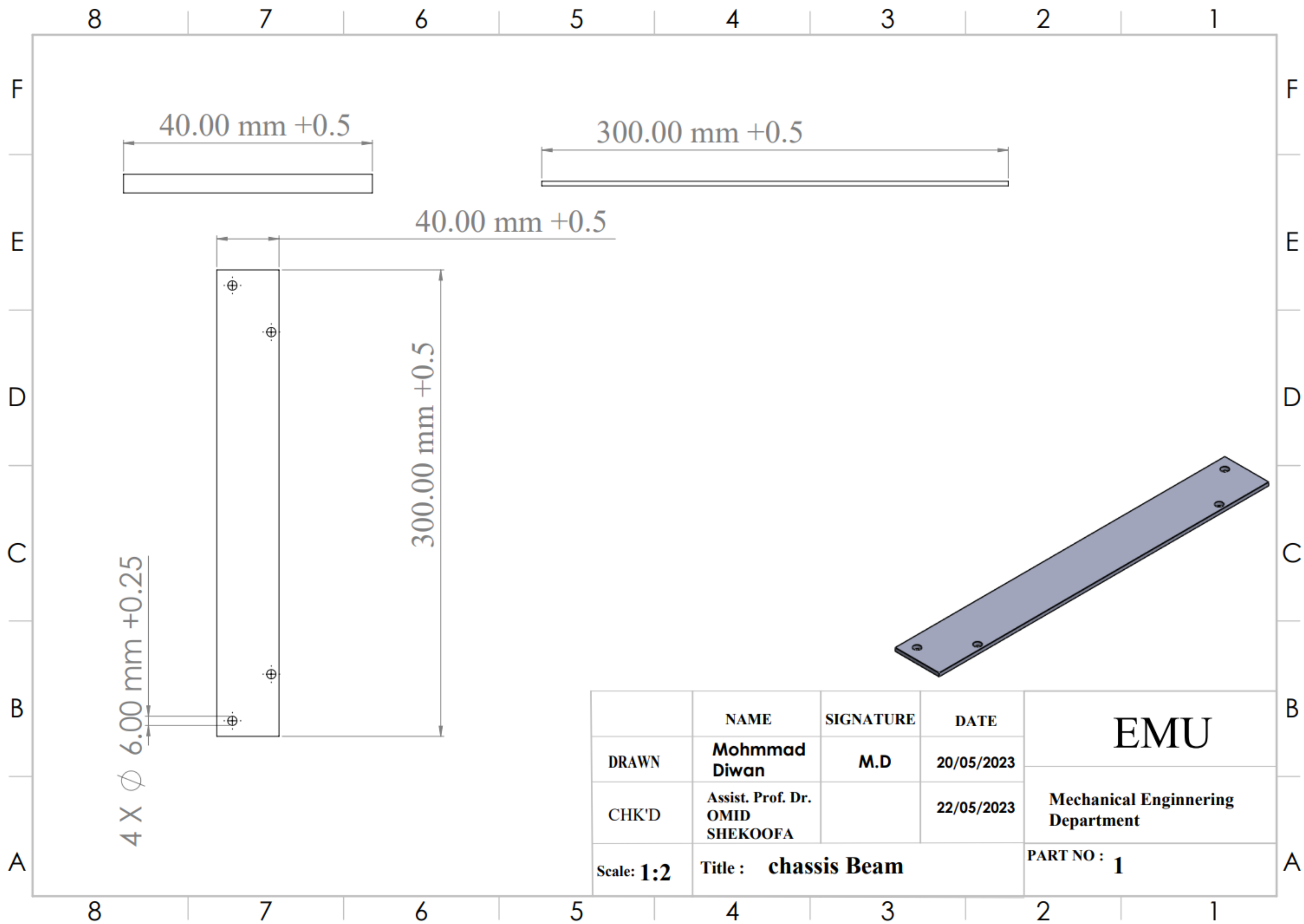

	NAME	SIGNATURE	DATE	EMU
DRAWN	Mohmmad Diwan	M.D	20/05/2023	Mechanical Enginnering Department
CHK'D	Assist. Prof. Dr. OMID SHEKOOFA		22/05/2023	
Scale: 1:2	Title : chassis Beam			PART NO : 1

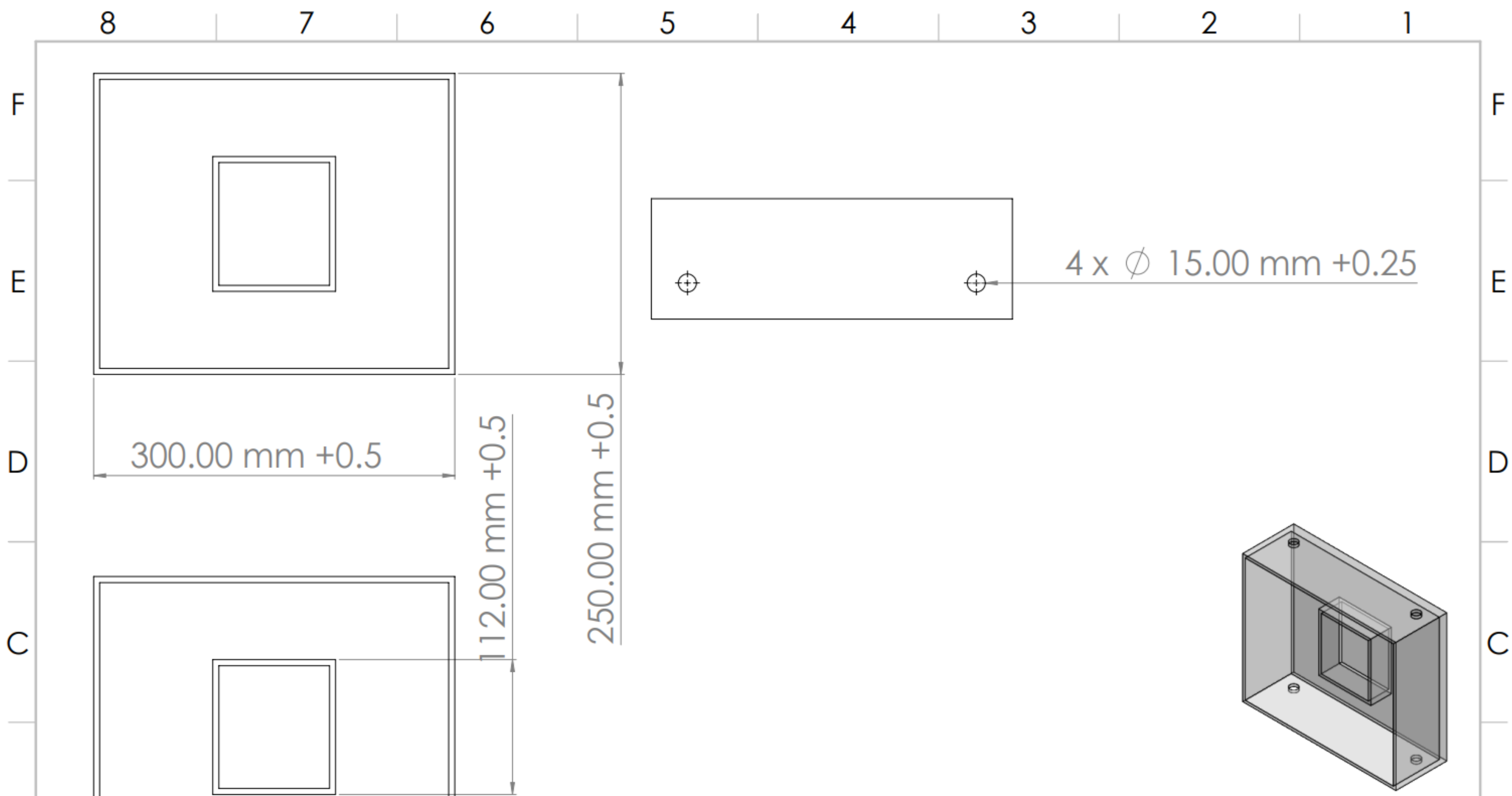

	NAME	SIGNATURE	DATE	EMU
DRAWN	Mohmmad Diwan	M.D	20/05/2023	Mechanical Enginnering Department
CHK'D	Assist. Prof. Dr. OMID SHEKOOFA		22/05/2023	
Scale: 1:3	Title : BOX			PART NO : 4

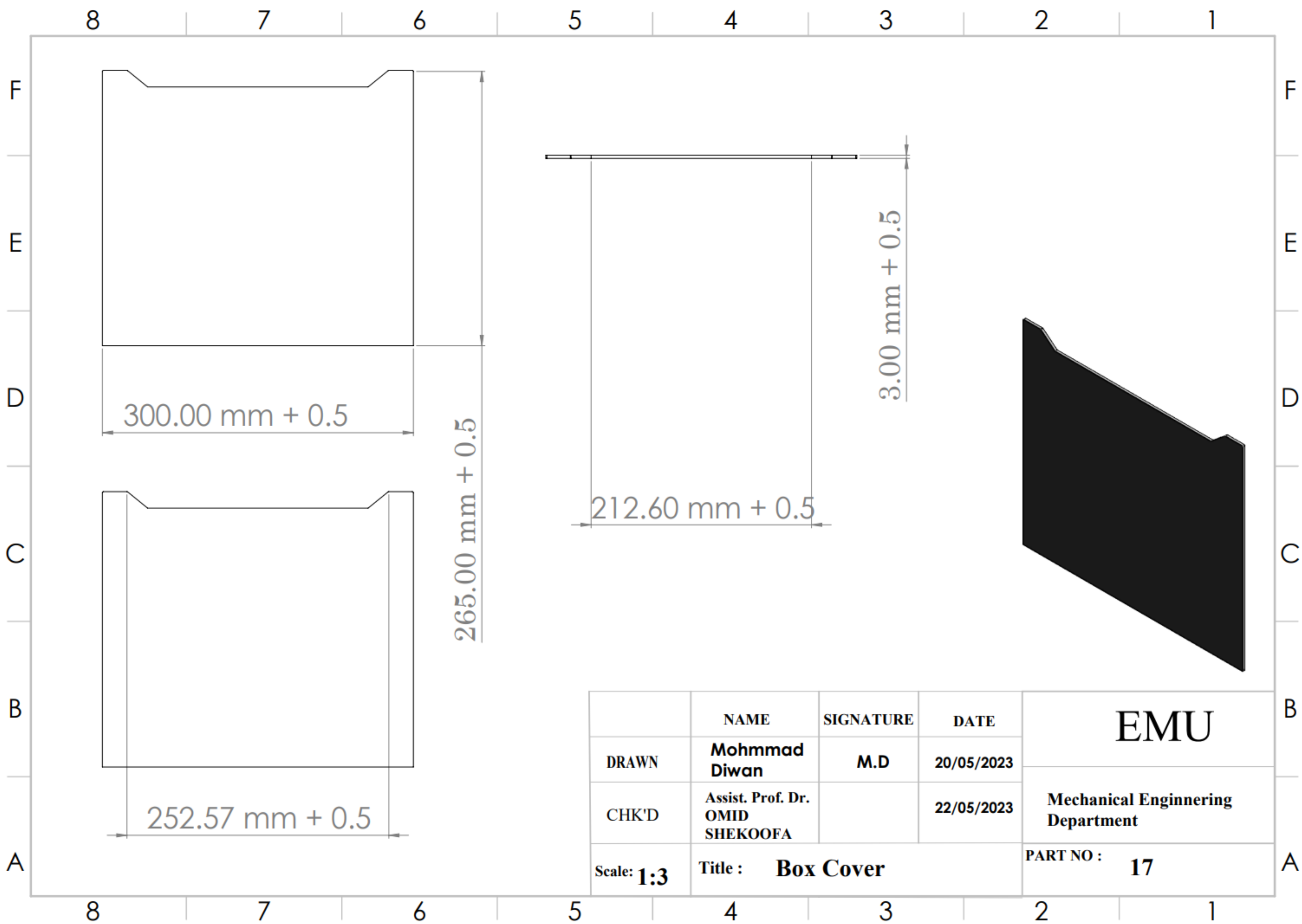

	NAME	SIGNATURE	DATE	EMU
DRAWN	Mohmmad Diwan	M.D	20/05/2023	
CHK'D	Assist. Prof. Dr. OMID SHEKOOFA		22/05/2023	Mechanical Enginnering Department
Scale: 1:3	Title : Box Cover			PART NO : 17

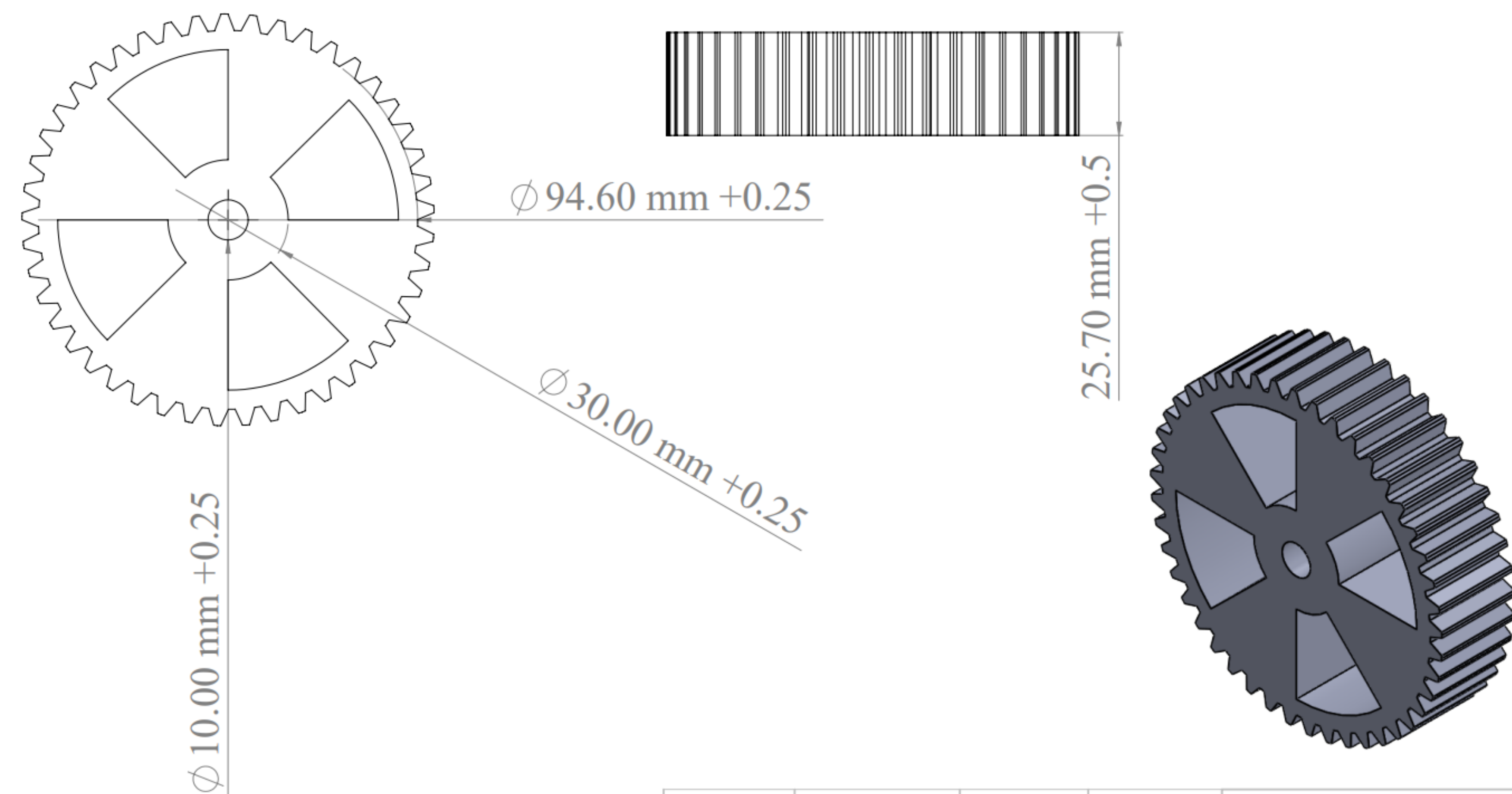

	NAME	SIGNATURE	DATE	EMU
DRAWN	Mohmmad Diwan	M.D	20/05/2023	
CHK'D	Assist. Prof. Dr. OMID SHEKOOFA		22/05/2023	Mechanical Enginnering Department
Scale: 1:1	Title : Front Wheel			PART NO : 29

	NAME	SIGNATURE	DATE	EMU
DRAWN	Mohmmad Diwan	M.D	20/05/2023	Mechanical Enginnering Department
CHK'D	Assist. Prof. Dr. OMID SHEKOOFA		22/05/2023	
Scale: 1:1	Title : Rear Wheel			PART NO : 28

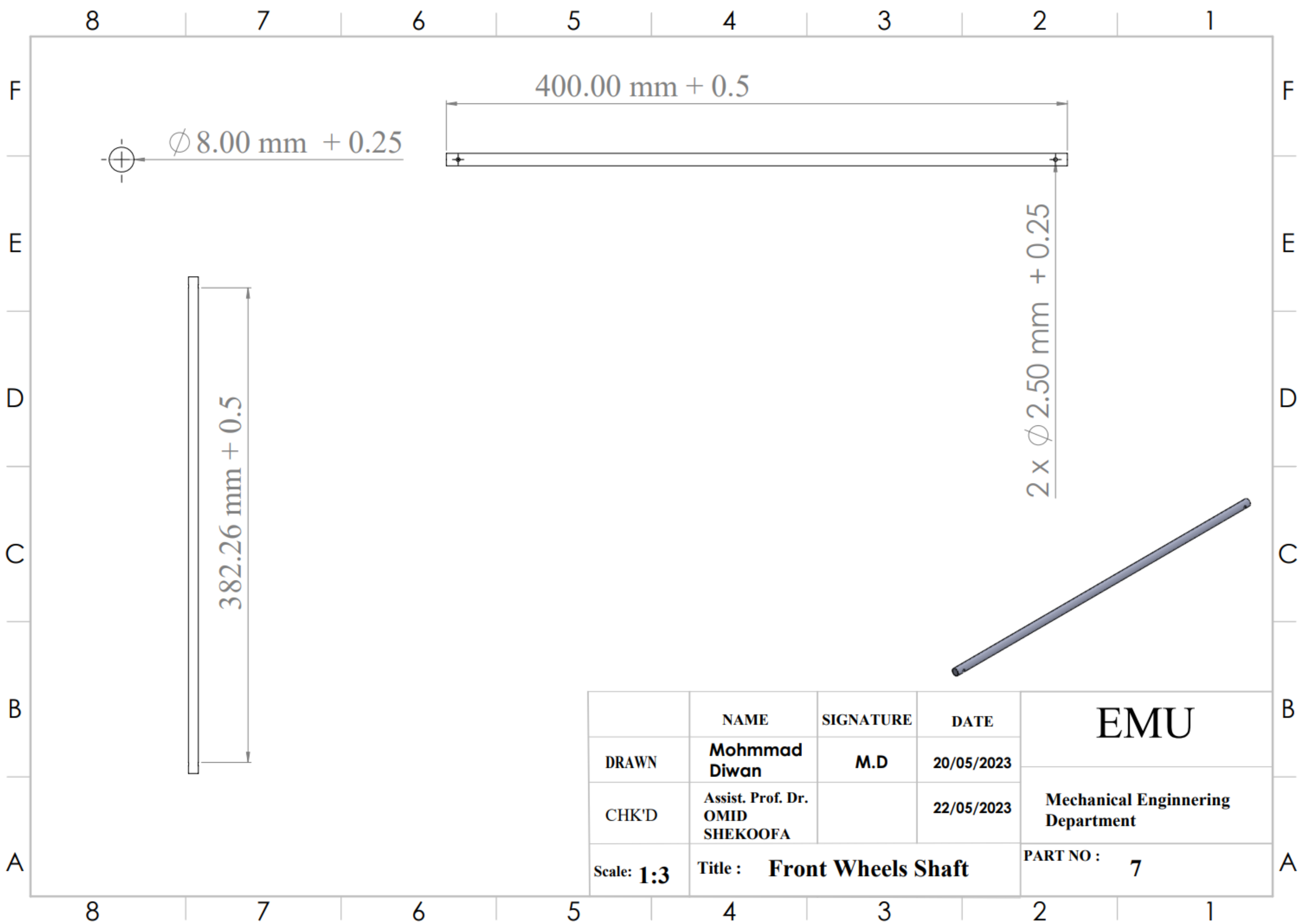

	NAME	SIGNATURE	DATE	EMU
DRAWN	Mohmmad Diwan	M.D	20/05/2023	Mechanical Enginnering Department
CHK'D	Assist. Prof. Dr. OMID SHEKOOFA		22/05/2023	
Scale: 1:3	Title : Front Wheels Shaft			PART NO : 7

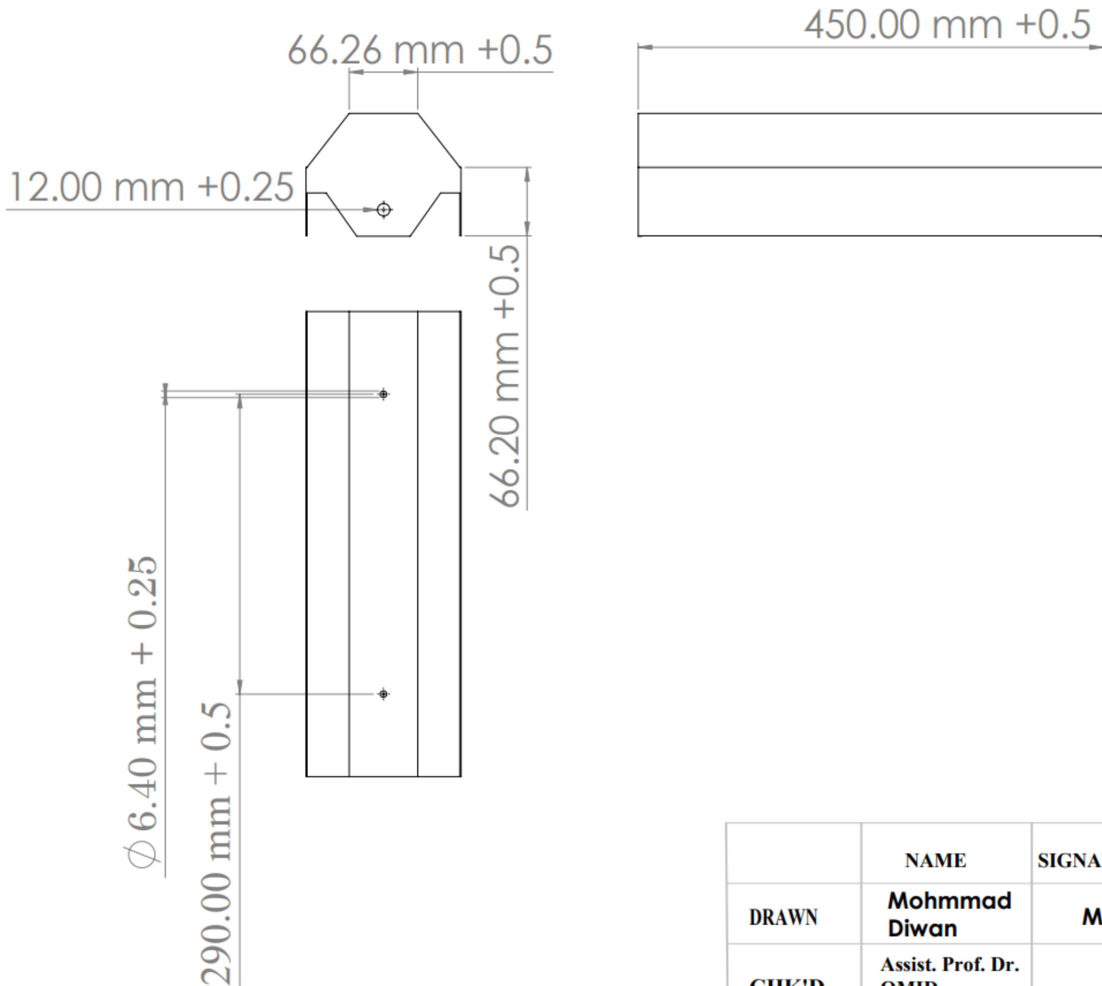

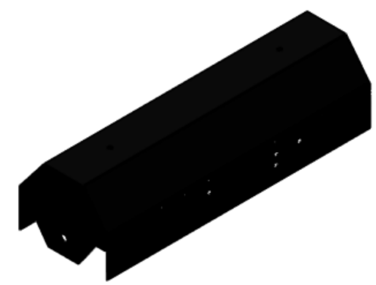

	NAME	SIGNATURE	DATE	EMU
DRAWN	Mohmmad Diwan	M.D	20/ 05/2023	Mechanical Enginnering Department
CHK'D	Assist. Prof. Dr. OMID SHEKOOFA		22/ 05/2023	
Scale: 1:4	Title : BRUSH CHASE			PART NO : 14

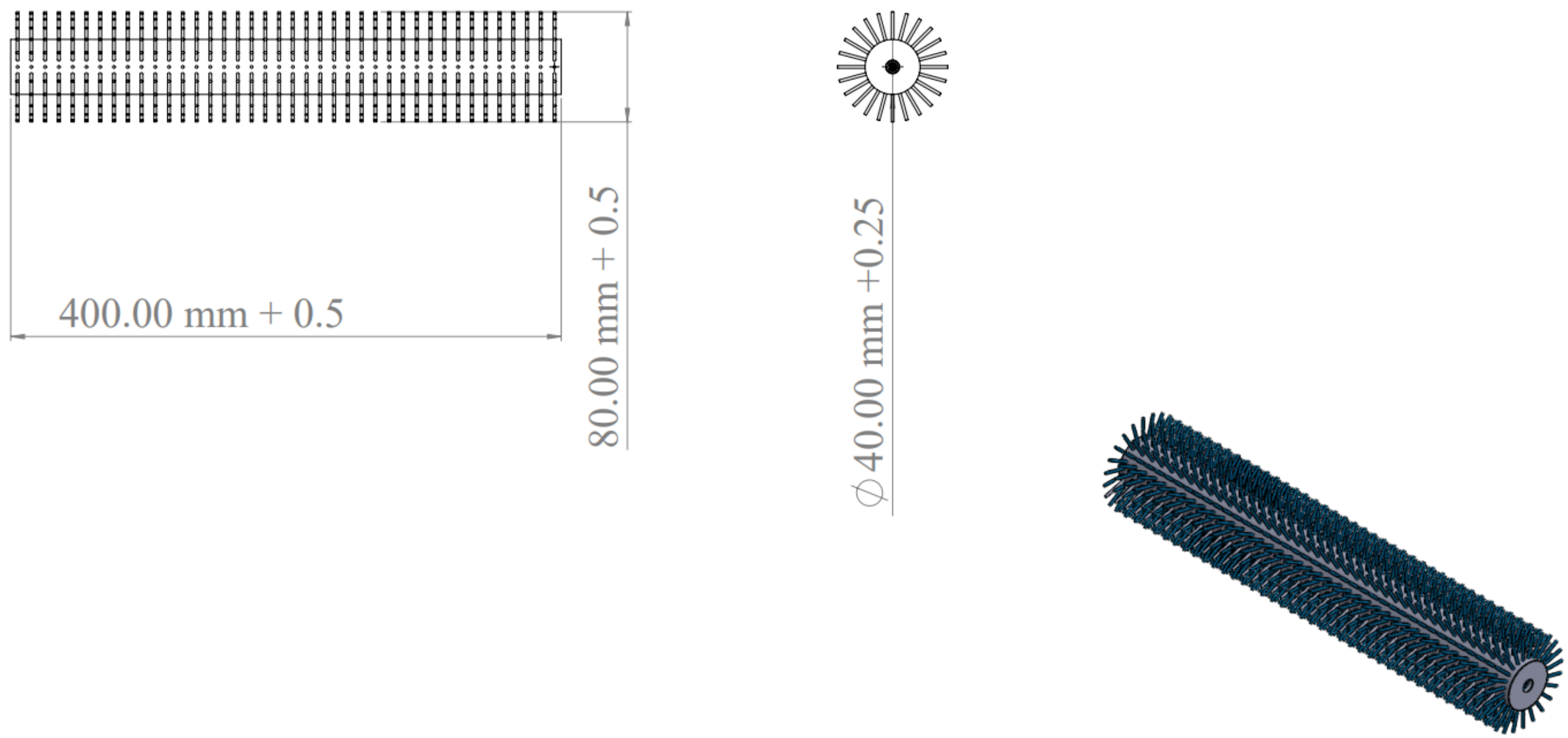

	NAME	SIGNATURE	DATE	EMU
DRAWN	Mohmmad Diwan	M.D	20/05/2023	Mechanical Enginnering Department
CHK'D	Assist. Prof. Dr. OMID SHEKOOFA		22/05/2023	
Scale: 1:3	Title : Brush			PART NO : 16

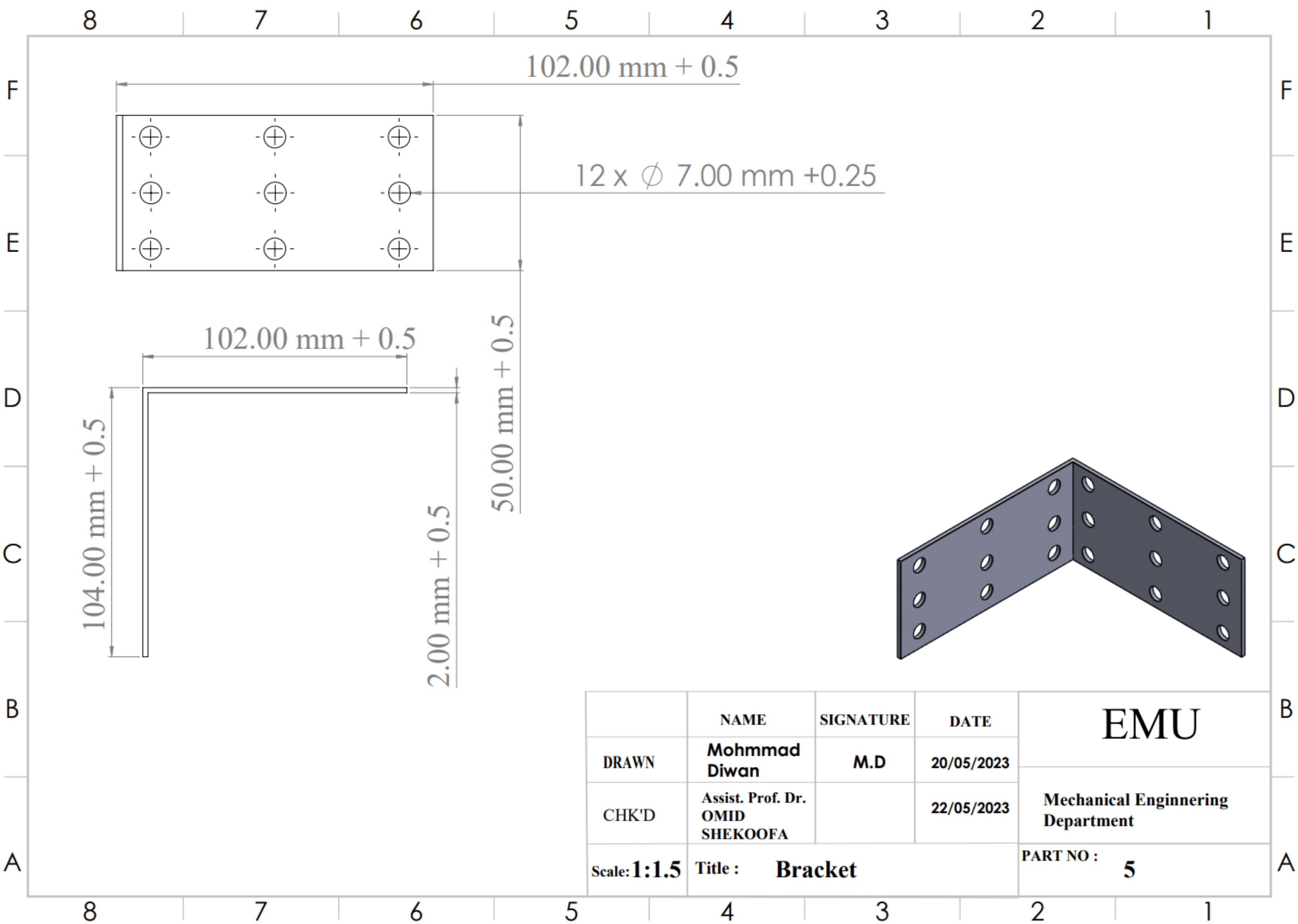

	NAME	SIGNATURE	DATE	EMU
DRAWN	Mohmmad Diwan	M.D	20/05/2023	Mechanical Enginnering Department
CHK'D	Assist. Prof. Dr. OMID SHEKOOFA		22/05/2023	
Scale: 1:1.5	Title : Bracket			PART NO : 5

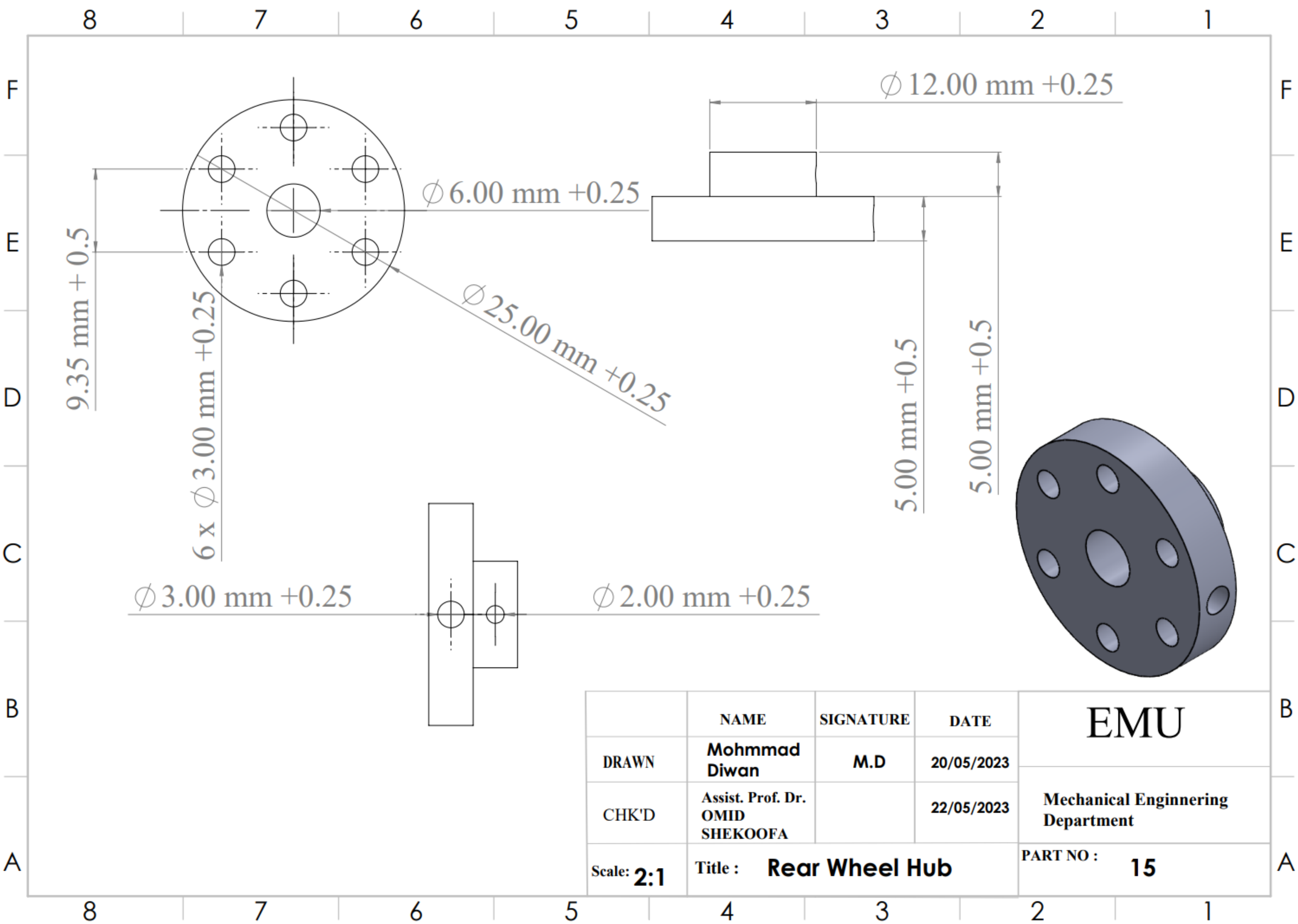

	NAME	SIGNATURE	DATE	EMU
DRAWN	Mohmmad Diwan	M.D	20/05/2023	Mechanical Enginnering Department
CHK'D	Assist. Prof. Dr. OMID SHEKOOFA		22/05/2023	
Scale: 2:1	Title : Rear Wheel Hub			PART NO : 15

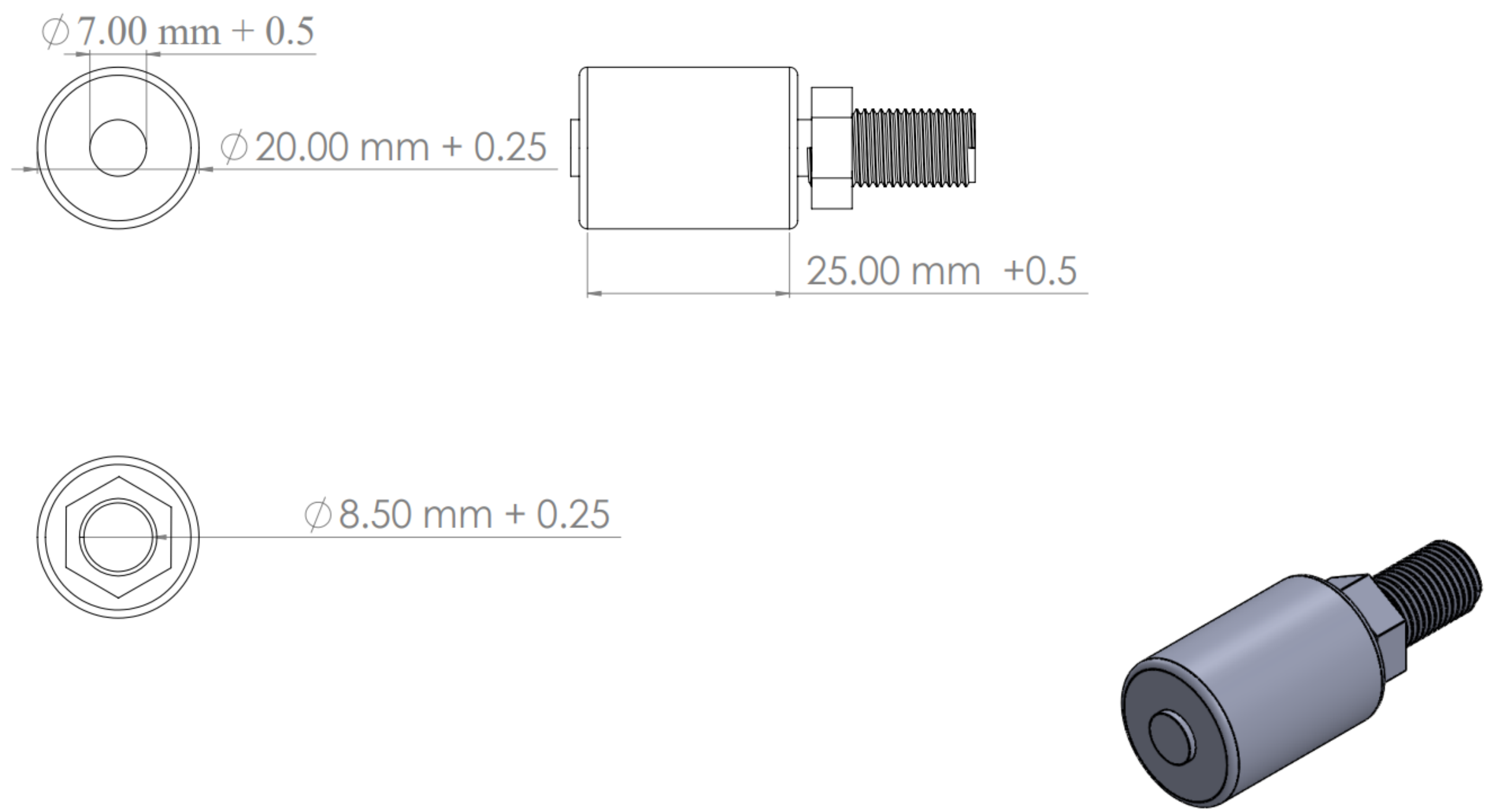

	NAME	SIGNATURE	DATE	Emu
DRAWN	Mohmmad Diwan	M.D	20/05/2023	
CHK'D	Assist. Prof. Dr. OMID SHEKOOFA		22/05/2023	Mechanical Enginnering Department
Scale: 2:1	Title : pulley			PART NO : 34

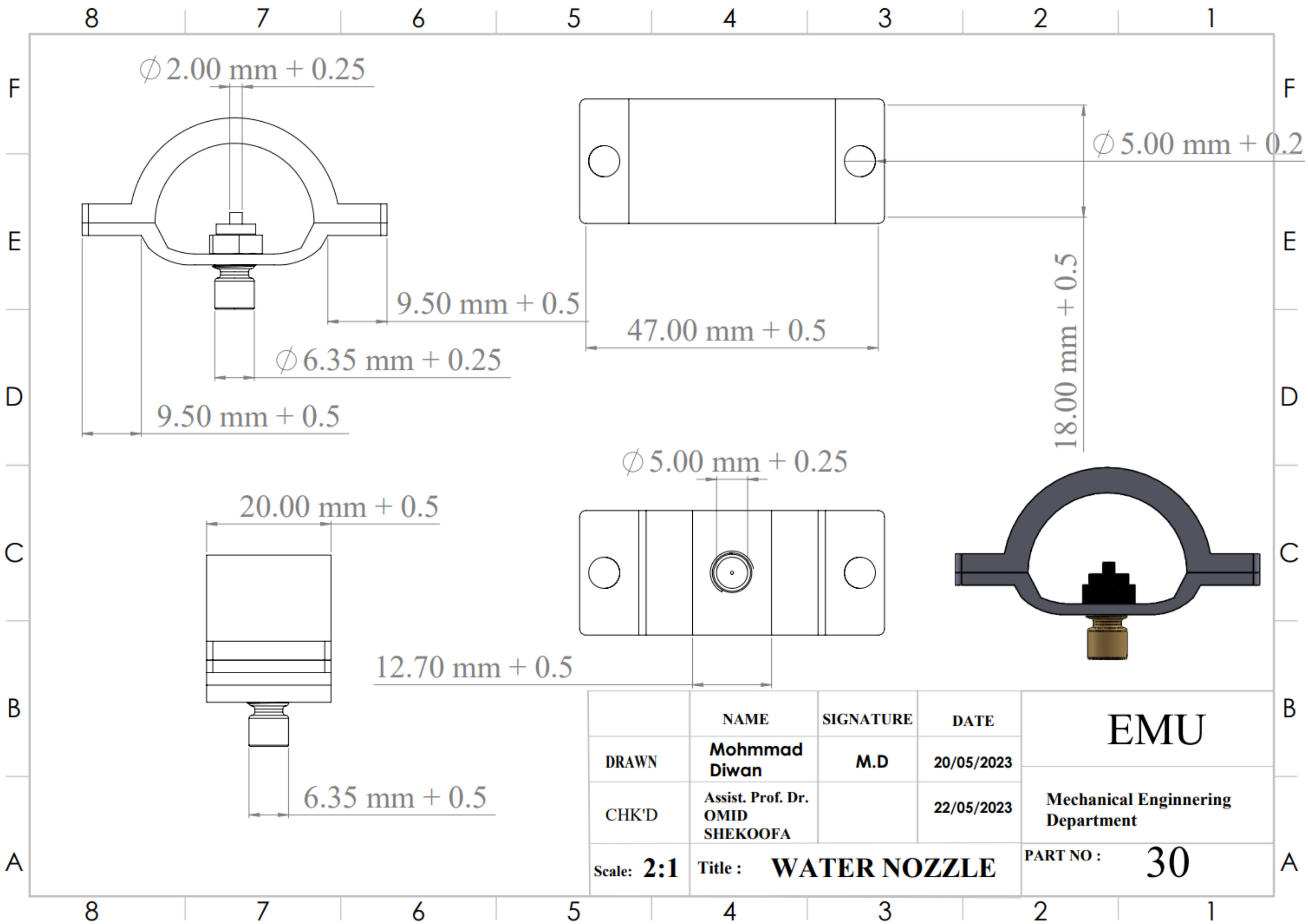

	NAME	SIGNATURE	DATE	EMU
DRAWN	Mohmmad Diwan	M.D	20/05/2023	Mechanical Enginnering Department
CHK'D	Assist. Prof. Dr. OMID SHEKOOFA		22/05/2023	
Scale: 2:1	Title : WATER NOZZLE			PART NO : 30

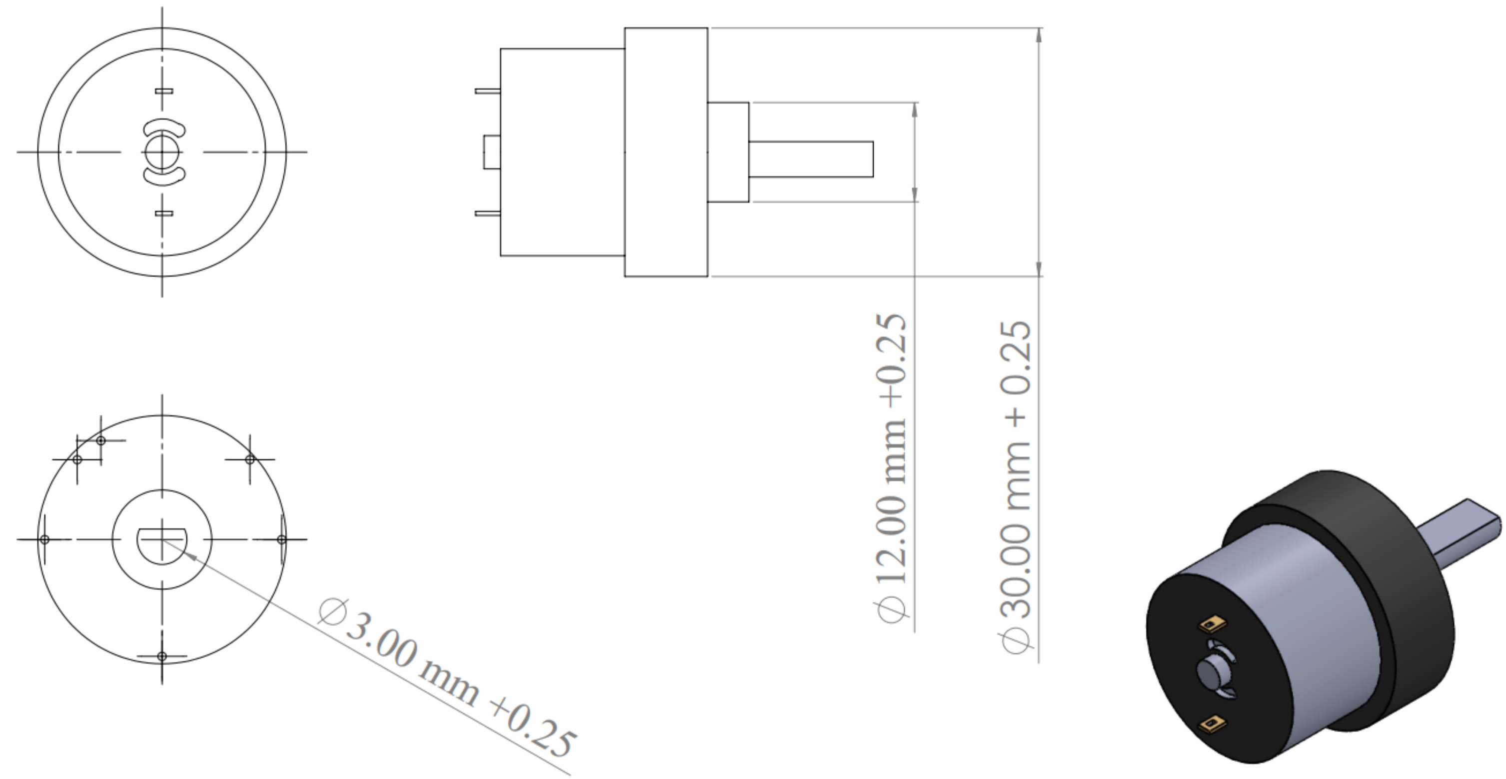

	NAME	SIGNATURE	DATE	EMU
DRAWN	Mohmmad Diwan	M.D	20/05/2023	
CHK'D	Assist. Prof. Dr. OMID SHEKOOFA		22/05/2023	Mechanical Enginnering Department
Scale: 2:1	Title : Brush Motor			PART NO : 21

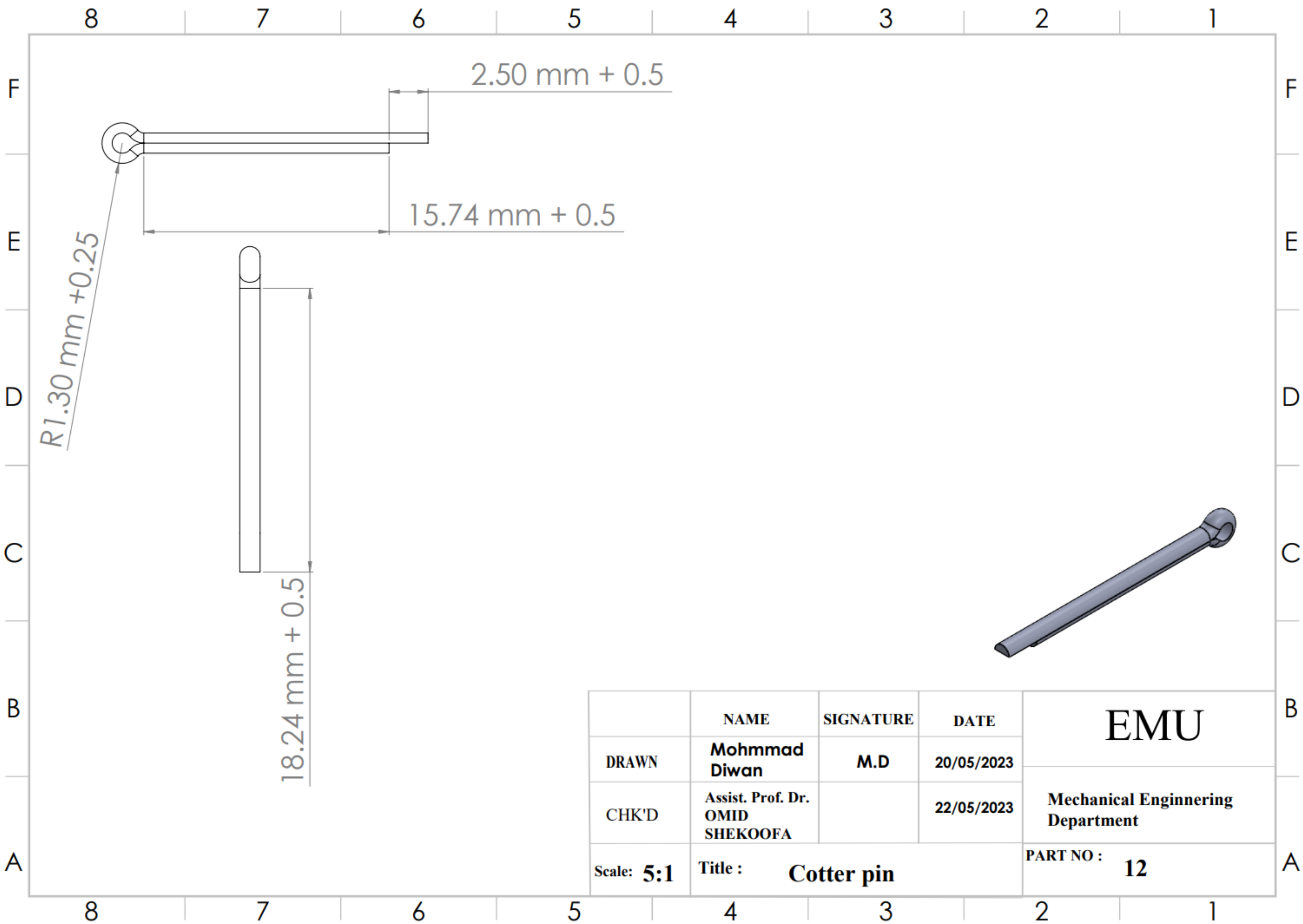

	NAME	SIGNATURE	DATE	EMU
DRAWN	Mohmmad Diwan	M.D	20/05/2023	Mechanical Enginnering Department
CHK'D	Assist. Prof. Dr. OMID SHEKOOFA		22/05/2023	
Scale: 5:1	Title : Cotter pin			PART NO : 12

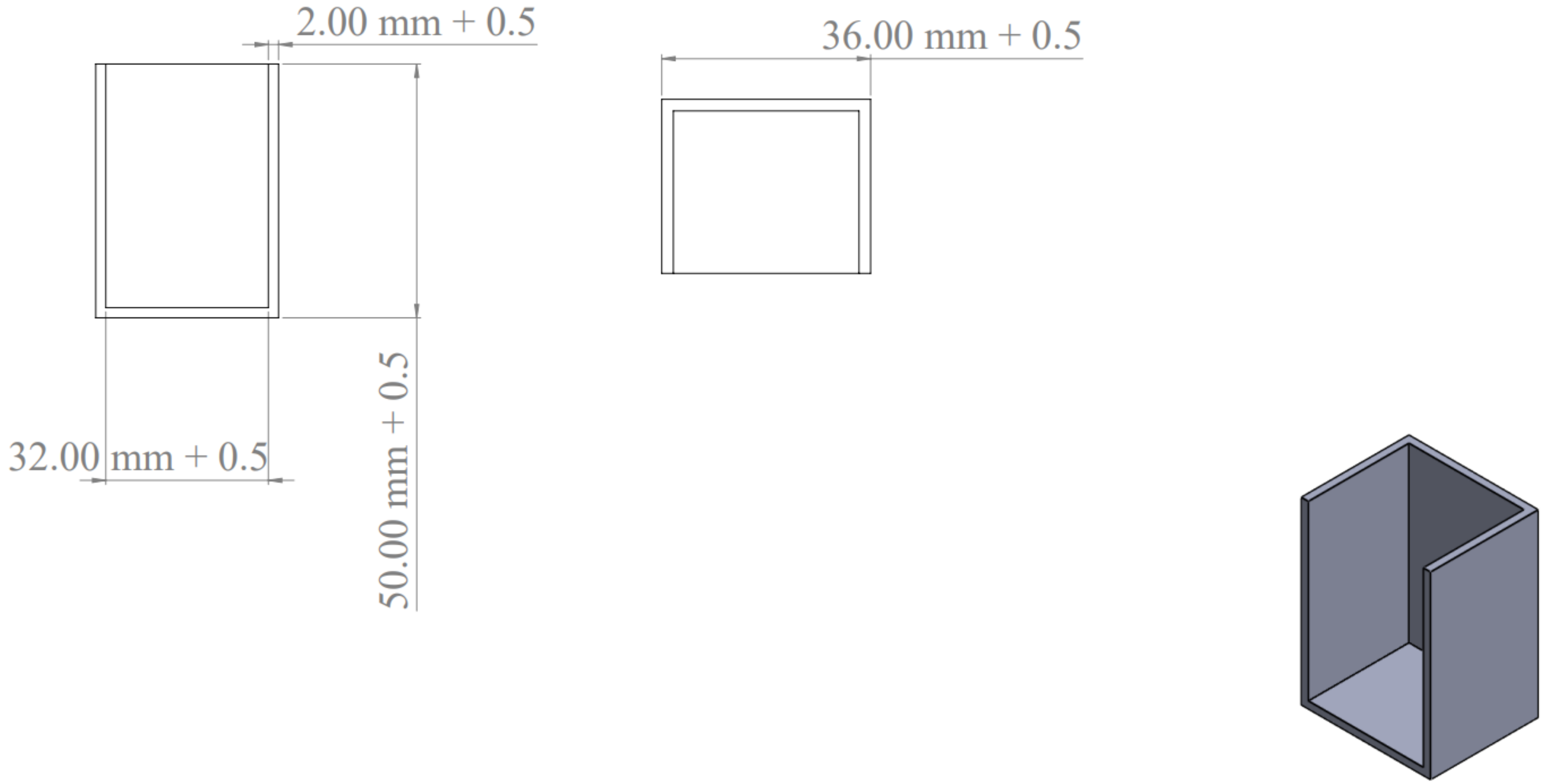

	NAME	SIGNATURE	DATE	EMU
DRAWN	Mohmmad Diwan	M.D	20/05/2023	
CHK'D	Assist. Prof. Dr. OMID SHEKOOFA		22/05/2023	Mechanical Enginnering Department
Scale: 1:1	Title : MOTOR INSULATION			PART NO : 31

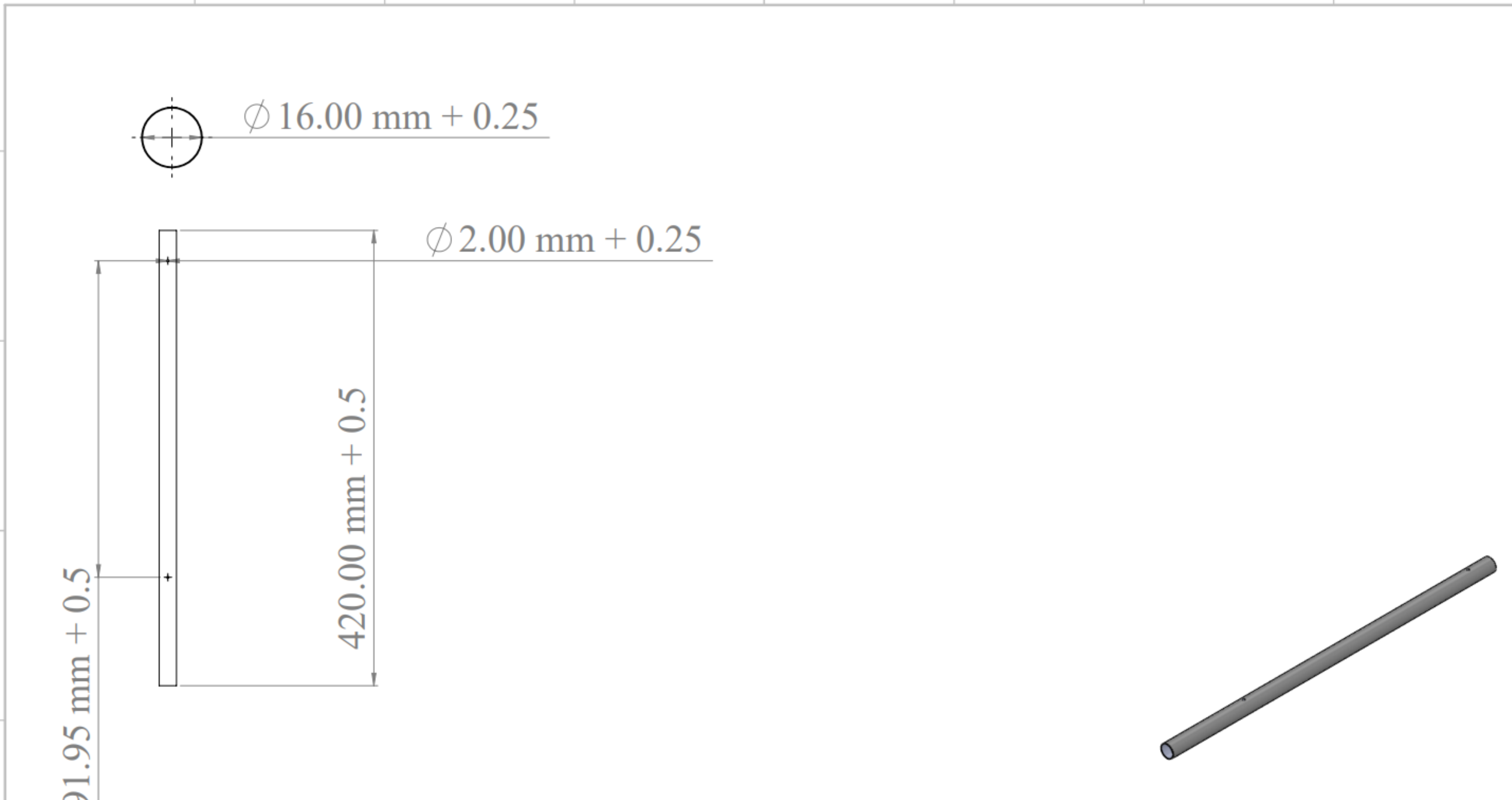

	NAME	SIGNATURE	DATE	EMU
DRAWN	Mohmmad Diwan	M.D	20/05/2023	Mechanical Enginnering Department
CHK'D	Assist. Prof. Dr. OMID SHEKOOFA		22/05/2023	
Scale: 1:3.5	Title : WATER PIPE			PART NO : 32

APPENDIX F: Component Specifications

ZGY370 DC6V Reduction Motor Worm Turbo Geared Motor

ZGY370-46/32		Technical Parameter						
No load		Load Torque				Sall		Reducer
Speed	Currend	speed	Current	Torque	Output	Torque	Current	Ratio
rpm	ma	rpm	ma	kg. cm	W	kg. cm	A	1:00
2	35	1.5	180	14.0	1.1	56	1	3000
5	35	4	180	14.0	1.1	50	1	970
10	35	8	180	8.0	1.1	32	1	588
15	35	13	180	4.8	1.1	21.3	1	324
20	35	15	180	4.0	1.1	16	1	278
30	35	28	180	2.7	1.1	11	1	160
50	35	34	180	1.6	1.1	6.4	1	135
100	35	68	180	0.8	1.1	3.2	1	50
150	35	128	180	0.5	1.1	2.1	1	37.3
200	35	136	180	0.4	1.1	1.6	1	25

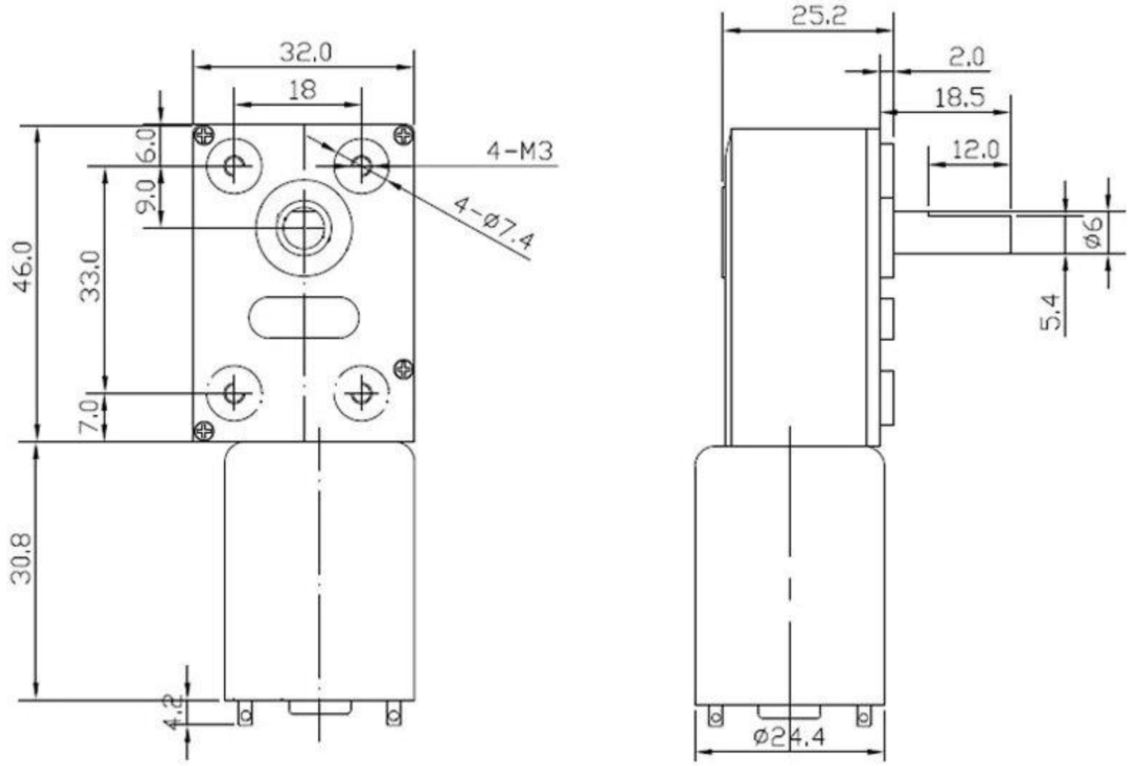
32.0
18
4-M3
4-Ø7.4
6.0
9.0
46.0
33.0
7.0
30.8
4.2
25.2
2.0
18.5
12.0
Ø6
5.4
Ø24.4

12V 35mm 960 RPM Geared DC Motor

Features:

Operating voltage	**12V**
Speed	**960RPM _**
Current Drawn	**160 mA ± 40mA**
Loading Torque	**0.38kg x cm**
Forcing Torque	**1.52kg xm**
Shaft Diameter	**6mm D**

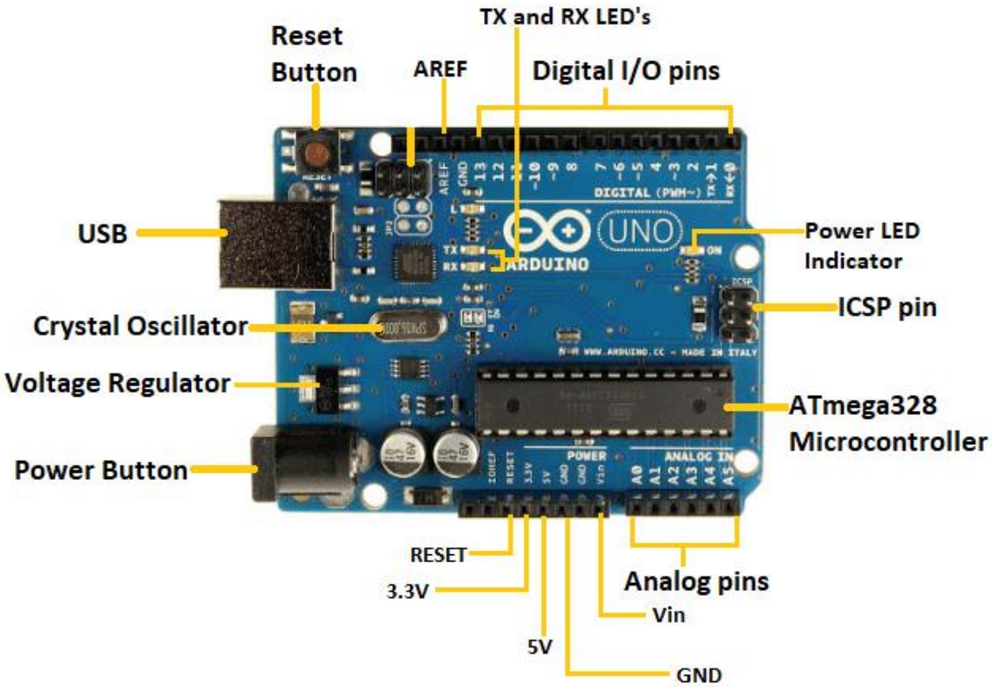

MCU	ATmega328P
Architecture	AVR
Operating Voltage	5V
Input Voltage	6V – 20V (limit) 7V – 12V (recommended)
Clock Speed	16 MHz
Flash Memory	32 KB (2 KB of this used by bootloader)
SRAM	2 KB
EEPROM	1 KB
Digital IO Pins	24 (of which 6 can produce PWM)
Analog Input Pins	6

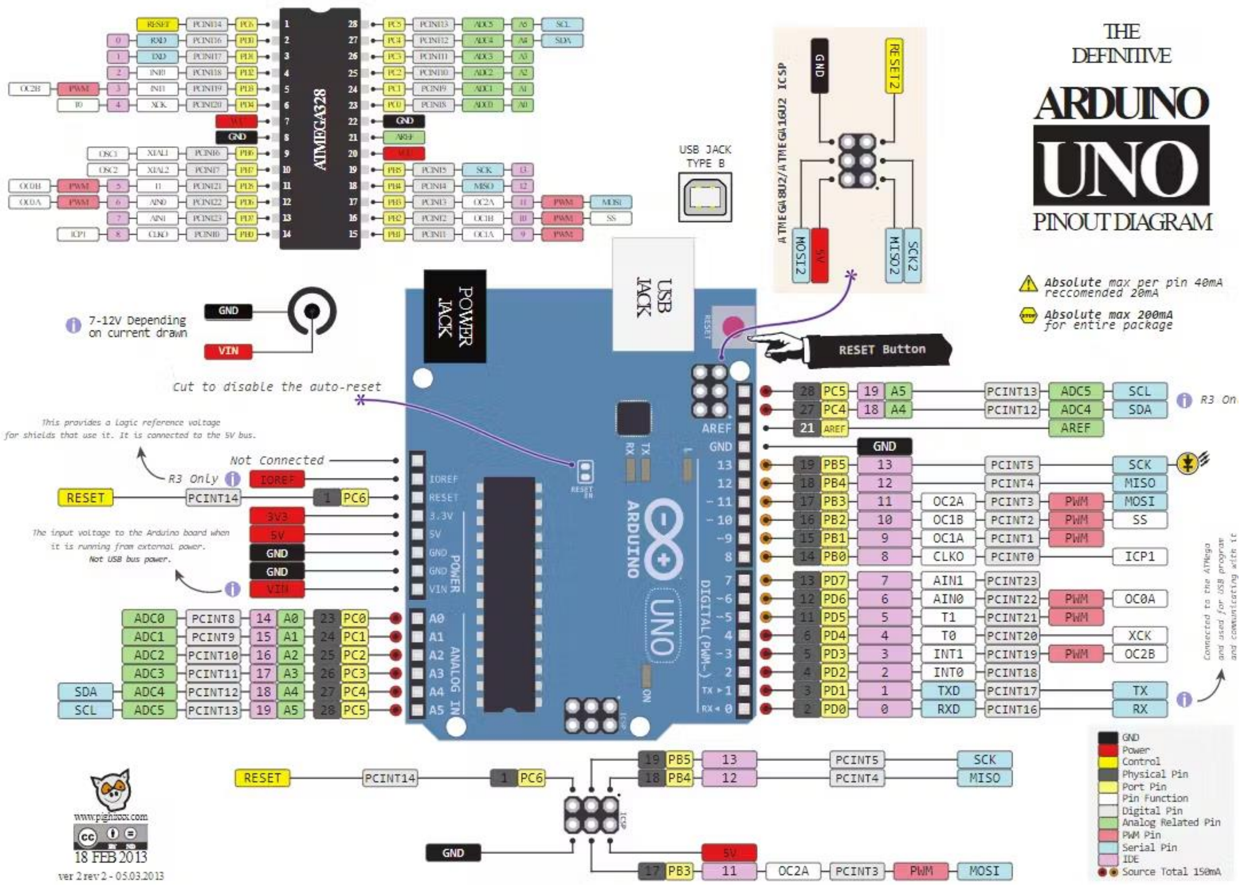
THE DEFINITIVE
ARDUINO
UNO
PINOUT DIAGRAM
Absolute max per pin 40mA reccomended 20mA
Absolute max 200mA for entire package
ATMEGA328
USB JACK TYPE B
ATMEGA8U2/ATMEGA16U2 ICSP
POWER JACK
USB JACK
RESET Button
7-12V Depending on current drawn
Cut to disable the auto-reset
This provides a logic reference voltage for shields that use it. It is connected to the 5V bus.
Not Connected
R3 Only
The input voltage to the Arduino board when it is running from external power. Not USB bus power.
Connected to the ATMega and used for USB program and communicating with it
www.pighixxx.com
18 FEB 2013
ver 2 rev 2 - 05.03.2013
GND
Power
Control
Physical Pin
Port Pin
Pin Function
Digital Pin
Analog Related Pin
PWM Pin
Serial Pin
IDE
Source Total 150mA

ASWAR 12V/4.5AH Rechargeable Battery

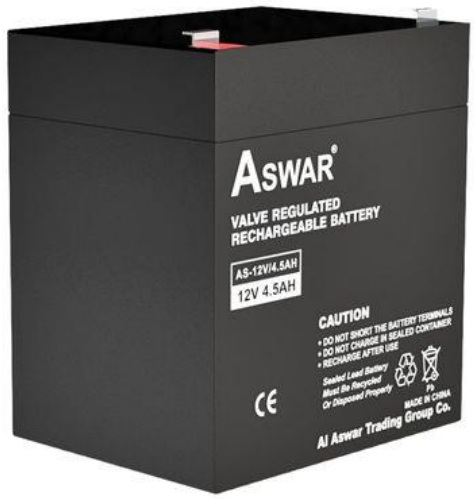

PRODUCT DESCRIPTION

Products	Voltage	Capacity	Dimensions /mm	Terminal /mm
 12V/4.5AH	12V	4.5AH	90x70x101x107	F4 (8×6.35×0.8)

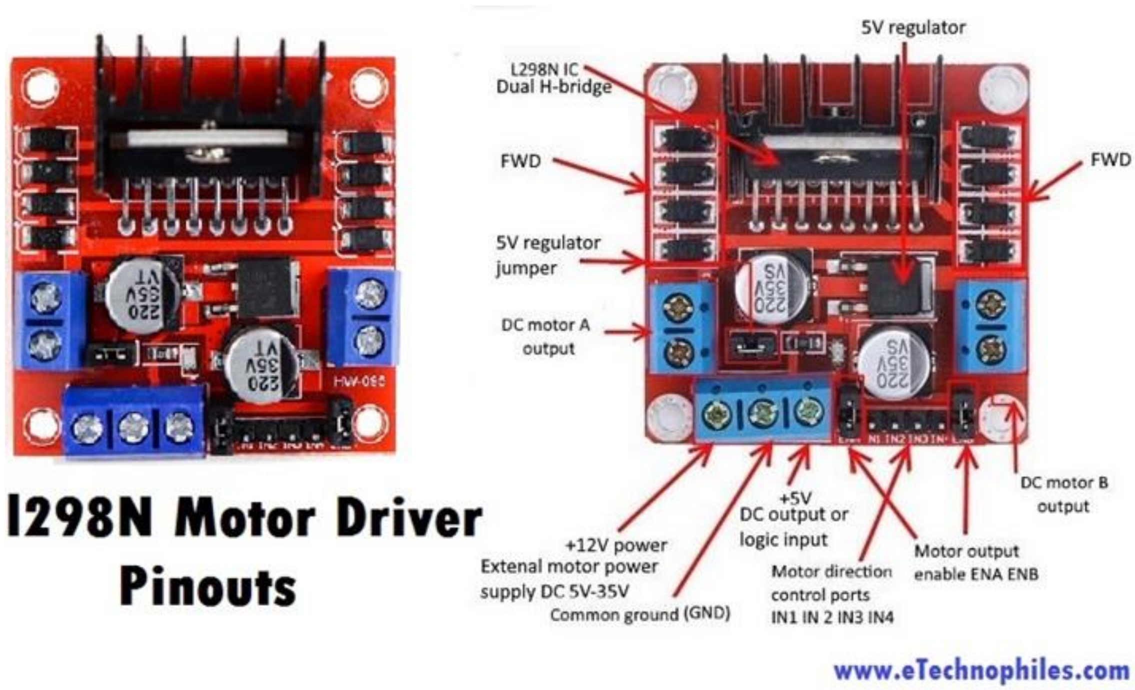

Dual H Bridge Motor Driver

L298N motor driver IC

Drives up to 2 bidirectional DC motors

Integrated 5V power regulator

5V – 35V drive voltage

2A max drive current

Technical Specifications	
Double H Bridge Drive chip	L298N
Logical Voltage	5V
Drive Voltage	5V -35V
Logical Current	0-36 mA
Driver Current	2A (Max Single bridge)
Max Power	25 W
Dimension	43 * 43 * 26 mm

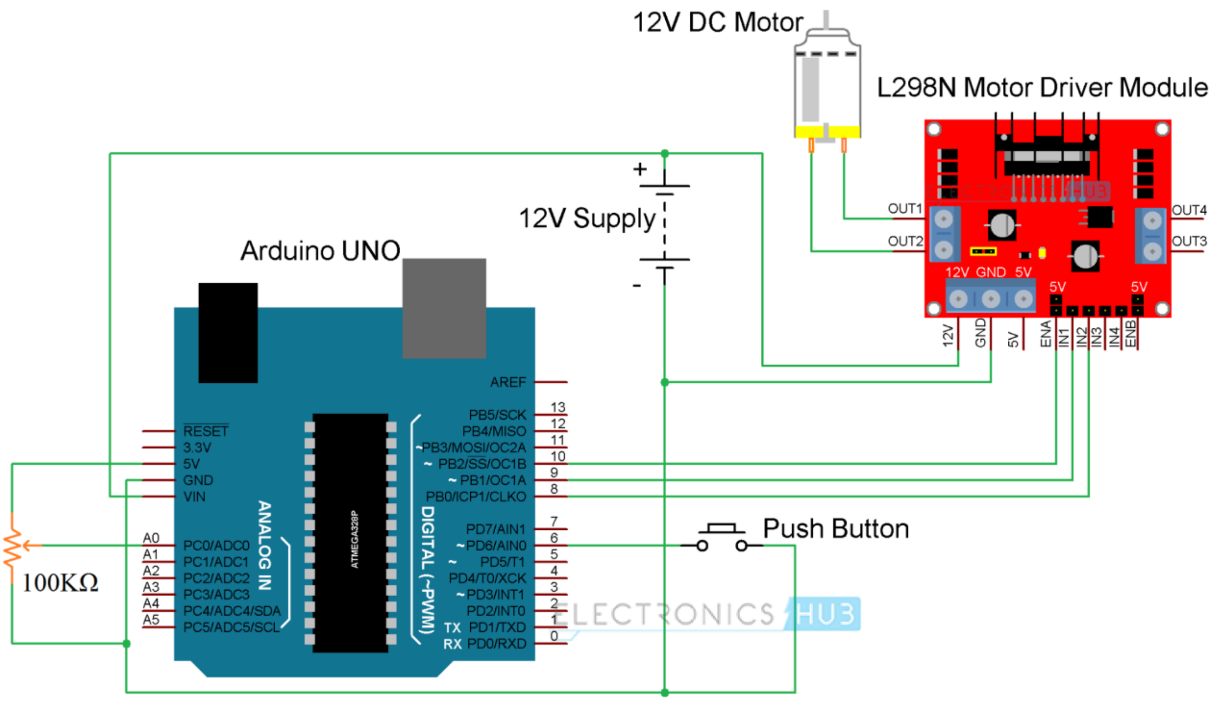
12V DC Motor
L298N Motor Driver Module
12V Supply
Arduino UNO
Push Button
100KΩ
OUT1
OUT2
OUT3
OUT4
12V GND 5V
5V
5V
12V
GND
5V
ENA
IN1
IN2
IN3
IN4
ENB
AREF
PB5/SCK
PB4/MISO
~PB3/MOSI/OC2A
~ PB2/SS/OC1B
~ PB1/OC1A
PB0/ICP1/CLKO
PD7/AIN1
~PD6/AIN0
~ PD5/T1
PD4/T0/XCK
~ PD3/INT1
PD2/INT0
TX PD1/TXD
RX PD0/RXD
13
12
11
10
9
8
7
6
5
4
3
2
1
0
RESET
3.3V
5V
GND
VIN
A0
A1
A2
A3
A4
A5
PC0/ADC0
PC1/ADC1
PC2/ADC2
PC3/ADC3
PC4/ADC4/SDA
PC5/ADC5/SCL
ANALOG IN
DIGITAL (~PWM)
ATMEGA328P
ELECTRONICS HUB

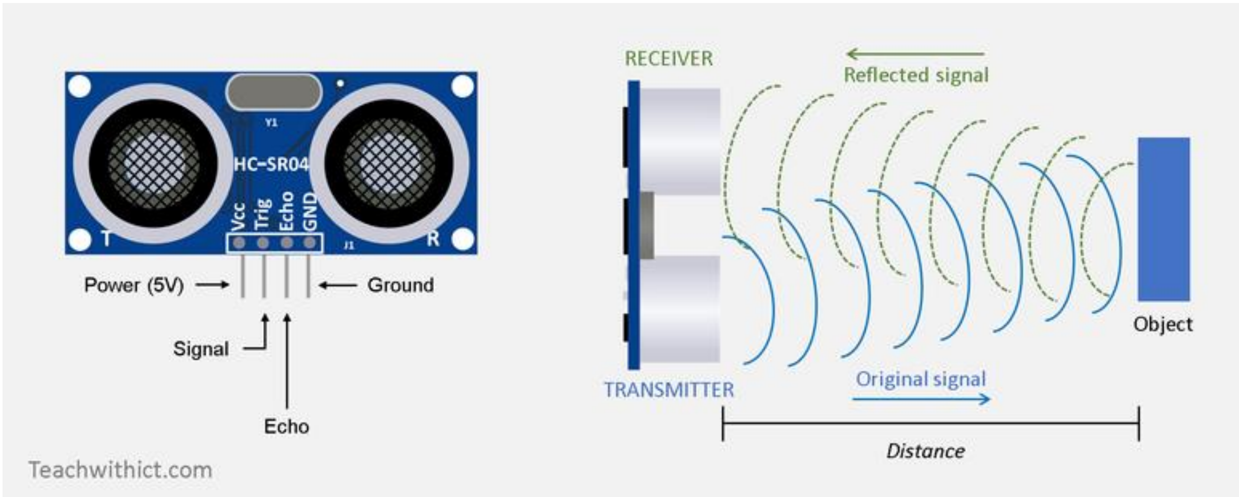
HC-SR04
Vcc
Trig
Echo
GND
T
R
Power (5V)
Ground
Signal
Echo
Teachwithict.com
RECEIVER
Reflected signal
TRANSMITTER
Original signal
Object
Distance

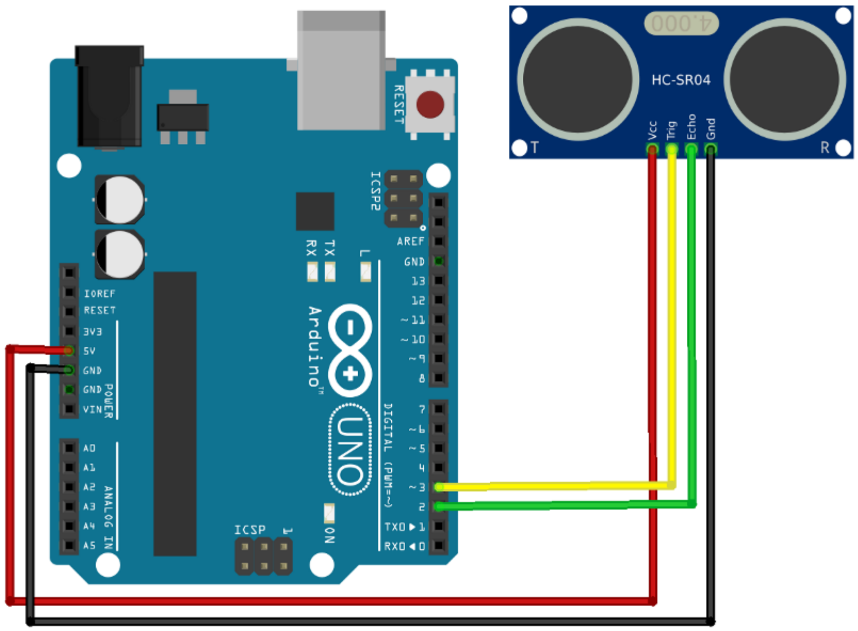
HC-SR04
Vcc
Trig
Echo
Gnd
RESET
ICSP2
AREF
GND
IOREF
RESET
3V3
5V
GND
GND
VIN
POWER
A0
A1
A2
A3
A4
A5
ANALOG IN
Arduino
UNO
DIGITAL (PWM=~)
ICSP
ON
TX
RX
L

HC-SR04

2.3、Module pin definitions

Types	Pin Symbol	Pin Function Description
HC-SR04	VCC	5V power supply
	Trig	Trigger pin
	Echo	Receive pin
	GND	Power ground

2.4、Electrical parameters

Electrical Parameters	HC-SR04 Ultrasonic Module
Operating Voltage	DC-5V
Operating Current	15mA
Operating Frequency	40KHZ
Farthest Range	4m
Nearest Range	2cm
Measuring Angle	15 Degree
Input Trigger Signal	10us TTL pulse
Output Echo Signal	Output TTL level signal, proportional with range
Dimensions	45*20*15mm

IR Sensor Module Circuit

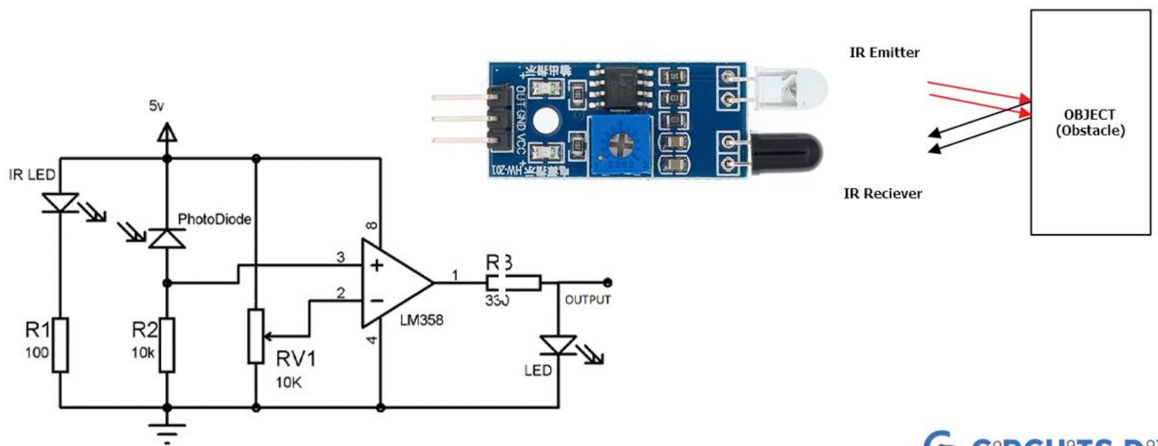

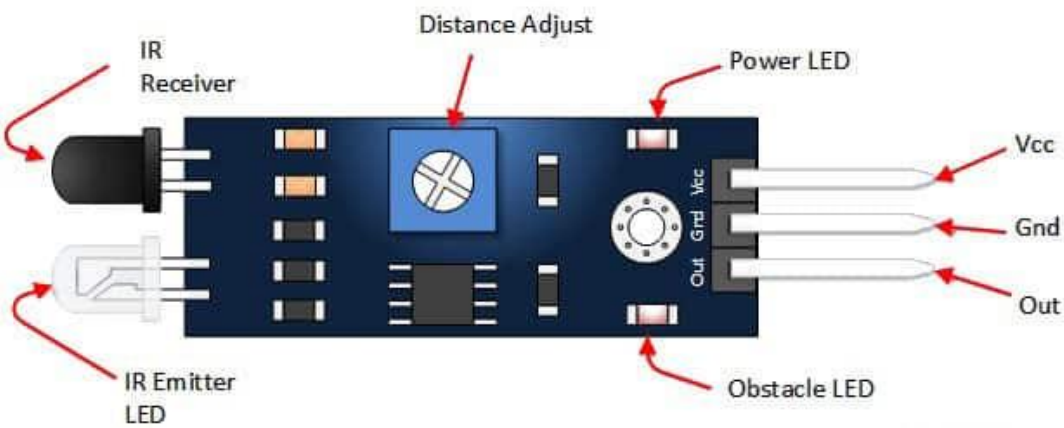

Pin Description

Vcc	3.3 to 5 Vdc Supply Input
GND	Ground Input
Out	The output that goes low when an obstacle is in range
Power LED	Illuminates when power is applied
Obstacle LED	Illuminates when an obstacle is detected
IR Emitter	Infrared emitter LED
IR Receiver	The infrared receiver that receives signal transmitted by Infrared emitter.

Specifications

Board Size	3.2 x 1.4cm
Working voltage	3.3 to 5V DC
Operating voltage	3.3V: ~23 mA, to 5V: ~43 mA
Detection range	2cm – 30cm (Adjustable using potentiometer)
Active output level	The output is “0” (Low) when an obstacle is detected

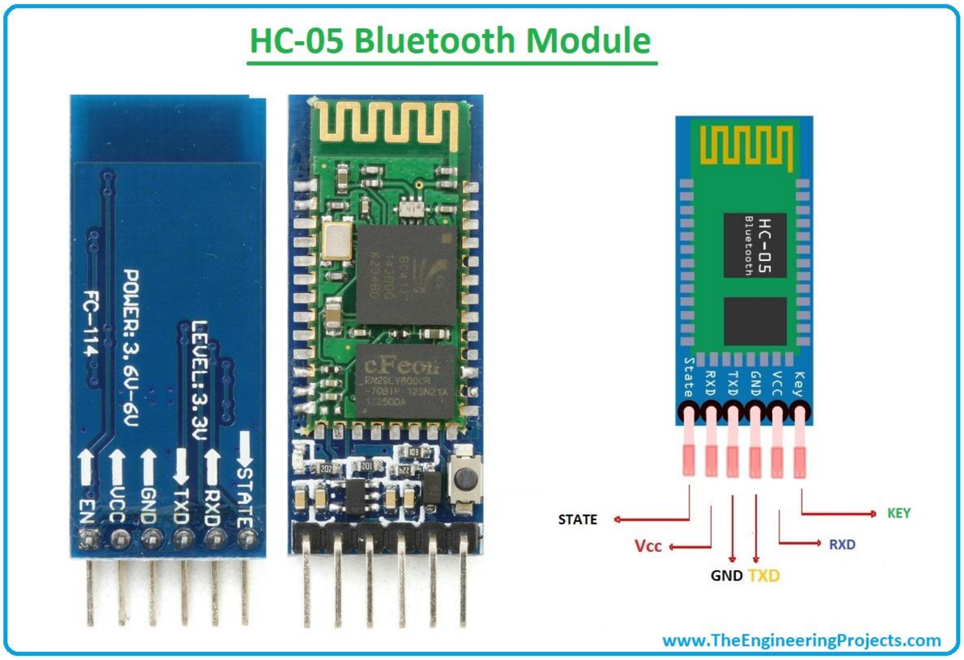

Configuration	Description
Bluetooth protocol	Bluetooth 2.0+ EDR standard
USB protocol	USB v1.1/2.0
Operating frequency	2.4GHz ISM frequency band
Modulation mode	Gauss frequency Shift Keying
Transmit power	≤ 4dBm, second stage
Sensitivity	≤-84dBm at 0.1 Bit Error Rate

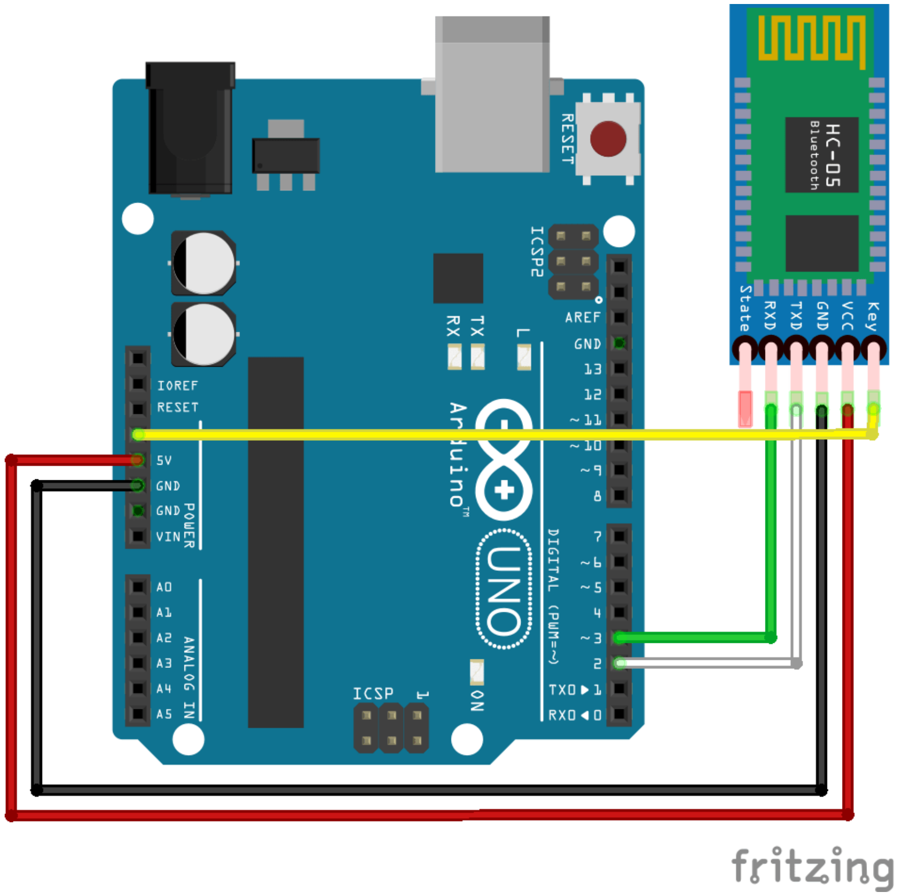
fritzing

Products name	C&U brand high quality metric miniature ball bearing 624rs 624 2rs 624z 624zz 624 small bearing
Brand name	neutral brand.imported brand or be customized to the customer's brand
Series	624ZZ .624 2RS.624 RZ.624Z.624 RS
ID size	4mm-13mm-5mm
material	Stainless steel.Gcr15.carbon steel
Precision	PO P6 P5 P4
Sealing	Open, Z, ZZ, RZ,2RZ,RS, 2RS
Quality standard	ISO9001:2000 standard

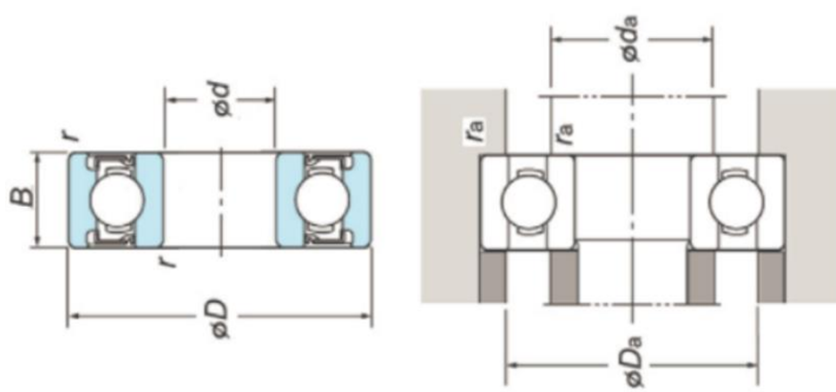

APPENDIX G: CODES

```
#include <SoftwareSerial.h>

#define rxPin A8
#define txPin A9
SoftwareSerial mySerial =  SoftwareSerial(rxPin, txPin);

int trig1 = 6;
int echo1 = A1;
int tim1;
int distanc1;

//second ultra
int trig2 = 10;
int echo2 = A2;
int tim2;
int distanc2;

int enA=9;
int in1=12;
int in2=7;

int enB=3;
int in3=5;
int in4=4;


int enC=20;
int in5=21;
int in6=22;

int brush=0;

char command;

void setup()
{
  pinMode(rxPin, INPUT);
  pinMode(txPin, OUTPUT);
  mySerial.begin(9600);
  pinMode(enA,OUTPUT);
  pinMode(in1,OUTPUT);
  pinMode(in2,OUTPUT);

  pinMode(enB,OUTPUT);
  pinMode(in3,OUTPUT);
  pinMode(in4,OUTPUT);

  pinMode(enC,OUTPUT);
  pinMode(in1,OUTPUT);
  pinMode(in2,OUTPUT);
```

```
 digitalWrite(in1,LOW);
 digitalWrite(in2,LOW);

 digitalWrite(in3,LOW);
 digitalWrite(in4,LOW);

 digitalWrite(in5,LOW);
 digitalWrite(in6,LOW);

  pinMode(5, OUTPUT);

  pinMode(6, OUTPUT);
  pinMode(A1, INPUT);

  pinMode(10, OUTPUT);
  pinMode(A2, INPUT);
}

void loop() {
  if (mySerial.available() > 0) {
    command = mySerial.read();
    stop();

  -digitalWrite(trig1, LOW);
  delayMicroseconds(2);
  digitalWrite(trig1, High);
  delayMicroseconds(10);
  digitalWrite(trig1, LOW);
  tim1 = pulseIn(echo1, HIGH);
  distanc1 = tim1 / 29 / 2;

  digitalWrite(trig2, LOW);
  delayMicroseconds(2);
  digitalWrite(trig2, High);
  delayMicroseconds(10);
  digitalWrite(trig2, LOW);
  tim2 = pulseIn(echo2, HIGH);
  distanc2 = tim2 / 29 / 2;

    If(command=='V'){
      brush==1
    }
    else if (command=='v'){
      brush==0;
    }
    while(brush=1){
      brushon();
    }



    switch (command) {
        case 'F':
        if(diatance1>220 || distance2>220){
```

```
        forward();
        }
        break;
        case 'B':
        backward();
        break;
        case 'L':
        left();
        break;
        case 'R':
        right();
        break;

    }

  }

}
void forward(){

  analogWrite(enA,255);
  digitalWrite(in1,HIGH);
  digitalWrite(in2,LOW);

  analogWrite(enB,255);
  digitalWrite(in3,HIGH);
  digitalWrite(in4,LOW);

}
void backward()
{
  analogWrite(enA,255);
  digitalWrite(in1,LOW);
  digitalWrite(in2,HIGH);

  analogWrite(enB,255);
  digitalWrite(in3,LOW);
  digitalWrite(in4,HIGH);
}
void left(){

  analogWrite(enA,10);
  digitalWrite(in1,LOW);
  digitalWrite(in2,HIGH);

  analogWrite(enB,255);
  digitalWrite(in3,HIGH);
  digitalWrite(in4,LOW);
}
void right(){
  analogWrite(enA,255);
  digitalWrite(in1,HIGH);
  digitalWrite(in2,LOW);
```

```
  analogWrite(enB,10);
  digitalWrite(in3,LOW);
  digitalWrite(in4,HIGH);
}
void stop(){
    analogWrite(enA,0);
    digitalWrite(in1,LOW);
    digitalWrite(in2,LOW);

    analogWrite(enB,0);
    digitalWrite(in3,LOW);
    digitalWrite(in4,LOW);
}
void brushon(){

  analogWrite(enC,255);
  digitalWrite(in5,HIGH);
  digitalWrite(in6,LOW);
```

APPENDIX H: Structural Analysis

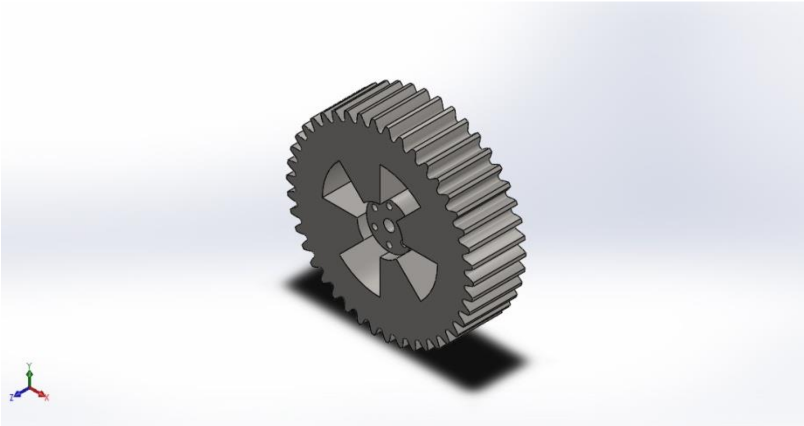

Simulation of rear wheel

Date: Saturday, May 20, 2023
Designer: SolidWorks
Study name: Static 1
Analysis type: Static

Model Information

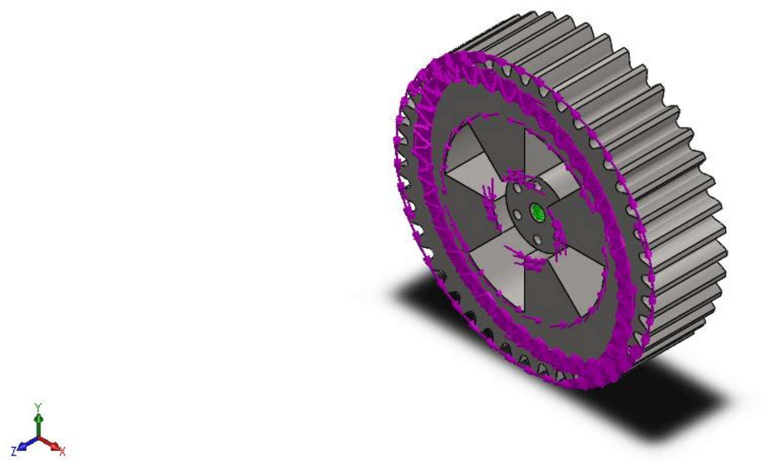

Model name: back wheels v1
Current Configuration: Default

Solid Bodies			
Document Name and Reference	**Treated As**	**Volumetric Properties**	**Document Path/Date Modified**
back wheels v1.step	Solid Body	**Mass:1.42253 kg** **Volume:0.000182376 m^3** **Density:7,800 kg/m^3** **Weight:13.9408 N**	**C:\Users\HP\AppData\Local\Temp\swx5928\IC~~\Spur Gear (42 teeth).step.SLDPRT** May 20 20:42:22 2023

Study Properties

Study name	Static 1
Analysis type	Static
Mesh type	Solid Mesh
Thermal Effect:	On
Thermal option	Include temperature loads
Zero strain temperature	298 Kelvin
Include fluid pressure effects from SOLIDWORKS Flow Simulation	Off
Solver type	FFEPlus
Inplane Effect:	Off
Soft Spring:	Off
Inertial Relief:	Off
Incompatible bonding options	Automatic
Large displacement	Off
Compute free body forces	On
Friction	Off
Use Adaptive Method:	Off
Result folder	SOLIDWORKS document (C:\Users\HP\Downloads)

Units

Unit system:	SI (MKS)
Length/Displacement	mm
Temperature	Kelvin
Angular velocity	Rad/sec
Pressure/Stress	N/m^2

Material Properties

Model Reference	Properties	Components
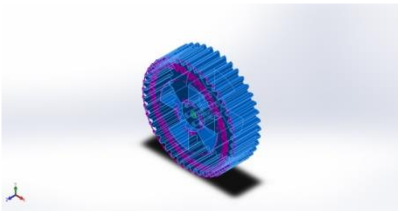	**Name:** Plain Carbon Steel **Model type:** Linear Elastic Isotropic **Default failure criterion:** Max von Mises Stress **Yield strength:** 2.20594e+08 N/m^2 **Tensile strength:** 3.99826e+08 N/m^2 **Elastic modulus:** 2.1e+11 N/m^2 **Poisson's ratio:** 0.28 **Mass density:** 7,800 kg/m^3 **Shear modulus:** 7.9e+10 N/m^2 **Thermal expansion coefficient:** 1.3e-05 /Kelvin	Solid Body 1(back wheels v1.step)(back wheels v1.step-1/Spur Gear (42 teeth).step-1)
Curve Data:N/A		

Loads and Fixtures

Fixture name	Fixture Image	Fixture Details
Fixed-1	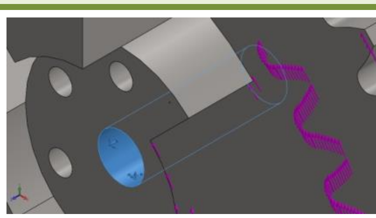	**Entities:** 1 face(s) **Type:** Fixed Geometry

Resultant Forces

Components	X	Y	Z	Resultant
Reaction force(N)	0.22876	0.132721	-0.164304	0.311355
Reaction Moment(N.m)	0	0	0	0

Load name	Load Image	Load Details
Torque-1	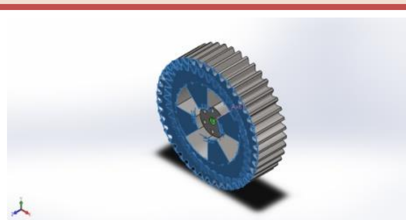	**Entities:** 1 face(s) **Reference:** Axis1 **Type:** Apply torque **Value:** 100 N.m

Mesh information

Mesh type	Solid Mesh
Mesher Used:	Standard mesh
Automatic Transition:	Off
Include Mesh Auto Loops:	Off
Jacobian points for High quality mesh	16 Points
Element Size	5.67187 mm
Tolerance	0.283593 mm
Mesh Quality	High
Remesh failed parts with incompatible mesh	Off

Mesh information - Details

Total Nodes	31778
Total Elements	19450
Maximum Aspect Ratio	12.114
% of elements with Aspect Ratio < 3	88.1
% of elements with Aspect Ratio > 10	0.0206
% of distorted elements(Jacobian)	0
Time to complete mesh(hh;mm;ss):	00:00:05
Computer name:	

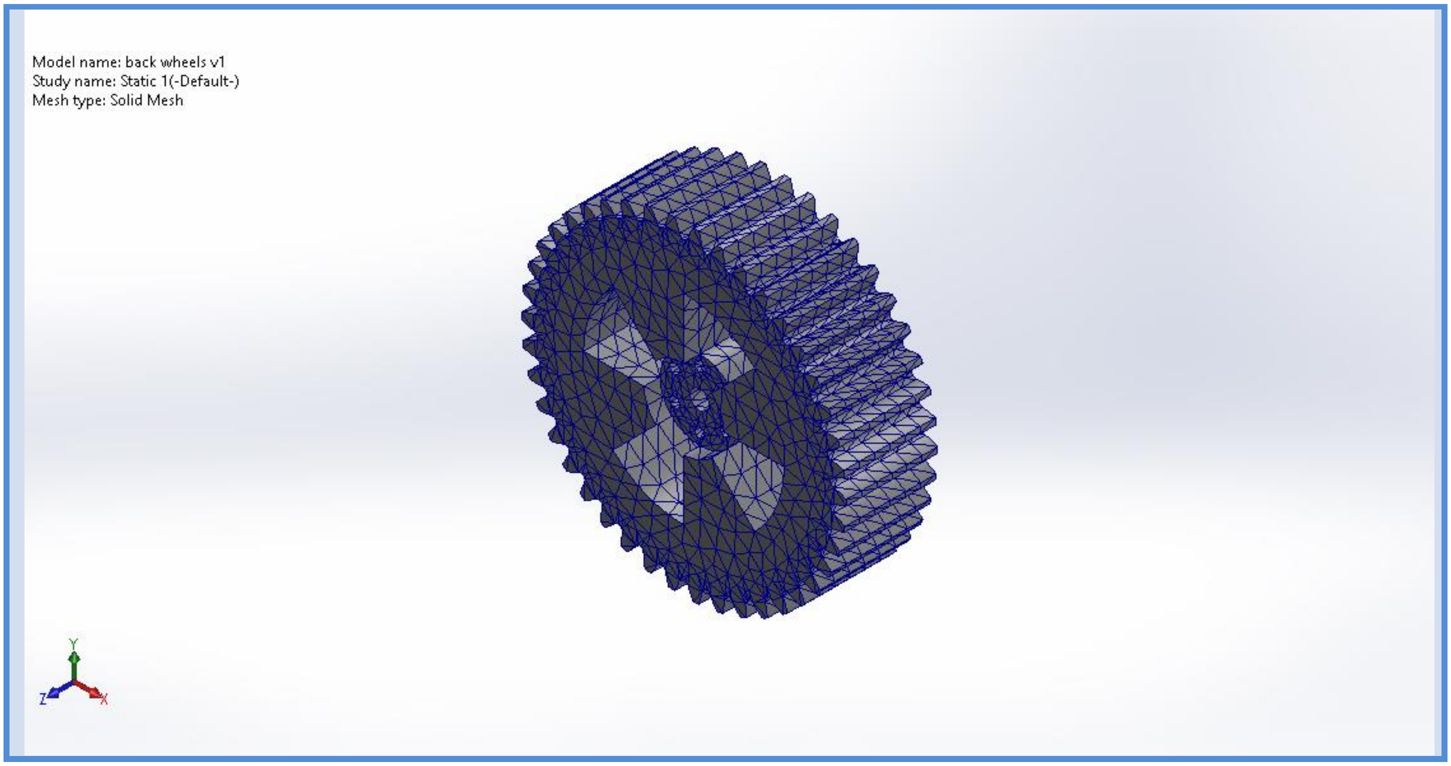

Resultant Forces

Reaction forces

Selection set	Units	Sum X	Sum Y	Sum Z	Resultant
Entire Model	N	0.22876	0.132721	-0.164304	0.311355

Reaction Moments

Selection set	Units	Sum X	Sum Y	Sum Z	Resultant
Entire Model	N.m	0	0	0	0

Free body forces

Selection set	Units	Sum X	Sum Y	Sum Z	Resultant
Entire Model	N	-0.296252	0.687684	0.0717873	0.752215

Free body moments

Selection set	Units	Sum X	Sum Y	Sum Z	Resultant
Entire Model	N.m	0	0	0	1e-33

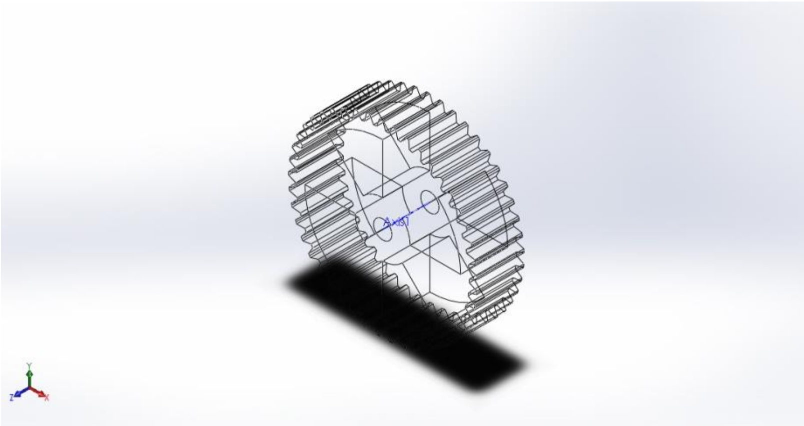

Simulation of front wheel

Date: Saturday, May 20, 2023
Designer: SolidWorks
Study name: Static 1
Analysis type: Static

Model Information

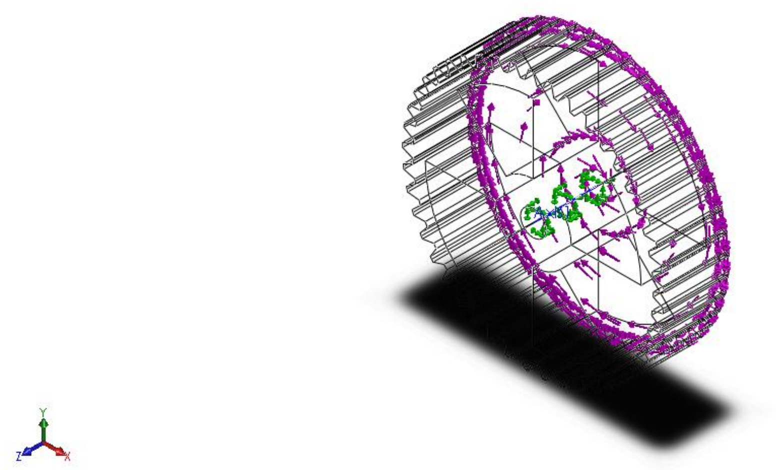

Model name: front wheels
Current Configuration: Default

Solid Bodies			
Document Name and Reference	**Treated As**	**Volumetric Properties**	**Document Path/Date Modified**
Cut-Extrude1 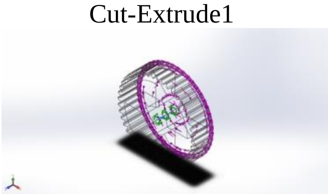	Solid Body	**Mass:1.02777 kg** **Volume:0.000130793 m^3** **Density:7,858 kg/m^3** **Weight:10.0722 N**	**C:\Users\HP\Desktop\Final capstone Design\front wheels.SLDPRT** May 19 19:34:12 2023

Study Properties

Study name	Static 1
Analysis type	Static
Mesh type	Solid Mesh
Thermal Effect:	On
Thermal option	Include temperature loads
Zero strain temperature	298 Kelvin
Include fluid pressure effects from SOLIDWORKS Flow Simulation	Off
Solver type	FFEPlus
Inplane Effect:	Off
Soft Spring:	Off
Inertial Relief:	Off
Incompatible bonding options	Automatic
Large displacement	Off
Compute free body forces	On
Friction	Off
Use Adaptive Method:	Off
Result folder	SOLIDWORKS document (C:\Users\HP\Desktop\Final capstone Design)

Units

Unit system:	SI (MKS)
Length/Displacement	mm
Temperature	Kelvin
Angular velocity	Rad/sec
Pressure/Stress	N/m^2

Material Properties

Model Reference	Properties	Components
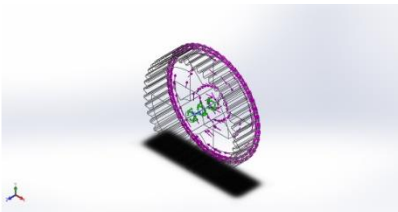	**Name:** 1023 Carbon Steel Sheet (SS) **Model type:** Linear Elastic Isotropic **Default failure criterion:** Max von Mises Stress **Yield strength:** 2.82685e+08 N/m^2 **Tensile strength:** 4.25e+08 N/m^2 **Elastic modulus:** 2.05e+11 N/m^2 **Poisson's ratio:** 0.29 **Mass density:** 7,858 kg/m^3 **Shear modulus:** 8e+10 N/m^2 **Thermal expansion coefficient:** 1.2e-05 /Kelvin	Solid Body 1(Cut-Extrude1)(front wheels)
Curve Data:N/A		

Loads and Fixtures

Fixture name	Fixture Image	Fixture Details
Fixed-1	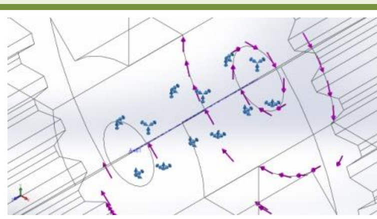	**Entities:** 1 face(s) **Type:** Fixed Geometry

Resultant Forces

Components	X	Y	Z	Resultant
Reaction force(N)	-0.0353374	-0.0356979	0.0325489	0.0598541
Reaction Moment(N.m)	0	0	0	0

Load name	Load Image	Load Details
Torque-1	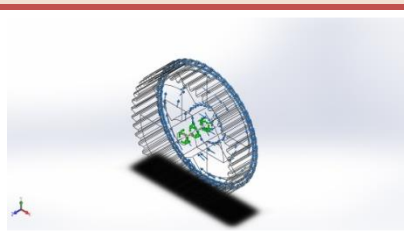	**Entities:** 1 face(s) **Reference:** Axis1 **Type:** Apply torque **Value:** 100 N.m

Mesh information

Mesh type	Solid Mesh
Mesher Used:	Standard mesh
Automatic Transition:	Off
Include Mesh Auto Loops:	Off
Jacobian points for High quality mesh	16 Points
Element Size	5.07759 mm
Tolerance	0.253879 mm
Mesh Quality	High

Mesh information - Details

Total Nodes	22374
Total Elements	12916
Maximum Aspect Ratio	9.5602
% of elements with Aspect Ratio < 3	79.8
% of elements with Aspect Ratio > 10	0
% of distorted elements(Jacobian)	0
Time to complete mesh(hh;mm;ss):	00:00:03
Computer name:	

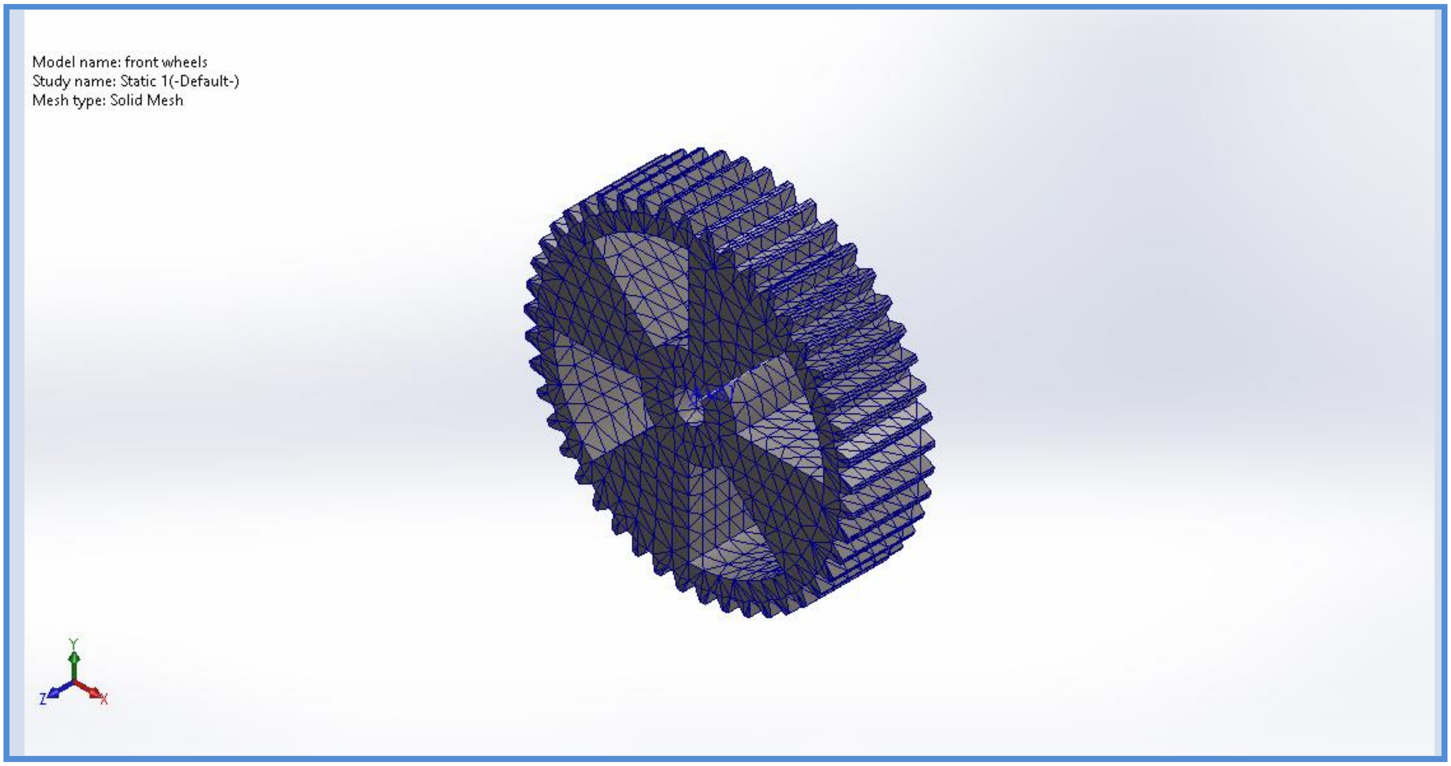

Resultant Forces

Reaction forces

Selection set	Units	Sum X	Sum Y	Sum Z	Resultant
Entire Model	N	-0.0353374	-0.0356979	0.0325489	0.0598541

Reaction Moments

Selection set	Units	Sum X	Sum Y	Sum Z	Resultant
Entire Model	N.m	0	0	0	0

Free body forces

Selection set	Units	Sum X	Sum Y	Sum Z	Resultant
Entire Model	N	1.23591	0.234528	0.447205	1.33509

Free body moments

Selection set	Units	Sum X	Sum Y	Sum Z	Resultant
Entire Model	N.m	0	0	0	1e-33

Study Results

Name	Type	Min	Max
Stress1	VON: von Mises Stress	6.863e+03N/m^2 Node: 19674	4.689e+07N/m^2 Node: 12283

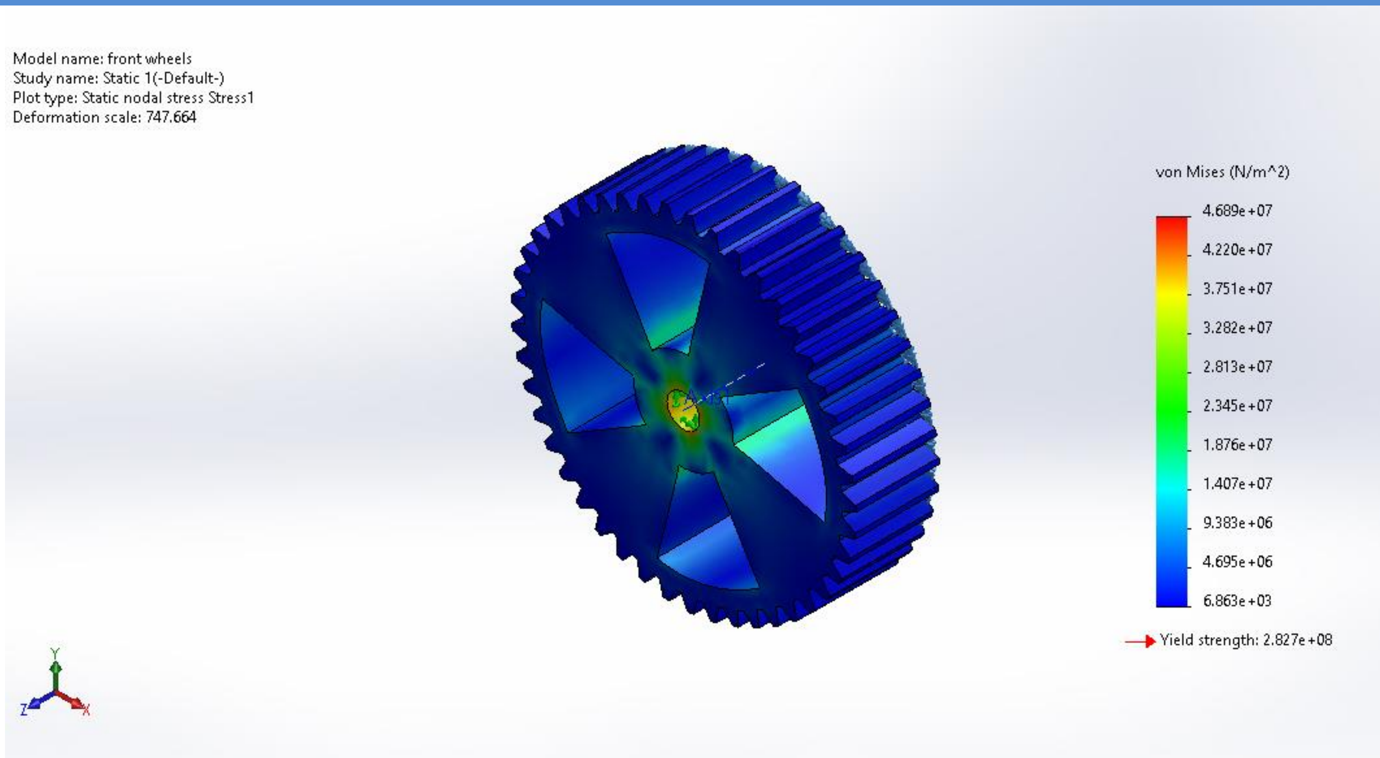

front wheels-Static 1-Stress-Stress1

Name	Type	Min	Max
Displacement1	URES: Resultant Displacement	0.000e+00mm Node: 1	1.376e-02mm Node: 103

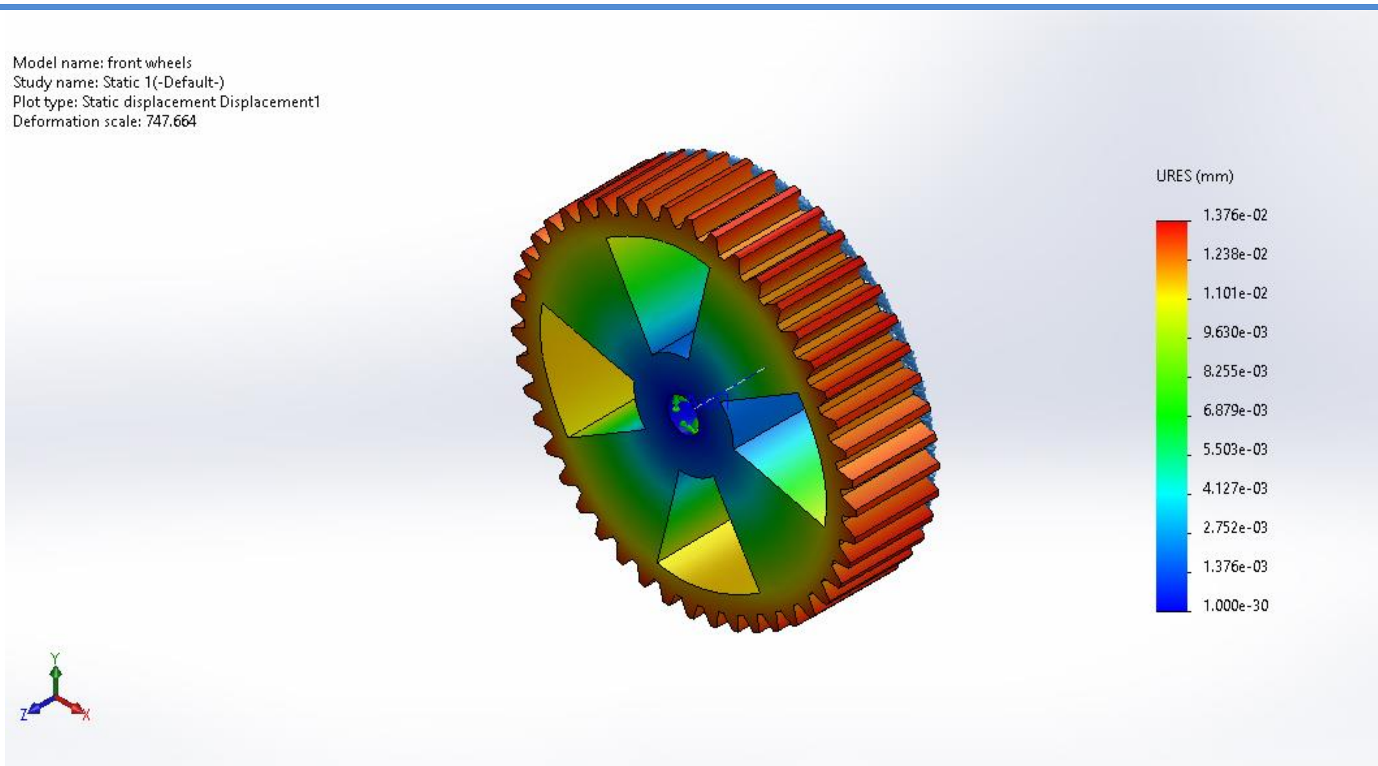

front wheels-Static 1-Displacement-Displacement1

Name	Type	Min	Max
Strain1	ESTRN: Equivalent Strain	2.775e-08 Element: 8762	1.529e-04 Element: 2350

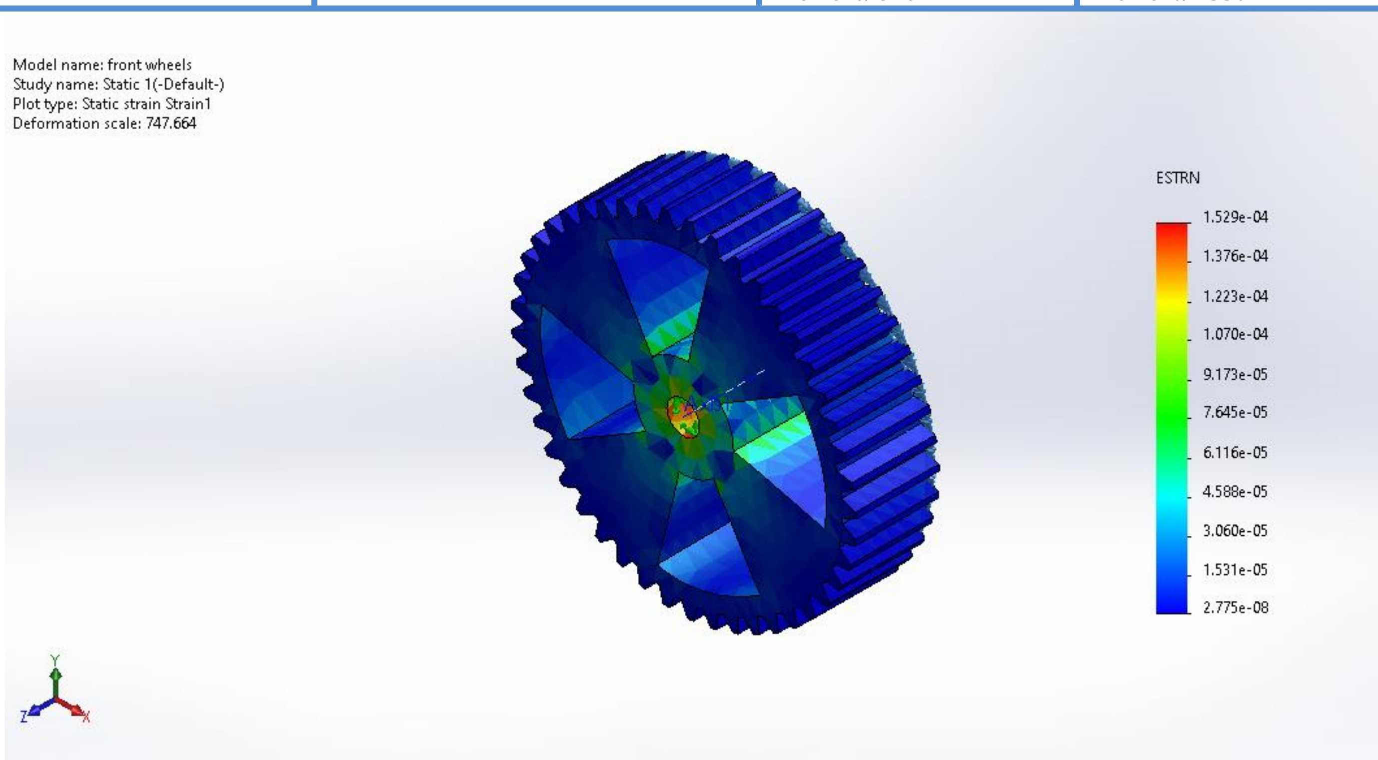

front wheels-Static 1-Strain-Strain1

Name	Type
Displacement1{1}	Deformed shape

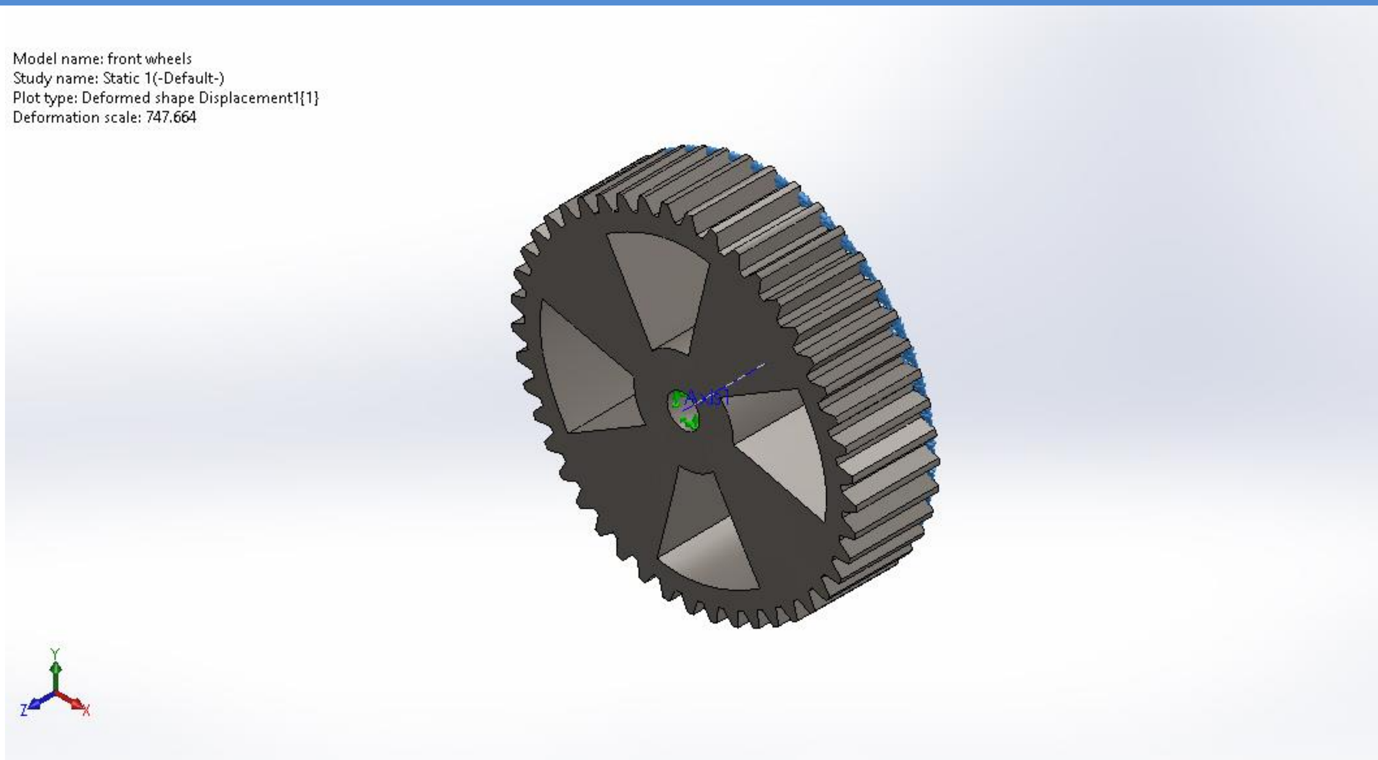

front wheels-Static 1-Displacement-Displacement1{1}

Conclusion :

The torque analysis was done to the front wheels with a support and with a 100 N.m the results showed that von misses stress is min 6.863e+03N/m^2 and max 4.689e+07N/m^2 And with Equivalent Strain of 2.775e-08 and 1.529e-04 max quantity .